EXPLORATION OF PHOTOAUTOTROPHIC HYDROGEN PRODUCTION IN *Synechocystis sp.* ATCC 27184

by

Arca Yılmaz

B.Sc. in Chemical Engineering, Boğaziçi University, 2017

Submitted to the Institute of Environmental Sciences in partial fulfillment of
the requirements for the degree of
Master of Science
in
Environmental Sciences

Boğaziçi University

2020

OPTIMIZATION OF PHOTOAUTOTROPHIC HYDROGEN PRODUCTION IN *Synechocystis sp.* ATCC 27184

APPROVED BY:

Assist. Prof. Dr. Berat Z. Haznedaroğlu Thesis Advisor	……..
Prof. Dr. Orhan Yenigün	……..
Assoc. Prof. Dr. Alper Uzun	……..

DATE OF APPROVAL: 15/09/2020

ACKNOWLEDGEMENTS

First of all, I would like to show my gratitude and respects to my advisor Assist. Prof. Dr. Berat Z. Haznedaroğlu for his guidance throughout the study. He was always accessible when needed and did everything he can to support me to overcome obstacles that I have faced. His dedication for research will be inspiring for my academic career. Also, I am very grateful to the members of my thesis committee Prof. Dr. Orhan Yenigün and Assoc. Prof. Dr. Alper Uzun for their valuable comments and contributions.

I was very lucky to work with Assist. Prof. Dr. Ulaş Tezel in laboratory environment. I learned a lot from him about the academic way of thinking, analytical equipment utilization and laboratory management. Also, problem solver Dr. Engin Bayram was a life saver in all gas analysis part of this thesis.

I also would like to acknowledge our funding support from The Scientific and Technological Research Council of Turkey (TÜBİTAK) 1001 Program with Project No: 115Y163.

Kilyos folks, starting from the first day, made the long way to laboratory more barrable. I am thankful to Fahri Koray Sakarya for his patience to every silly question. To Sevda Avcı, Emren Borhan, Elifcan Çalışkan, Gizem Çetin, Seyed Mehdi Emadian, İrem Karamollaoğlu, Dila Hocaoğlu and Emre Karakaya, I am very happy that we had the chance to work together. I thank Duygu Özçelik for all we share. Fortunately, Neowise was appeared in Kilyos sky in the last days of my laboratory work. Even I was quite absent, I happily shared the office with Ece Özön and F. Öykü Sefiloğlu. I will miss the energy of my roomies.

For Zeynep Karagöz and good people of KALT 2.0; Murat Sarıhan, Yunus Şeker, Kubilay Temurhan and Tezcan Gönüllü, your places in my life are irreplaceable.

Alexandra Elbakyan, a Don Quite against windmills, split the ocean and let us walk through.

Not only these years, but I always feel unrequited love and support of my family, Berna Yılmaz and Turgay Yılmaz. It is such a joy to make them proud.

ABSTRACT

EXPLORATION OF PHOTOAUTOTROPHIC HYDROGEN PRODUCTION IN *Synechocystis sp.* ATCC 27184

Anthropogenic carbon dioxide emissions possess severe treats to Earth's climate balance and warms the planet. In order to reverse this trend, conventional energy production from fossil fuels must be abandoned in near future. It is an urgent and critical need to shift towards low carbon intensive energy production technologies. While solar and wind energy mainly focus on electricity production, hydrogen technologies remains as notable energy carrier which requires more sustainable production methods. On this manner, innovative biofuel applications open new horizons. Cyanobacteria are alternative third generation biofuel resources for hydrogen technologies. Cyanobacterium *Synechocystis sp.* strain ATCC 27184 (also designated as PCC 6803 [N-1]) is known for its hydrogenase enzyme which is able to produce hydrogen gas by direct photolysis of water molecules. However, oxygen is a strong inhibitor for the enzyme. In this study, hydrogenase activity and total hydrogen gas production potential are explored in various growth media. Culture media BG-11 is modified by removing nitrogen and sulfur nutrients separately. Plus, the effect of strong reducing agent sodium thioglycolate salt is investigated. Although sodium thioglycolate is effective in removing both dissolved oxygen and photosynthetic oxygen gas, hydrogenase activity is not significantly increased. Highest hydrogenase activity is observed in sulphur deprived medium. Direct hydrogen production is not observed in any of experimental media in the course of the study.

ÖZET

İnsan kaynaklı karbondioksit salımları dünyanın iklim dengesini ciddi şekilde etkilemekte ve gezegenin ısınmasına sebep olmaktadır. Bu gidişatı tersine çevirmek için fosil yakıtlardan enerji üretimi yakın gelecekte terk edilmelidir. Düşük karbon yoğun enerji üretim teknolojilerine geçiş bu yüzden acil ve kritik bir ihtiyaçtır. Güneş ve rüzgar enerjisi esas olarak elektrik üretimine odaklanırken, artık daha sürdürülebilir üretim yöntemleri gerektiren hidrojen teknolojileri kayda değer enerji taşıyıcısı olmaya adaydır. Bu yolda, yenilikçi biyoyakıt uygulamaları yeni ufuklar sunmaktadır. Siyanobakteriler ise hidrojen teknolojileri için alternatif üçüncü nesil biyoyakıt kaynaklarıdır. *Synechocystis* sp. siyanobakterisinin ATCC 27184 suşu (PCC 6803 [N-1] olarak da adlandırılır) su molekülünden doğrudan fotoliz ile hidrojen gazı üretebilen hidrojenaz enzimine sahip olması ile bilinir. Ancak oksijen gazı hidrojenaz enzimi için güçlü bir inhibitördür. Bu çalışmada, çeşitli besi yerlerinin hidrojenaz aktivitesi üzerindeki etkisi ve toplam hidrojen gazı üretim potansiyeli araştırılmıştır. Bu doğrultuda BG-11 besi yeri nitrojen ve kükürt bileşenlerinin çıkarılmasıyla ayrı ayrı modifiye edildi. Ayrıca, güçlü indirgeyici madde olan sodyum tiyoglikolat tuzunun etkisi araştırıldı. Sodyum tiyoglikolat, hem çözünmüş oksijenin hem de fotosentetik oksijen gazının uzaklaştırılmasında etkili olmasına rağmen, hidrojenaz aktivitesini arttırmada etkili olmadı. En yüksek hidrojenaz aktivitesi kükürtsüz besi yerinde gözlemlendi. Çalışma boyunca deneysel ortamların hiçbirinde doğrudan hidrojen üretimi gözlemlenmedi.

TABLE OF CONTENTS

ACKNOWLEDGEMENTS iii

ABSTRACT iv

ÖZET v

TABLE OF CONTENTS vi

LIST OF FIGURES ix

LIST OF TABLES xi

LIST OF SYMBOLS/ABBREVIATIONS xii

1. INTRODUCTION 1

2. LITERATURE REVIEW 5

2.1. Biological Hydrogen Production 5

2.2. Fundamentals of Photolysis 6

2.3. Photobiological Hydrogen Production 7

2.3.1. Direct Photolysis 8

2.3.2. Indirect Photolysis 9

2.4. Photofermentation 10

2.5. Dark Fermentation 11

2.6. Enzymes 11

2.6.1. Hydrogenase 12

2.6.2. Nitrogenase 14

2.7. Improvements for Hydrogen Production 15

2.7.1. Genetic Modifications 16

2.7.2. Medium Modifications 18

2.7.3. Immobilization 19

2.7.4. Use of Reducing Agents 20

2.8. Photoautotrophic Species 21

2.9. Use of Methyl Viologen in Biohydrogen Analysis 24
2.10. Chlorophyll a Measurements 24
2.10.1. Spectrophotometric Chlorophyll a Determination 25
3. MATERIALS AND METHODS 27
3.1. Culture Maintenance 27
3.2. Culture Maintenance and Seed Preparation 28
3.3. Experimental Reactor Setup 29
3.4. Experimental Conditions 29
3.5. Measurements 31
3.5.1. Headspace Sampling 31
3.5.2. Small vial sampling 31
3.5.3. Sampling for Hydrogenase Activity 31
3.5.4. Gas Analysis Method 32
3.5.5. Dissolved Oxygen Measurement 36
3.6. Chlorophyll a Analysis 36
4. RESULTS AND DISCUSSION 39
4.1. Growth of *Synechocystis sp.* 39
4.2. Initial Screening Experiments 41
4.3. Chlorophyll a Content 46
4.4. Overall Biological Hydrogen Production 48
4.5. Hydrogenase Activity 54
5. CONCLUSION 59
REFERENCES 61
APPENDIX A 75
APPENDIX B 75
APPENDIX C 77
APPENDIX D 83

APPENDIX E……86

APPENDIX F……88

LIST OF FIGURES

Figure 2.1. Electron flow in photosynthesis, also known as Z scheme..... 7

Figure 2.2. Mechanism of direct photolysis..... 9

Figure 2.3. Mechanism of indirect photolysis..... 9

Figure 2.4. Mechanism of photofermentation..... 11

Figure 2.5. Exact electron transfer pathway in hydrogen production in *Synechocystis sp* 23

Figure 3.1. Reactor for seed growth……..28

Figure 3.2. *Synechocystis sp.* cells under light microscope…….29

Figure 3.3. Experimental setup……..30

Figure 3.4. Hydrogen calibration curve…….34

Figure 3.5. Oxygen calibration curve..... 34

Figure 3.6. Nitrogen calibration curve 35

Figure 3.7. Chlorophyll a extraction steps 37

Figure 4.1. Growth curve for *Synechocystis sp*. 40

Figure 4.2. pH vs time..... 40

Figure 4.3. Cell density vs time..... 41

Figure 4.4. Chl a concentration of R1……..……...47

Figure 4.5. Chl a concentration of R2……...……..47

Figure 4.6. Chl a concentration of R3…….47

Figure 4.7. Chl a concentration of R4……47

Figure 4.8. Reactors on 6th day. (A) BG-11; (B) BG-11 (-S); (C) BG-11 (-N); (D) BG-11° 48

Figure 4.9. Oxygen concentration in the headspace of R1..... 50

Figure 4.10. Oxygen concentration in the headspace of R2..... 51

Figure 4.11. Oxygen concentration in the headspace of R3..... 52

Figure 4.12. Oxygen concentration in the headspace of R4..... 53

Figure 4.13. Dissolved oxygen in BG-11° setup..... 53

Figure 4.14. Hydrogenase activity of R1 54

Figure 4.15. Hydrogenase activity of R2 56

Figure 4.16. Hydrogenase activity of R3 57

Figure 4.17. Hydrogenase activity of R4 58

LIST OF TABLES

Table 2.1. Genetically engineered cyanobacteria, their targeted genes and enhanced hydrogen production rates 16

Table 3.1. Composition of BG-11 medium 27

Table 3.2. Composition of BG-11 trace metals solution 27

Table 3.3. Experimental conditions 30

Table 4.1. Initial screening experiments for hydrogen detection 43

Table 4.2. Hydrogenase activity in the presence of reduced MV 55

LIST OF SYMBOLS/ABBREVIATIONS

Symbol	Explanation	Unit
A	Gas Peak Area	-
a	Slope of Gas Calibration Curve	mol
b	Gas Calibration Curve Constant	mol
DO	Dissolved Oxygen	mg/L
n_i	Amount of Gas	mol
P_i	Pressure	bar
R	Gas Constant	Lbar/Kmol
T	Temperature	Kelvin (K)
V_i	Volume	Liter (L)

Abbreviation	Explanation
AEM	Anion Exchange Membrane
ATP	Adenosine Triphosphate
BG-11	Blue-Green Medium
BG-11(-N)	Nitrogen deprived Blue-Green Medium
BG-11(-S)	Sulphur Blue-Green Medium
$CaCl_2 \cdot 2H_2O$	Calcium Chloride Dihydrate
Chl a	Chlorophyll a
Citric Acid$\cdot H_2O$	Citric Acid Monohydrate
$Co(NO_3)_2.6H_2O$	Cobalt (II) Nitrate Hexahydrate
$CuSO_4.5H_2O$	Copper (II) Sulfate Pentahydrate
Cyt	Cytochrome
DDT	1,4 dithiothreitol
DMF	N,N'-dimethylformamide
DMSO	Dimethyl Sulfoxide
EIA	Energy Information Administration
Fd	Ferredoxin
FNR	Ferredoxin NADP Reductase
GC	Gas Chromatography
GHG	Greenhouse Gases

H_3BO_3	Boric Acid
HCO_3^-	Bicarbonate Ion
Hmd	[Fe]-hydrogenase
HPLC	High-Performance Liquid Chromatography
HydA	Fd-dependent Hydrogenase
IEA	International Energy Agency
IPCC	Intergovernmental Panel on Climate Change
K_2HPO_4	Dipotassium Hydrogen Phosphate
LED	Light-emitting Diode
LH	Light Harvesting
LHC	Light-Harvesting Complex
$MgCl_2.6H_2O$	Magnesium Chloride Hexahydrate
$MgSO_4 \cdot 7H_2O$	Magnesium Sulfate Heptahydrate
$MnCl_2.4H_2O$	Manganese (II) Chloride Tetrahydrate
Na_2CO_3	Sodium Carbonate
$Na_2EDTA \cdot 2H_2O$	EDTA Disodium Salt Dihydrate
$Na_2MoO_4.2H_2O$	Sodium Molybdate Dihydrate
$NADP^+$	Nicotinamide Adenine Dinucleotide Phosphate
NADPH	Reduced Nicotinamide Adenine Dinucleotide Phosphate
$NaNO_3$	Sodium Nitrate
NDH1	Complex I-like NADPH Dehydrogenase
NDH2	Type II NADPH Dehydrogenase
NH_4^+	Ammonium Ion
OD	Optical Density
Pc	Plastocyanin
PEM	Proton Exchange Membrane
Ph	Pheophytin
PSI	Photosystem I
PSII	Photosystem II
Q	Quinone
Q_A	Quinone A
Q_B	Quinone B
RC	Reaction Center
rpm	Revolutions per Minute

RSM	Response Surface Methodology
SDH	Succinate Dehydrogenase
SO_4^{2-}	Sulfate Ion
TCD	Thermal Conductivity Detector
$ZnSO_4.7H_2O$	Zinc (II) Sulfate Heptahydrate

1. INTRODUCTION

Intergovernmental Panel on Climate Change (IPCC) Special Report 1.5 °C foresees severe uncertainties in global climate in near future due to human induced climate change with very high probability, additional to previous occurrences to this date (Allen et al., 2018). Most critical action is to reduce fossil fuel consumption and deforestation to limit greenhouse gas (GHG) emissions and to protect carbon sinks (Allen et al., 2018). These efforts will hopefully be followed by net-zero carbon dioxide emission policies for a more stable climate. Meanwhile, global energy consumption shows an increasing trend over the years, while some government policies have started to shift towards renewable resources. Based on International Energy Agency's (IEA) recent report, even though fossil fuel share is as high as 81% in 2017 frame challenging base for future, a certain momentum in renewable energy capacity indicates the potential and the interest towards alternatives (IEA, 2018). In the same report, a possible sustainable development scenario suggests much higher share of renewable resources by 2040 (IEA, 2018). Being still out of the track of IPCC's net-zero recommendations, it shows how deterministic policies are required for more stabilized climate in future (IEA, 2019).

Another overlook made by The U.S. Energy Information Administration (EIA) shows that energy supply from renewables will increase significantly while coal usage will be decreasing until 2040 (EIA, 2016). Even though hydropower remains controversial as a renewable energy source, it still leads the alternative energy sources and solar power will also have important impact on future energy generation (EIA, 2016). Every projection shows that GHG emissions are the main focus of concern on energy shifting policies. A consensus among scientists has already been reached that elevated GHG emissions are the prime cause of global warming and the anthropogenic climate change is certain without any doubts (Oreskes, 2005). Thus, policymakers and scientists have the tendency to work more on low or non-carbon emitting energy sources.

Hydropower is still the main driver in renewable electricity production (IHA, 2020). Plus, apart from other purposes, agricultural crops are widely used to produce alternative liquid fuels, such as ethanol or biodiesel (Demirbaş, 2008). Biogas, a substitute for natural gas, is a mix of methane and carbon dioxide, mostly produced by anaerobic digestion of various biomass sources (Weiland, 2010). Hydrogen is another important alternative for future energy needs, having higher energy density than conventional hydrocarbon sources, indicating its role as an efficient energy carrier (Pandey and

Mohan, 2014). In reality, hydrogen cannot be considered as primary energy source, as it is not found naturally. It is an energy storage medium, needed to be obtained from other resources and then used in internal combustion engines or in hydrogen fuel cells (Nikolaidis and Poullikkas, 2017).

There are several different ways for hydrogen production, ranging from reforming of fossil fuels to biological routes. Today, majority of hydrogen is still produced commercially from carbon dioxide emitting resources (Dinçer and Acar, 2015). International Energy Agency (IEA) estimates that 75% of hydrogen production comes from natural gas, which sums up 6% of global natural gas use, and 23% uses coal as raw material (IEA, 2019). Only very small portion corresponding to 0.1% is produced from electrolysis, which remains controversial due to source of the electricity and utilization of water in water-stressed areas. Declining costs of solar and wind energy also offers promise for large scale production. Although the potential of hydrogen technologies has been discussed for years, it is underrepresented in future energy scenarios (Quarton et al., 2020). Combining with alternative production pathways and decoupling current mainstream production from coal and natural gas, hydrogen may have the power to shift both transport and industry sectors.

Conventional hydrogen production pathways are mainly as follows; coal gasification, natural gas reforming, electrolysis of water and biomass processing (IEA, 2019). Highest amount of hydrogen generation comes from reforming of natural gas. It includes multiple steps to obtain pure hydrogen; first natural gas, or methane, as the feedstock is processed in catalytic steam reforming at high temperature, following a water-gas-shift reaction is conducted the product becomes synthetic gas (a.k.a. syngas) composed of hydrogen, carbon monoxide and carbon dioxide. In the last step, a pressure-swing adsorption stage separates hydrogen gas from carbon dioxide (Amin et al., 2011).

Another fossil fuel based method is the gasification of coal. The main product is syngas, which can later be separated to its components via water-gas-shift reaction (Ratnasamy and Wagner, 2009). Whereas the syngas from coal gasification is largely produced and utilized for ammonia production in China, there are no industrial scale coal gasification plant operation for pure hydrogen production elsewhere (IEA, 2019). This pathway has the largest carbon emission with a ratio of 15 carbon dioxide to hydrogen per weight, the highest global warming vector among all (Muradov, 2017).

While having the smallest share in overall production, electrolysis is possibly the cleanest way with respect to GHG emissions depending highly on the primary electricity source. Electrolysis of water generates oxygen and hydrogen molecules, and it is one of the purest ways to obtain hydrogen

(Ursua, et al., 2011). The most established technology is alkaline electrolysis, followed by proton exchange membrane (PEM) and anion exchange membrane (AEM) (FCHJU, 2014). Anion exchange membrane technology is still under developmental state, seeking further investigations and cost reduction analysis to become commercially available (Vincent and Bessarabov, 2018). IEA estimates the cost of hydrogen production from water electrolysis is the highest, almost double the cost of production from coal gasification and natural gas reforming (IEA, 2019). Water splitting by photocatalysts is another promising technology, focusing on different semiconductors and co-catalysts to produce hydrogen from water (Kothari et al., 2008).

Biological hydrogen production is an upcoming, yet a challenging option, yielding hydrogen from metabolic activities of microorganisms (Hallenbeck, 2013). Some studies include the use of microbial biomass as substrate for hydrogen production in thermochemical processes such as gasification or pyrolysis (Pandey and Mohan, 2014). Hydrogen can be produced in several microorganisms by biological pathways of biophotolysis, photofermentation, dark fermentation or microbial electrolysis cell (Hallenbeck, 2013). Potentially, light dependent biohydrogen production from biophotolysis can be carbon neutral or negative. During direct biophotolysis, water molecule is converted into hydrogen and oxygen gases by means of photosynthetic pathways using only solar energy while fixing atmospheric carbon (Bozoglan et al., 2012). On the other hand, photosynthetically produced carbon-based substrate is utilized for the conversion of water into hydrogen and carbon dioxide in indirect biophotolysis (Voloshin et al., 2016). Both mechanisms are catalyzed; hydrogenase enzyme is responsible for both biophotolytic hydrogen production in non nitrogen-fixing green algae and cyanobacteria, whereas in nitrogen-fixing cyanobacteria nitrogenase enzyme is effective through indirect biophotolysis (Anwar et al., 2019). Photosynthetic bacteria, such as purple non-sulphur bacteria, are effectively capable of performing photofermentation for biomass production utilizing sunlight, which generates hydrogen and carbon dioxide as by-products in the absence of oxygen (Eroğlu and Melis, 2011). Dark fermentation happens in fermentative microorganisms under dark anoxic environments, where complex organic molecules are degraded into smaller organic acids or alcohols, and hydrogen is produced as a by-product (Anwar et al., 2019). Thus, the potential of removing waste organic matter while producing hydrogen gas makes dark fermentation an appealing option. Microbial electrolysis cell, inspired from microbial fuel cell, is capable of generating hydrogen in the cathode from organic matters using electron transfer from anode through cathode (Call and Logan, 2008). It requires small voltage application to trigger substrate degradation (Call and Logan, 2008). Significant challenges needed to be addressed, and current research is focused on optimization of the enzymatic pathway (Rao and Cammack, 2001).

Without demanding any source apart from sunlight and water, photobiological hydrogen production might be a sustainable and environmentally friendly approach for future hydrogen needs.

Biological production of hydrogen has been known and studied for decades. On the way towards bioeconomy-focused sustainable production of raw materials, it is highly sought to develop more efficient methods of biohydrogen production. The main objective of this study is to explore possible alternative ways to seek biological hydrogen production from cyanobacterium *Synechocystis sp.* To achieve this objective, various culture media compositions were used to determine hydrogen production capacity and oxygen reducing agents were experimented to decrease inhibitory effect of oxygen on enzyme (i.e. hydrogenase) during hydrogen production metabolism. Cells were cultivated in BG-11 medium, BG-11 without nitrogen, BG-11 without sulphur and BG-11 with 5 g/L of sodium thioglycolate.

2. LITERATURE REVIEW

2.1. Biological Hydrogen Production

As the effects of climate crisis buildups drastically, carbon dioxide emissions have to be minimized by shifting from fossil fuel consumption towards sustainable fuel alternatives. In the search of alternatives following the oil crisis in 1970s, hydrogen became a focal point being a promising energy carrier (IEA, 2019). However, there was a decline in interest since then due to decreasing oil prices, and the controversy about hydrogen utilization since the feedstock for hydrogen is almost completely fossil-fuel based. While slow interest on hydrogen technologies focused on fuel cell and transportation, debates have been increased on if the clean fuel proposal of hydrogen is hypocrisy. Nowadays, it has been argued once again that hydrogen-based economy in the scope of emission reduction for hard-to-abate industries; policy shifts on clean air, economic development and energy access; ability to encourage renewable electricity production; and energy transition is possible (IEA, 2019). Yet, there still exists challenges to be faced, such as policy and technology uncertainties, need for infrastructure towards hydrogen-based economy, and acceptance from governments and public (IEA, 2019). Nevertheless, hydrogen's high energy density comparing to other conventional fuels makes it attractive for further investigations on alternative production opportunities.

Among those, biological hydrogen production from microorganisms might be a plausible option for future hydrogen-based economy. There are numerous photosynthetic and non-photosynthetic microorganisms such as green algae, cyanobacteria and dark fermentative bacteria capable of producing biohydrogen through their primary metabolic pathways. Effective water splitting capacity, fast growth and higher carbon utilization rates of cyanobacteria offer valuable sustainability metrics in hydrogen production. Despite these advantages, the progress in biohydrogen production from cyanobacteria has been relatively slow. The metabolic production efficiency is lower than the desired level due to inhibitory effects of oxygen gas (formed during photosynthesis) on hydrogenase enzyme. Hydrogen production is achieved nearly under anaerobic conditions since the formation of oxygen instantaneously stops hydrogen generation (Appel et al., 2000). Although various strains and species have been investigated and genetically modified to increase the hydrogenase enzyme activity, there are still gaps in literature to understand the regulatory functions of these enzymes, especially [NiFe]-hydrogenase (Tamagnini et al., 2002). Since substrates such as glucose and sucrose increase the operational expenses, waste materials are appealing for hydrogen production during dark

fermentation (Pandey and Mohan, 2014). But still, biophotolytical methods provide an alternative approach due to effective use of light energy with water, without any other input requirements.

2.2. Fundamentals of Photolysis

When a water molecule is disassociated into hydrogen and oxygen under light energy, which is absorbed by chlorophyll pigments, by the means of biological systems, it is described as biophotolysis (Khetkorn et al., 2017). Light harvesting by Light Harvesting Complex (LHC) and by Reaction Center (RC) of photosystems I and II (PSI and PSII), and oxygen generation are the first steps of photosynthesis (Madigan et al., 2015). RC of PSII and PSI are named as P680 and P700, respectively indicating their maximum wavelength that can be absorbed (Madigan et al., 2015). LHC in green algae and light harvesting (LH) in cyanobacteria comprise of pigments such as chlorophylls and carotenoids in microalgae and chlorophyll a and phycobilisome in cyanobacteria respectively (Weber et al., 2014). Among them, chlorophyll located in RC is the main pigment and exited by light energy and transfers electron through Z scheme of biophotolysis (Madigan et al., 2015). When the light is harvested, photons excite chlorophyll molecule P680 in PSII to a higher state. This exited molecule, sometimes referred as PSII* or P680*, is an extremely good electron donor and is willing to give its electron to pheophytin (Ph) (Madigan et al., 2015). Thus, PSII becomes strong electropositive and accepts two electrons from each water molecule. Oxidation of two water molecules by PSII is catalyzed by Mn_4 cluster, resulting in 4 H^+ and oxygen gas (O_2) (Madigan et al., 2015). This is how water splitting occurs. Meanwhile, electrons transferred to Ph continue to travel through other proteins; quinone a and b (Q_A and Q_B), plastoquinone pool, plastocyanin (Pc) and results in PSI (Madigan et al., 2015). The pigment P700 in PSI can accept electron from Pc when it is excited by light energy (Madigan et al., 2015). Excited PSI* transfers electron through quinone molecules to ferredoxin (Fd) and at the end, $NADP^+$ molecules are reduced to NADPH (Madigan et al., 2015). This Z scheme can be seen on Figure 2.1. The energy is driven from RCs, and then continuously flows into the mechanisms of ATP synthesis and NADPH formation (Weber et al., 2014). In photosynthesis, electron carriers and generated ATP flow through carbon fixation pathways, i.e. Calvin Cycle. In case of hydrogen production, NADPH or Fd are catalyzed by either hydrogenase or nitrogenase to form hydrogen gas, which will be discussed in following sections.

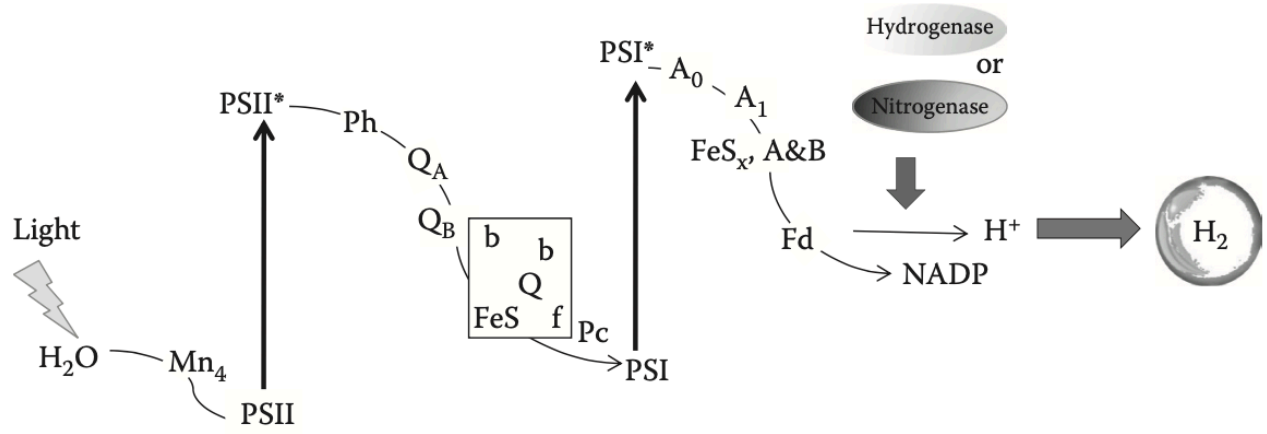

Figure 2.1. Electron flow in photosynthesis, also known as the Z scheme. PSI* and PSII*: exited states of photosystems, Ph: pheophytin, Q: quinone, Cyt: cytochrome, Pc: plastocyanin, A_0: quinones, Fd: ferredoxin. Under ideal conditions for hydrogen production, NADPH or reduced Fd is catalyzed by either hydrogenase or nitrogenase (adopted from Das et al., 2014).

In prokaryotic organisms, such as cyanobacteria, there are no specific organelle for photosynthesis to take a place as chloroplast in photosynthetic eukaryotes. Instead, there exists thylakoids, a cytoplasmic membrane (Madigan et al., 2015).

2.3. Photobiological Hydrogen Production

In cyanobacteria, two different enzymes are capable of hydrogen generation; nitrogenase and reversible hydrogenase. Nitrogenase is responsible of the reduction of nitrogen into NH_4^+, functions mainly during nitrogen fixing bioprocess (Burris, 1991). Hydrogen production remains limited in these organisms, as the hydrogen recycle is quite efficient by the help of the uptake [NiFe]-hydrogenase (Cournac et al., 2004). However, some non-nitrogen fixing cyanobacteria, such as *Synechocystis*, have only reversible (or bidirectional) [NiFe]-hydrogenase enzyme, allowing them to produce hydrogen photoautotrophically (Cournac et al., 2004). Both enzymes are highly sensitive to oxygen presence. Whereas hydrogenase activity is only suppressed under aerobic conditions, nitrogenase becomes inactive irreversibly (Eroğlu and Melis, 2011).

Hydrogen production by photolysis is a thermodynamically feasible process. Two PSs capture radiative energy from the light and can insert an electron from water-oxygen couple to a negative value, then becomes more negative than hydrogen electrode (Das et al., 2014).

There are two types of photolysis in microorganisms. Direct photolysis refers water splitting in electron flow of photosynthesis and generation of electrons and oxygen gas (Hallenbeck, 2013). Electrons, which reduce electron carrier $NADP^+$, are redirected towards hydrogenase enzyme and therefore hydrogen gas is produced (Das et al., 2014). In other words, NADPH reacts with a proton, H^+, in the presence of hydrogenase enzyme and forms hydrogen gas. In indirect photolysis, electron carriers, i.e. NADPH, are oxidized back to $NADP^+$ in autotrophic pathways and energy is stored as organic molecules (Antal et al., 2012). These molecules are then utilized to produce hydrogen gas later.

2.3.1. Direct Photolysis

Direct photolysis refers water splitting through biological means under the light irradiation. Electrons generated from water splitting are carried into PSI and PSII by utilizing absorbed light energy. These electrons pass through PSI and PSII towards Fd. In photosynthesis, Fd donates an electron to $NADP^+$, which goes to the Calvin Cycle for carbon fixation (Madigan et al., 2015). When oxygen is not present, reduced Fd donates an electron to hydrogenase enzyme in green algae (Eroğlu and Melis, 2011). Thus, some of the energy is stored as another final product, hydrogen gas, whereas the rest is kept as carbohydrates and lipids (Das et al., 2014). Figure 2.2. shows stepwise direct photolysis.

Electron carrier depends on the organism. In cyanobacteria electrons are transferred to NADPH, which is then oxidized back to $NADP^+$, and hydrogen is produced with the help of [NiFe]-hydrogenase (Montagud et al., 2015). However in green algae, the last electron carrier in photosystem, reduced Fd, works as an electron donor to [FeFe]-hydrogenase, which catalyzes H^+ to form hydrogen gas as shown in equations 2.1 and 2.2 (Melis et al., 2000):

$$NADPH + 2H^+ \leftrightarrow H_2 + NADP^+ \quad (2.1)$$

or;

$$2H^+ + 2Fd^- \leftrightarrow H_2 + 2Fd \quad (2.2)$$

Direction of reduced Fd in green algae highly depends on oxidation reduction potential, $NADP^+$/NADPH ratio or ATP level (Das et al., 2014). Once again, oxygen is a strong inhibitor in this pathway.

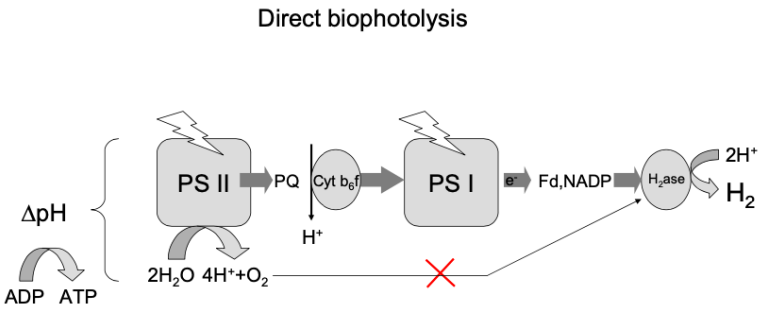

Figure 2.2. Mechanism of direct photolysis (adopted from Antal et al., 2012).

2.3.2. Indirect Photolysis

In the case of indirect photolysis, solar energy is captured, and generated ATP and electrons are directed to carbohydrate production. In ideal circumstances, stored carbohydrates can be converted into hydrogen during dark cycles. There are two types of indirect photolysis. In one case, it is suggested that photosynthesis is coupled with hydrogen production with a time delay (Pandey and Mohan, 2014). The metabolic pathway is same as direct photolysis, however, some of the ATP, reduced Fd and NADPH are used in Calvin cycle for carbohydrate production. In Figure 2.3. indirect photolysis can be seen. After the aerobic stage, carbohydrates are catabolized smaller molecules and electrons are then given to electron carriers under anaerobiosis (Antal et al., 2012). Then, reduced Fd and NADPH from both carbohydrates and PSI* can give an electron to H^+ ions under presence of either hydrogenase or nitrogenase.

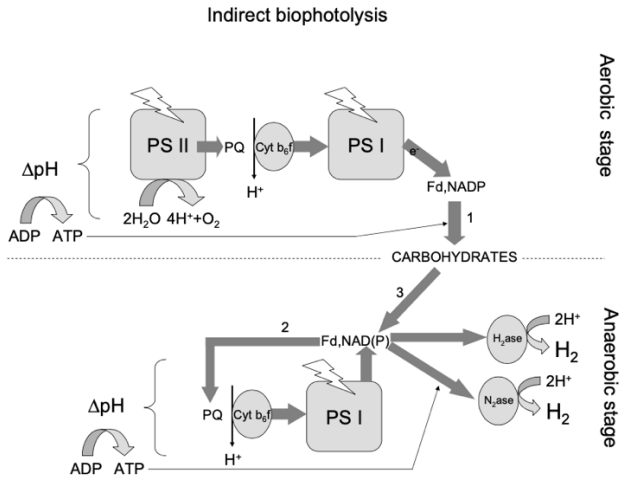

Figure 2.3. Mechanism of indirect photolysis (adopted from Antal et al., 2012).

Another type of indirect photolysis occurs in cyanobacteria when hydrogen production and oxygen generation are separated with space. In some filamentous cyanobacteria, there are specialized cells within the filament called heterocyst. These specialized cells are encoded with only PSI but not PSII, thus oxygen generation from the photolysis of water does not occur here. Plus, they are embedded within nonoxygen permeable cell walls, meaning that anaerobiosis can be achieved within the cell (Das et al., 2014). Hydrogen evolution, simultaneously with nitrogen fixation, is catalyzed by nitrogenase in heterocyst in anoxic environment (Schütz et al., 2004). However, the energy requirement for this energy intensive reaction comes from generated hydrogen molecules, which are consumed in the presence of uptake hydrogenase enzyme (Schütz et al., 2004). This enzyme helps to recover energy and reducing equivalent lost by recirculating electrons from hydrogen gas.

2.4. Photofermentation

Apart from other metabolic production means, hydrogen can also be generated by non-sulfur photosynthetic bacteria using additional light energy and consuming various substrates where dark fermentation is not an option. Generally exploiting waste streams or organic acids as substrates, hydrogen is produced as a side-product of nitrogen fixing metabolism. ATP, generated through photophosphorylation, is hydrolyzed to release electrons and reduced by the nitrogenase enzyme. Nitrogenase catalyzes nitrogen gas reduction into ammonia in nitrogen fixing bacteria, producing one to one ratio of hydrogen to nitrogen as shown in equations 2.3 and 2.4. If other reducible organic substrates do not exist in the environment, nitrogenase keeps reducing protons into hydrogen (Hallenbeck, 2013).

The bioprocess is also called anoxygenic photosynthesis. This series of reaction is irreversible and very energy intensive, where nitrogenase is highly sensitive to ammonium and oxygen. However, when substrates are provided, especially organic acids, under anoxic conditions with the presence of limited nitrogen, hydrogen production is viable (Masepohl and Hallenbeck, 2010). Figure 2.4. shows stepwise photofermentation.

$$N_2+8H^++8e^-+16ATP\rightarrow 2NH_3+ H_2+16ADP+16Pi \quad (2.3)$$

$$2H^++2e^-+4ATP\rightarrow H_2+4ADP+4Pi \quad (2.4)$$

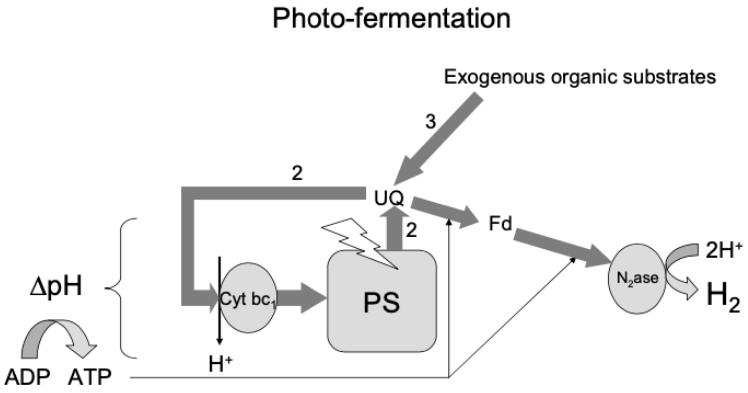

Figure 2.4. Mechanism of photofermentation (adopted from Antal et al., 2012).

2.5. Dark Fermentation

With the absence of light, facultative bacteria, obligate anaerobic bacteria and thermophiles are able to generate hydrogen gas (Hallenbeck, 2013). In dark fermentative biological hydrogen production, organic substrates are used as only electron source and this enables waster material utilization as substrate. There are three biochemical pathways for hydrogen production in dark fermentation that use different enzymes: Pyruvate:formate lyase and formate:hydrogen lyase enzymes are used in the first type of reactions and it is commonly seen in *Escherichia coli* and Enterobacteriaceae; Pyruvate:ferrodoxin oxidoreductase and Fd-dependent hydrogenase (HydA) are utilized in the second type; and NADPH:ferrodoxin oxidoreductase and HydA are used in the third one, where second and third type of reactions are common in *Clostridium* species (Oh et al., 2013). One ease of application for this process is an established large scale fermentation technologies, however some drawbacks exist such as high production of side organic acid products (i.e. acetic acid) and difficult fermentation of widely abundant substrates (i.e. lignocellulosic materials) (Hallenbeck et al., 2012).

2.6. Enzymes

Hydrogen production is catalyzed by two different enzyme groups (Tamagnini et al., 2002). Hydrogenase is directly responsible for the production with use of various electron carriers coming from cellular metabolic activities, such as biophotolysis, carbohydrate decomposition or fermentation. Hydrogen can be generated reversibly depending on cell redox potential shown on equation 2.5.

$$2H^{+}+2e^{-}\leftrightarrow H_2 \quad (2.5)$$

This is the simplest form of reaction catalyzed by hydrogenase. Cyanobacteria and photofermentative bacteria possess hydrogenase in their cytoplasm, whereas in microalgae it is located in chloroplast. Types of hydrogenase will be discussed in section 2.6.1.

Similarly, nitrogenase enzyme is able to catalyze nitrogen fixation reaction, and meantime hydrogen gas is produced to store energy for later consumption. Dinitrogen molecule is reduced to ammonia with an overall reaction of:

$$N_2+8e^{-}+8H^{+}+16ATP\rightarrow 2NH_3+H_2+16ADP+16P_i \quad (2.6)$$

One molecule hydrogen is generated from 8 protons and electrons, while consuming 16 ATP. Nitrogenase is found in cyanobacteria or in purple non-sulphur bacteria (Burris, 1991). In some cyanobacteria, it is active in heterocyst cell with uptake hydrogenase enzyme, and hydrogen gas product is therefore consumed by uptake hydrogenase to obtain energy (Eroğlu and Melis, 2011). Both enzymes are metalloproteins which contain iron-sulphur clusters (Carere and Levinli, 2012).

2.6.1. Hydrogenase

The activity of the hydrogenase enzyme depends on redox potential in the cell. When hydrogen gas and an electron acceptor is present, the enzyme works as uptake hydrogenase; but when an electron donor with a low potential is found, protons from water molecule work as electron acceptor with the help of biophotolysis and generates hydrogen (Vignais and Billoud, 2007). There are three types of hydrogenase exist in cells depending on their metal content in the active site. Among them, [FeFe]-hydrogenase is found in microalgae and some obligate anaerobic fermentative bacteria. This the most well-known type enzyme studied extensively (Eroğlu and Melis, 2011). [NiFe]-hydrogenase is abundant within cyanobacteria and photosynthetic bacteria. Lastly, some of thermophilic and mesophilic methanogens possess the rarest type, [Fe]-hydrogenase (Vignais and Billoud, 2007).

[FeFe]-hydrogenase is the only type of hydrogenase found in eukaryotes; therefore, it is mostly located in organelles, chloroplast or hydrogenosome. In addition, it is also found in anaerobic bacteria, anaerobic fungi and ciliates, trichomonads, and green algae, where the enzyme is located in stroma where it takes part in electron transport chain by accepting electrons from Fd (Vignais and Billoud, 2007). [FeFe]-hydrogenase has an active site “H-cluster”, having binuclear iron center

(2FeH) attached to [4Fe4S] cluster (Meyer, 2007). [FeFe]-hydrogenase is highly sensitive and becomes irreversibly inactive when intact with oxygen and carbon monoxide and its activity is 100 fold higher than [NiFe],hydrogenase (Melis and Happe, 2001). In a *Chlamydomonas reinhardtii* mutant, it was found by absorption X-ray spectroscopy that a contact with oxygen leads to destruction of [4Fe4S] cluster without harming the 2FeH center (Allakhverdiev et al., 2010).

[NiFe]-hydrogenase found in nature more extensively than [FeFe]-hydrogenase. As mentioned earlier, many domains of bacteria and archaea have [NiFe]-hydrogenase in their physiology. This type of hydrogenase is evaluated in subgroups depending on its subunit composition, conserved cysteine motif and catalytic bias: (1) Hydrogen uptake hydrogenase (encoded by gene Hup), which is linked to respiration; (2) cyanobacterial uptake hydrogenase, linked to nitrogen fixation and cytoplasmic hydrogen sensor hydrogenases; (3) bidirectional cytoplasmic hydrogenase (encoded by gene Hox); (4) and membrane bound, hydrogen evolving hydrogenase (Eckert et al., 2012). The enzyme consists of two subunits: large (α) subunit is 60 kDa and hosts bimetallic active site; small subunit (β) 30 kDa and hosts Fe-S clusters (Vignais and Billoud, 2007). α-subunit contains two cyanide (CN^-) and one carbon monoxide (CO) ligands, which are essential for hydrogen activation. These non-protein ligands are bound to Fe atom of [NiFe] active site, and four cysteine residues work for coordination of Ni atom and Ni-Fe bridge within the enzyme (Eckert et al., 2012). From this point forward, the main focus is cyanobacterial hydrogenases.

Cyanobacteria possess two different [NiFe]-hydrogenases: uptake and bidirectional hydrogenase. Uptake hydrogenase is highly linked with nitrogen fixation process in filamentous cyanobacteria (Tamagnini et al., 1997). The three main benefits of uptake hydrogenase are providing some of required ATP to the cell using oxyhydrogen reaction, removing oxygen gas and therefore preventing any inactivation, and delivering electrons to nitrogenase for nitrogen fixation (Tamagnini et al., 2002). As a result, generated hydrogen gas is consumed by uptake hydrogenase and transformed into energy for the use of energy-intensive nitrogen-fixing process. In heterocystous cyanobacteria, uptake hydrogenase is protected from oxygen and mostly located in heterocyst cell, where activity of nitrogenase enzyme is spatially separated from oxygen existence (Tamagnini et al., 2007). In non-heterocystous cyanobacteria, this separation is maintained with a time delay. On the other hand, uptake hydrogenase enzyme presence and existence is dependent on growth conditions, plus the precise location of the enzyme should be investigated further both in heterocystous and non-heterocystous cyanobacteria (Tamagnini et al., 2007).

Bidirectional hydrogenase is generally more susceptible to oxygen, but more tolerant to temperature and has higher affinity to hydrogen (Tamagnini et al., 2002). It is a pentameric enzyme, encoded by *hoxEFUYH* (Kaneko et al., 1996). It works bidirectionally, both generating and consuming hydrogen depending on inner cell parameters, such as redox potential. It engages with electron transport chain; it is suggested that it works as an electron valve during photosynthesis (Appel et al., 2000). Different strains have varying hydrogenase sensitivity to oxygen; in heterocystous species demand either anaerobic or microaerobic conditions, whereas for some non nitrogen-fixing species such as *Gloeocapsa alpicola* or *Chroococcidiopsis thermalis* gaseous oxygen presence is not an issue (Tamagnini et al., 2002).

[Fe]-hydrogenase, or iron-sulphur-cluster-free hydrogenase, is the least studied enzyme which is found in methanogens. Another name is hydrogen-forming methylenetetrahydromethanopterin dehydrogenase, abbreviated as Hmd. Main differences from other hydrogenases are that this enzyme does not contain [FeS]-clusters and it has mononuclear metal center rather than those of dinuclear enzymes in its active site (Das et al., 2014). Actually, it does not effectively catalyze reversible reaction of $2H^{+}+2e^{-}\leftrightarrow H_2$, rather it is responsible of an intermediate reaction of carbon dioxide reduction with hydrogen to form methane under nickel limitation (Thauer, 1998). This enzyme reversibly catalyzes the reduction of methenyltetrahydromethanopterin (methenyl-H_4MPT^{+}) with hydrogen to methylene-H_4MPT and H^{+}. However, it is not active by itself and requires iron-containing cofactor for its activity (Vignais and Billoud, 2007). Differing from other hydrogenases that can catalyze hydrogen-water exchange under exogenous electron acceptor, prior existence of electron acceptor Methenyl- H_4MPT^{+} is required for [Fe]-hydrogenase activity (Vogt et al., 2008).

2.6.2. Nitrogenase

Nitrogenase is the key enzyme that catalyzes hydrogen production in heterocystous cyanobacteria and purple non-sulphur bacteria. It is responsible for nitrogen gas reduction into ammonia, however, when there is no nitrogen gas in the environment, nitrogenase catalyzes only hydrogen production as shown in following reaction (Antal et al., 2012);

$$2H^{+}2e^{-}+4ATP\rightarrow H_2+4ADP+4Pi \qquad (2.7)$$

It is formed by dinitrogenase and dinitrogenase reductase proteins (Burris, 1991). It is very sensitive to oxygen presence, therefore in some cyanobacteria it is protected either by temporal or spatial separation of oxygen generation and nitrogen fixation (Tamagnini et al., 2002). The nitrogen

fixation process is very energy intensive, but the reaction is irreversible; meaning that produced hydrogen is not consumed by nitrogenase (Hallenbeck, 2013). On the other hand, in many cyanobacteria possess uptake hydrogenase within nitrogen fixation process to derivate additional energy from generated hydrogen and therefore lowering the yield. Generally, there are three types of nitrogenases found abundantly in microorganisms: Mo-nitrogenase, V-nitrogenase and Fe-nitrogenase (Burris, 1991).

2.7. Improvements for Hydrogen Production

There are a series of challenges needed to be addressed for improvements in biological hydrogen production. Oxygen sensitivity of reversible hydrogenase enzyme in algae is so high that when oxygen reaches a partial pressure more than 2%, the enzyme is deactivated (Ghirardi et al., 1997). Due to complex structure of hydrogenase enzyme, current research is mainly concentrated on oxygen removal or inhibition of oxygen generation in metabolic pathways.

Some approach follows modification of design parameters, applied to increase the rate. Although it is more applicable on laboratory scale and cost inefficient in large scale, one effective option for oxygen removal method is stripping reactor with inert gas, such as argon or nitrogen (Eroğlu and Melis, 2011). Once the anoxic environment is achieved, hydrogenase is reactivated. Interestingly, anaerobiosis can be achieved in [FeFe]-hydrogenase possessing alga *Chlamydomonas reinhardtii* by applying pulse illumination, causing directly conducting electrons towards the hydrogenase enzyme rather than carbon fixation and therefore increasing sustainable hydrogen production (Kosourov et al., 2018).

Backpressure of hydrogen in the reactor system can be a hindering factor for gaseous hydrogen generation (Das et al., 2014). To overcome this challenge, one possibility is to target thermodynamics of hydrogenase enzymatic reaction and extracting hydrogen gas from the reaction medium by directly consuming hydrogen in an electrochemical cell, which results in shifting the reaction equilibrium towards the product and increase both the yield and rate of hydrogen with a maximum number of 11 and 3.4 fold comparing to that of in the headspace accumulation, respectively (Ananyev et al., 2012).

There are also new strains that can surprisingly generate hydrogen under atmospheric oxygen concentrations. *Chlorella vulgaris* strain YSL01 and YSL16 have active hydrogenase enzyme using carbon dioxide as the only carbon source under aerobic conditions with different oxygen levels

(Hwang et al., 2014). Some other *Chlorella* strains were also found to be hydrogen productive under oxygen partial pressure of 15% under sulphur deprived conditions (Chader et al., 2009). Other intensively studied methodologies are discussed in following subsections.

2.7.1. Genetic Modifications

Main motivations on referring genetic engineering are to decrease oxygen generation or to redirect electrons towards hydrogenase or nitrogenase. Plus, some studies focus on deactivation of uptake hydrogenase enzyme to limit hydrogen consumption within the cell. Nitrogenase possessing cyanobacteria also have uptake hydrogenase involving hydrogen recycling and consumption. Uptake hydrogenase depleted strains have the ability to produce significantly higher hydrogen in *Anabaena sp.* (Khetkorn et al., 2017).

Table 2.1. Genetically engineered cyanobacteria, their targeted genes and enhanced hydrogen production rates (adopted from Khetkorn et al., 2017).

Microalgal strains	Engineered Gene	Hydrogen production rate (μmol H_2 mg chl a $^{-1}$ h^{-1})	Conditions	Reference
Inactivation of uptake hydrogenase				
Anabaena variabilis strain AVM13	hupSL	135	Ar, 100 μ$Em^{-2}s^{-1}$, nitrogen- fixing	(Happe et al., 2000)
Nostoc punctiforme strain NHM5	hupL	14	Light and nitrogen-fixing	(Lindberg et al., 2002; Tamagnini et al., 2002)
Anabaena sp. PCC 7120	hupL/hoxH	53	Ar, 10 Wm-2 s-1, nitrogen- fixing	(Masukawa et al., 2002)
Anabaena sp. PCC 7120	hupW	3.3	Ar, 10 Wm-2 s-1, nitrogen- fixing	(Lindberg, et al., 2012)
Anabaena siamensis TISTR 8012	hupS	29.7	Ar, 100 μEm-2 s-1, nitrogen- fixing	(Khetkorn et al.,2012)
Eliminating pathways competing for electrons				
Synechocystis strain M55	ndhB	12	Anaerobic and nitrogen deprivation	(Cournac et al., 2004)
Synechocystis sp. PCC 6803	ctaI/cyd	11.4	Anaerobic and nitrogen deprivation	(Gutthann et al., 2007)
Synechocystis sp. PCC 6803	ctaII/cyd	6.9	Anaerobic and nitrogen deprivation	(Gutthann et al., 2007)
Synechocystis sp. PCC 6803	narB/nirA	18	Ar, darkness and nitrogen deprivation	(Baebprasert et al., 2011)

Table 2.1. shows some genetic modifications applied on two cyanobacteria species; *Anabaena* and *Synechocystis*. In studies focusing *Anabaena*, the target gene uptake hydrogenase (hup) is disrupted, resulting less to none hydrogen consumption and in increase in production either under dark anoxic atmosphere or illumination. On the other hand, genetic engineering in *Synechocystis* is mostly studied on elimination of pathways competing for electrons with hydrogenase. Under nitrogen limiting conditions, inhibiting independently NDH-1 enzyme, respiratory terminal oxidases (such as quinol oxidase) or nitrite and nitrate reductase can yield higher activity of bidirectional hydrogenase enzyme as shown in Table 2.1.

It is worth to mention *Synechocystis* strain in more detail. Cournac and colleagues found that hydrogen production in *Synechocystis* is limited due to recycling of NADPH through the NDH-1 complex (Cournac et al., 2002). When ndhB gene is inactivated, meaning the lack of NDH-1 enzyme working for pairing carbon dioxide fixation and oxygen generation, sustained hydrogen production is observed (Cournac et al., 2002).

Under low oxygen conditions quinol oxidase, respiratory redox regulation enzyme, works as electron valve and block reduction of PSII active site. Inhibition of this enzyme effectively increase hydrogen production in *Synechocystis sp.*(Gutthann et al., 2007). Similar effect was observed with nitrate reductase enzyme, which takes part in nitrate assimilation. This bioprocess is a strong electron sink, competing with hydrogenase; therefore inhibition of this enzyme results in higher hydrogen yield (Gutthann et al., 2007). When both nitrite and nitrate reductase enzymes are inhibited, the effect is even higher than that of separate inhibition (Baebprasert et al., 2011).

Green algae and cyanobacteria grow under sunlight are able to collect solar energy for photosynthetic growth by means of pigments located in LHC. These are shaped as antenna, and actually the size of antenna is inversely correlated with solar energy conversion efficiency (Tanaka and Melis, 1997). Three mutants of *Synechocystis sp*. with different antenna size were studied for their performance on cyclic and linear electron transport, and it was found that higher linear electron transport of mutant cells grown under bright light indicates a good candidate for biohydrogen production (Rögner, 2009).

2.7.2. Medium Modifications

Various medium modification is highly preferred in hydrogen production. Essential elements in microbial growth, sulphur, nitrogen, carbon and phosphorous, are investigated greatly for various microorganisms. Similarly, effect of some trace metal elements can be incremental for hydrogen generation.

A revolutionary approach to biological hydrogen production was introduced by Melis et al. In 2000, they exposed *Chlamydomonas reinhardtii* cells to sulphur starvation after a normal growth. It was found that lack of sulphur first converts Q_B-reducing capability of PSII centers into Q_B-non-reducing form, and then loss of PSII centers from thylakoid (Melis et al., 2000). Thus, electron carriers come to hydrogenase enzyme only through PSI and carbohydrate decomposition. Meaning that sulphur deprivation causes hydrogen production similar to indirect photolysis by separating carbon accumulation and hydrogen production into two stage. Similar approach was investigated in *Synechocystis sp*. and *Gloeocapsa alpicola* by Antal and Lindblad (Antal and Lindblad, 2005). Cells grown in sulphur depleted media were then transferred to dark anoxic environment to trigger hydrogen production, optimizing the production rate by creating methane atmosphere and pH adjustment. Hydrogen production were prolonged under 100% methane atmosphere and at 5.0-5.5 pH level (Antal and Lindblad, 2005).

Non-starving nitrogen depletion growth conditions have remarkable effects on hydrogen production of *Synechocystis sp*. When cells are incubated with medium with 1mM nitrate, the production rate becomes at its highest after 40 hours, and very compatible among cyanobacteria and green algae (Schütz et al., 2004). Nitrogen starvation causes pigment loss, especially light harvesting antenna, PSI and PSII reaction centers. Also, it is proposed that this situation decelerate reoxidation of electron carriers, and down-regulate electron transfer capability (Antal et al., 2006). It is stated that hydrogenase is vital in *Synechocystis sp.* to survive under mixotrophic, nitrogen limiting environment (Gutekunst et al., 2014). Gutthann et al., also showed that higher production rates in medium when limited ammonium ion, 5 mM, is present (Gutthann et al., 2007).

Burrows et al., proposed medium optimization in photofermentative hydrogen production in *Synechocystis sp.* by manipulating ammonium, bicarbonate, sulfate and phosphate ions. By screening experiments, it was found that concentrations of 0.52 mM NH_4^+, 20.1 μM SO_4^{2-} and 46 mM HCO_3^- are the most effective compositions for hydrogen production, whereas effect of phosphorus does not

seem to be statistically significant (Burrows et al., 2008). Thereafter, new medium compositions by machine learning methods of Response Surface Methodology (RSM) and Q2 algorithm were estimated even higher production rates, including optimum pH of 7.77 or 7.88 for designated medium (Burrows et al., 2009). However, the improvement was not very high, and nitrogen compositions were designated as 0.63 mM and 0.36 mM, respectively (Burrows et al., 2009).

One of the positive sides of sulphur deprivation is the enzyme activity can be reversibly inverted by switching from depleted to non-depleted medium (Melis et al., 2000). Effect of nutrient limitations may be justified by disruptions on intracellular redox states by reregulating electron carriers (Antal et al., 2006). On the other hand, total starvation of sulphur or nitrogen may change biological pathways within the cell, where sulphur is required for protein synthesis and nitrogen is an essential part of pyridine dinucleotides (Burrows et al., 2008). Starvation may affect NADPH formation, therefore decreasing in hydrogen production.

Addition of tungstate (O_4W^{-2}) also increase both photohydrogen and fermentative hydrogen production in *Synechocystis sp.*, due to inhibition of nitrate reductase, which is a competitor enzyme for electron carriers with hydrogenase (Gutthann et al., 2007).

Another alternative approach was undertaken by Surzycki et al., coupling genetic suppression with manipulation of copper concentration in medium. The coding sequence of the nucleus-encoded Nac2 chloroplast protein was combined with copper-sensitive cytochrome c6 promoter to repress PSII activity in *Chlamydomonas reinhardtii* (Surzycki et al., 2007). When copper was reinserted in cells grown in copper-depleted medium, PSII activity level fell below respiration rate; resulting anaerobic atmosphere and induce hydrogen production (Surzycki et al., 2007).

2.7.3. Immobilization

One reasonable approach for augmentation in hydrogen production is cell immobilization. The method can be applied in four different ways; surface attachment; entrapment in porous matrices; containment behind a barrier; and self-aggregation (Azbar and Kapdan, 2012). One advantageous outcome is that it enables reuse and recycle the reactor system (Das and Veziroğlu, 2001). Different materials; activated carbon, glass beads, clay, sponge, inert stone chips, for surface absorbance can be used. Porous materials such as ceramic fittings and pine wood shavings providing high surface area for cells to attach give high hydrogen production rates; however the later can be consumed as

organic material in the absence of any other external carbon source (Ivanova et al. , 2008). One drawback of these materials is that they consume considerable volume in the reactor and they are hard to replace (Azbar and Kapdan, 2012). Hahn et al., explored binding efficiency of algae cells onto silica particles to maintain immobilization, an example for surface attachment of cells (Hahn et al., 2007). The experiment was done in two stage processes; the first is the growth of algae in sulphur rich medium and the second was in sulphur deprivation, and immobilization reveals easiness of algae collection by filtering and performs as good as free floating algae in hydrogen production (Hahn et al., 2007). As an example for entrapment material, when anoxygenic phototrophic bacterium *Rhodobacter sphaeroides* was assayed for hydrogen by using tofu wastewater, it was found that immobilization in agar gel worked as shield against inhibitory factor of ammonium ion (Zhu et al., 1999). Cells can be incubated in permeable membrane, such as alginate, agar beads or hydrogels. Dickson et al. applied silica-sol gel encapsulation for *Synechocystis sp.* cells and found similar production rates to those of non-immobilized (Dickson et al., 2009).

In containment method, cells are immobilized behind a barrier. The setup can be two-staged and continuous. As an example, completely different reactor design was undertaken; cells were immobilized in a textile-like glass sheet containing narrow glass wires, and it was tauten in between glass plates with illumination (Laurinavichene et al., 2006). The continuous reactor design with this immobilization technique prolonged phototrophic hydrogen production while maintaining similar rates to those of suspension cultures (Laurinavichene et al., 2006).

Lastly, self-aggregation method proposes cell to cell attachment induced either natural or artificially by cross linking agents (Azbar and Kapdan, 2012). When floc of cells is formed and separated from the bulk liquid medium by fast sedimentation or course screen, immobilization has been done. Therefore, effective size or density of cells are increased by aggregation. Even though long duration for floc formation, this method can be chosen for cost reduction, no requirement for spare particles and applicability in larger scale (Azbar and Kapdan, 2012). Self-aggregation for hydrogen production assays is not very abundant, however when it is preferred, the biological metabolism is dark fermentation application using mixed seed culture.

2.7.4. Use of Reducing Agents

Using oxygen reductants may have significant effect on hydrogenase activity for *Synechocystis sp*. Thiol compounds are very reactive and can be used as reducing agent in medium. Baebpresert et

al. showed that 750 μM β-mercaptoethanol is an efficient reductant for augmentation of hydrogen production with an activity rate of 14.32 μmol H_2 mg chl $a^{-1}min^{-1}$, only when it is used in nitrogen and sulphur deprived BG-11 medium (Baebprasert et al., 2010). Another thiol compound 1,4 dithiothreitol (DTT) and β-mercaptoethanol with concentrations of 100 μM in original BG-11 medium provides only small increment in enzyme activity (Baebprasert et al., 2010)

Dutta and Vermaas found that sodium dithionite and external reduced Fd also has small effect on hydrogen production. Hydrogenase deletion strain and wild-type *Synechocystis sp.* show similar hydrogen production trend in cell extracts, however it is argued that either [FeS] clusters in broken cells catalyzed H^+ ions with reduced Fd and dithionite, or measurement device gave false positive record (Dutta and Vermaas, 2016). It is known that dithionite does not induce hydrogen production in whole cells. Therefore, in this study where it was desired to observe activity *in vivo,* cells were not extracted.

Another thiol solution is thioglycolic acid, which can be obtained from sodium thioglycolate salt. It is frequently used in Brewer's medium along with cysteine to maintain anaerobic conditions in the liquid which is exposed to air (Brewer, 1940). Sodium thioglycolate can lower the redox potential of the medium by removing oxygen. Note that when medium is prepared, a red color indicating sulphydryl (thiol) group appears (Cook and Steel, 1959). The absence of color signifies complete reduction of thioglycolate. Main oxidation products of thioglycolic acid is dithiodiglycolitic acid, which is a disulfide (Cook and Steel, 1959). In this research, reducing effect of sodium thioglycolate is investigated.

2.8. Photoautotrophic Species

Depending on hydrogen production mechanism and enzyme in action, good variety of algae and cyanobacteria are under investigation. Microalgae having [FeFe]-hydrogenase, such as *Chlamydomonas reinhardtii, Chlorella fusca, Scenedesmus obliquus, Chlorococcum littorale* and *Platymonas subcordiformis*; heterocyst cell containing nitrogen-fixing filamentous cyanobacteria genuses such as *Nostoc*, *Anabaena*, *Calothrix* and *Oscillatoria*; non nitrogen-fixing genus such as *Synechocystis, Synechococcus* and *Gloebacter*; photofermentative purple non-sulphur bacteria *Rhodospirillum rubrum, Rhodopseudomonas palustris, Rhodobacter sphaeroides* and *Rhodobacter capsulatus* have been explored for their hydrogen production capacities (Eroğlu and Melis, 2011). Among them, cyanobacteria are oldest photosynthetic organisms which are able to convert carbon

dioxide into biomass by the help of sunlight from evolutionary point of view (Knoop et al., 2010). It is worth to choose cyanobacteria for hydrogen production due to their fast growth rate, vigor against contamination and relatively simple biochemical mechanism. *Synechocystis sp.* is one of the extensively studied cyanobacteria, metabolic, biochemical and physiochemical pathways are deeply investigated (Knoop et al., 2010), and its genome was fully sequenced (Kaneko et al., 1996). It has been investigated for several metabolite production; such as isoprene, poly-beta-hydroxybutyrate, alcohols, biohydrogen and several other biofuels (Montagud et al., 2015). Focusing on hydrogen, it is also important that this non nitrogen-fixing cyanobacterium has probably no encoded uptake hydrogenase enzyme, the only enzyme responsible both for hydrogen production and consumption is bidirectional [NiFe]-hydrogenase enzyme (Cournac et al., 2002). This makes the biochemistry relatively less complicated. Also, [NiFe]-hydrogenase is more resistant than [FeFe]-hydrogenase to oxygen gas (Frey, 2002).

For this research, cyanobacteria species *Synechocystis* sp. strain ATCC 27184 (also designated as strain PCC 6803 [N-1]) is selected. Main focus of this research is to generate biological hydrogen by means of photolytic biomechanism utilizing water and light energy. *Synechocystis sp*. is a model organism for biological hydrogen production, consequently some of [NiFe]-hydrogenase related interpretation can be made based on previous studies. It was found that its bidirectional [NiFe]-hydrogenase enzyme actively works as an electron valve in photosynthesis (Appel et al., 2000). In another words, hydrogenase in *Synechocystis sp.* works completely bidirectional in the cell highly depending on redox potentials (Gutthann et al., 2007). It is known that highest enzymatic activity is observed at high photosynthetic activity and low respiration rates, plus under oxygen presence the enzyme becomes totally inactive (Germer et al., 2009). In *Synechocystis sp.*, NADPH, the common cofactor taking place in both photosynthesis and autotrophic carbon fixation, is the substrate for hydrogen production of bidirectional hydrogenase, meaning that both metabolic activities affect hydrogen generation (Cournac et al., 2002). Hydrogenase is in competition with cyclic electron transport and respiration for reducing equivalents, plus it was estimated that the competition is against other carbon sinks; protons, oxygen, nitrate and Calvin cycle (Gutthann et al., 2007). There are different views in which electron donor is primarily responsible for photohydrogen production in *Synechocystis sp.*. It was previously stated that electron comes from NADPH only, assuming that hydrogen production is NADPH dependent in the cyanobacterium (Tamagnini et al., 2002). However, more recent research revealed that even though NADPH takes in part in minor production, in fact, [NiFe]-hydrogenase in *Synechocystis sp.* uses reduced Fd and flavodoxin as the principal electron donor in hydrogen production (Gutekunst et al., 2014). The latter was introduced relatively new,

challenging extensive research on the hypothesis that NADPH is the leading electron carrier. Figure 2.5. Exact electron transfer pathway in hydrogen production in *Synechocystis sp*. H_2ase: hydrogenase; PSI: photosystem I; PSII: photosystem II; cyt: cytochrome; SDH: succinatedehydrogenase; NDH1 Complex I-like NAD(P)H dehydrogenase; NDH2: type II NAD(P)H dehydrogenase; PQ: plastoquinone; PC: plastocyanin; FNR: Ferredoxin-$NADP^+$ reductase; Fd: ferredoxin; ATPase: ATP synthase. Photolysis takes places in thylakoid membrane. bold arrows indicates electron transfer, and dotted arrows that of proton (adopted from Cournac et al., 2002) shows proposed hydrogen production bioprocess in *Synechocystis sp.*

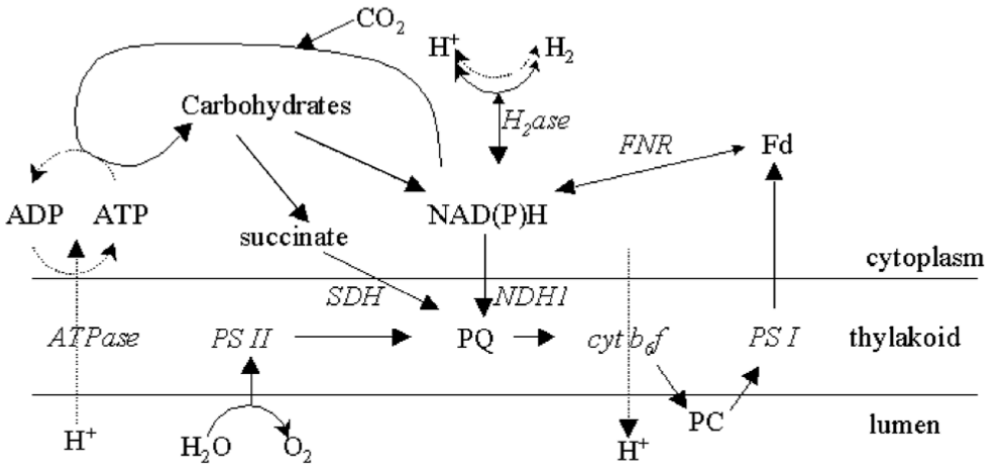

Figure 2.5. Exact electron transfer pathway in hydrogen production in *Synechocystis sp*. H_2ase: hydrogenase; PSI: photosystem I; PSII: photosystem II; cyt: cytochrome; SDH: succinatedehydrogenase; NDH1 Complex I-like NAD(P)H dehydrogenase; NDH2: type II NAD(P)H dehydrogenase; PQ: plastoquinone; PC: plastocyanin; FNR: Ferredoxin-$NADP^+$ reductase; Fd: ferredoxin; ATPase: ATP synthase. Photolysis takes places in thylakoid membrane. bold arrows indicates electron transfer, and dotted arrows that of proton (adopted from Cournac et al., 2002).

In cyanobacteria, while photosynthetic electron transport mechanism occurs in thylakoid membrane, respiratory transport chain happens both in cytoplasm and thylakoid membrane (Schmetterer, 1994). It is suggested that due to organism's parallel activity of hydrogen uptake and photosynthetic electron transport, bidirectional hydrogenase might be attached to thylakoid membrane in *Synechocystis sp.* (Appel et al., 2000). But it is more likely that the enzyme is located in cytoplasm and catalysis hydrogen production from electron donor with electrons in cytoplasm (Cournac et al., 2002). In terms of hydrogen gas generation, its potential is competitively higher than that of some other microorganisms regarding hydrogenase activity measurements when an artificial electron donor methyl viologen (MV) is present (Schütz et al., 2004).

2.9. Use of Methyl Viologen in Biohydrogen Analysis

Methyl viologen (MV) is a highly soluble compound with a low normal potential of -0.446 V and of which the solution gives a blue-purple color when reduced (Michaelis and Hill, 1933). Single reduced form is a widely used electron donor in bidirectional hydrogenase enzyme activity measurement (Tamagnini et al., 2002). It accepts electrons from PSI, preventing it to direct towards NADPH, and lead through PSII (Trebst, 1972). At this state, it is very sensitive to oxygen presence and oxidized back very fast (Farrington et al., 1973).

There are some effective utilization in photosynthetic metabolism activity; when MV reduced by sodium dithionite is used for activity measurement, the specific activity of the enzyme is 31.25 times higher than that of NADH plus sodium dithionite in extracts from cyanobacteria *Anacystis nidulans* (Schmitz et al., 1995). Another comparison was made by Schütz et al., comparing bidirectional hydrogenase activity of *Lyngbya majuscula* CCAP 1446/4, *Anabaena variabilis* ATCC 29413, *Anabaena sp.* PCC 7120 and *Synechocystis sp*. PCC 6803 with reduced MV, obtaining highest activity in *Synechocystis sp*. PCC 6803 under nitrogen depletion and continuous light, with a rate of 235.5 μmol H_2 mg Chl a^{-1} h^{-1} (Schütz et al., 2004).

2.10. Chlorophyll a Measurements

Total hydrogen production rate must be given with respect to a criterion. There are various options to determine hydrogen production from algae and cyanobacteria. It is possible to indicate the rate values as total hydrogen production over time (Laurinavichene et al., 2006). Some studies prefer dry biomass weight (Ananyev et al., 2012) or total protein content (Schmitz et al., 2002). When total protein is preferred, Lowry method itself or its modifications can be used for protein determination (Peterson, 1977). In other studies, hydrogen concentration over time was preferred (Dickson et al., 2009; Cournac et al., 2002; Burrows et al., 2008). Rarely, hydrogen production rate was given with respect to total culture medium volume (Zhu et al., 1999; Hahn et al., 2007). Even though this type of reporting is practically less time consuming, it is less precise and may vary with parameters such as growth phase of the studied microorganism. Nevertheless, the most commonly utilized hydrogen production rate is given with respect to photosynthetic organism's chlorophyll content (Burrows et al., 2009; Schütz et al., 2004; Touloupakis et al., 2016; Jokel et al., 2019) . Most of the time, the measurement method depends on hydrogen production mechanism. Photoautotrophic hydrogen production is highly related with PS and chlorophyll content. Determining hydrogen production

regarding chlorophyll is more accurate and unbinds possibility for comparison between hydrogen producing species, e.g. shown by Schütz et al. (Schütz et al., 2004).

Chlorophyll pigment is a complex molecule where the light energy is harvested and used for electron exchange mechanisms during PS in photosynthetic organisms (Tanaka and Tanaka, 2006). Apart from few species, most cyanobacteria contain only chlorophyll a pigment (Ritchie, 2006). Hydrogenase is active in photosynthetic electron transport chain, where water molecule is split under solar energy in chlorophyll a found in PSI and PSII (Tamagnini et al., 2002). This happens for direct biophotolysis. Therefore, determining total chlorophyll a amount to give hydrogen production rate becomes meaningful.

Chlorophyll can be determined either by High-Performance Liquid Chromatography (HPLC), fluorimetry or spectrophotometry. Spectrophotometric method is the most commonly used analytical method due to its ease of application and low capital cost for instrumentation (Steinman et al., 2017). No significant systematic differences were observed between HPLC and other methods, however phaeophytin estimations may be unpredictable if HPLC is not used (Murray et al., 1986).

2.10.1. Spectrophotometric Chlorophyll a Determination

Spectrophotometric method relies on light absorbance of the pigment. Chlorophyll a is a green molecule, meaning that it transmits green light, that absorbs red and blue light at around 430 nm and 680 nm (Madigan et al., 2015). To be able to determine absorbance level of the pigment, extraction process is a must. In general, chlorophyll a extraction method includes collection of cells from medium and their disruption, extraction with a solvent and spectrophotometric absorbance measurement. Absorbance is then converted into chlorophyll concentration by series of empirical equations.

The main interference on chlorophyll a determination is degraded products. In acidic environment, chlorophyll a pigment loses its central Mg^{2+} ion and degraded into pheophytin a and pheophorbide a (Steinman et al., 2017). In natural water samples, degradation may add up to significant percentages of total pigments, therefore an acidification step may be added before and after absorbance measurements for correction of pheophytin a presence (Steinman et al., 2017).

First, liquid sample is filtered or centrifuged to obtain cyanobacteria or green algae pellet. In each case, samples can be stored at -20°C until analysis, however if the wet pellet is obtained, it should be freeze dried under nitrogen atmosphere (Ritchie, 2006). Filter paper should be stored at the freezer under dark conditions after drying (Steinman et al., 2017). Some studies propose that mechanical cell disruption methods of homogenization and sonication are not necessary to improve extraction efficiency of solvent (Sartory and Grobbelaar, 1984). Another technique, freezing with liquid nitrogen and thawing, was an effective cell wall disruption tool shown by Henriques et al. when methanol is used (Henriques et al., 2007).

After filtration, cell samples should be extracted. Extraction efficiency is highly dependent on the solvent choice. Organic solvents can easily extract fat-soluble pigment molecules from cell material (Lichthentaler, 1987). On the UV-visible light absorbance spectrum, the wavelength of highest peaks indicates chlorophyll pigment absorbance, thus these absorbance values are used in empirical equations to determine chlorophyll concentration in the sample (Lichthentaler, 1987). For spectrophotometric calculations, generally two dichroic equations are generated for chlorophyll a and b estimation based on absorbance values, and each solvent has its own coefficients for red and blue peaks (Ritchie, 2006). However, in the case of cyanobacteria, which possess only chlorophyll a, the empirical equation is generally based on one absorbance value (Ritchie, 2006). Some of the common organic solvents used for extraction are acetone, methanol, ethanol, dimethyl ether, dimethyl sulfoxide (DMSO) or N,N'-dimethylformamide (DMF) (Mackinney, 1941; Porra, 2002). The last two are more toxic and therefore, not frequently used (Porra, 2002). Traditionally, aqueous acetone was a common choice for extraction of chlorophyll pigments. However, it is very volatile and flammable. Plus depending on species, methanol performs better than dimethyl ether and acetone (Dere et al., 1998). It should be taken into consideration that methanol is toxic as well and should be handled with care. Extraction time is another parameter that affects performance. Solvent contact duration should be longer than 2 hours and not exceed 24 hours to ensure total extraction (Arar, 1997). However, it is also argued that there is no need 24 hours of extraction, since as the time elongates, the possibility of breaking down into pheophytin pigments increases (Ritchie, 2006). Crude cell should be in contact with the solvent at 4°C in dark (Arar, 1997). Finally, absorbance values can be read instead of empirically determined wavelength, it is possible to correct those values with absorbance maxima observed in spectrum for species studied (Dere et al., 1998). To prevent any interference, plastic spectrophotometer cuvettes, especially polystyrene and polymethylacrylates, are not eligible for measurements, since it can interfere analyses with organic solvents (Ritchie, 2006). Quartz cuvettes are safer to work with.

3. MATERIALS AND METHODS

3.1. Culture Maintenance

Synechocystis sp. strain ATCC 27184 (also designated as strain PCC 6803 [N-1]) is a unicellular non-nitrogen fixing freshwater cyanobacterium used as model organism throughout the study. Axenic cultures were maintained in Blue Green Medium (referred as BG-11) both on agar and liquid medium (Rippka et al., 1979). Composition for BG-11 medium is given on 3.1. and 3.2. Culture has been maintained on plates and in tissue cell culture flasks in a growth chamber (GC 401, Nüve, Ankara, Turkey) at 25 °C under 1200 lux light density with light:dark cycle of 14h:10h and has been sub-cultured biweekly.

Table 3.1. Composition of BG-11 medium (adopted from Rippka et al., 1979).

	Component	**Amount**	**Stock Solution Concentration**	**Final Concentration**
1	$NaNO_3$	30 mL/L	10 g/400mL dH2O	8.82 mM
2	$CaCl_2 \cdot 2H_2O$	10 mL/L	1 g/400mL dH2O	0.17 mM
3	$MgSO_4 \cdot 7H_2O$	10 mL/L	3 g/400mL dH2O	0.3 mM
4	K_2HPO_4	10 mL/L	3 g/400mL dH2O	0.43 mM
5	Citric Acid$\cdot H_2O$	10 mL/L	0.12 g/200 mL dH2O	0.031 mM
6	Ferric Ammonium Citrate	10 mL/L	0.12 g/200 mL dH2O	0.021 mM
7	$Na_2EDTA \cdot 2H_2O$	6 mL/L	0.02 g/200 mL dH2O	0.0027 mM
8	Na_2CO_3	40 mL/L	0.4 g/200 mL dH2O	0.19 mM
9	BG-11 Trace Metals Solution*	1 mL/L		

**Composition given in Table 3.2.*

Table 3.2. Composition of BG-11 trace metals solution (adopted from Rippka et al., 1979).

	Component	**Amount**	**Final Concentration**
1	H_3BO_3	2.86 g/L	46 mM
2	$MnCl_2.4H_2O$	1.81 g/L	9 mM
3	$ZnSO_4.7H_2O$	0.22 g/L	0.77 mM
4	$Na_2MoO_4.2H_2O$	0.39 g/L	1.6 mM
5	$CuSO_4.5H_2O$	0.079 g/L	0.3 mM
6	$Co(NO_3)_2.6H_2O$	49.4 mg/L	0.17 mM

3.2. Culture Maintenance and Seed Preparation

Once culture plates were on the 5th to 8th days, they were inoculated in 1L glass Erlenmeyer flasks (with a working volume of 400 mL) and operated as a batch type reactor. The opening of the reactor was covered with a rubber stopper having three 0.22 µm pore size filters, one of which is for air inlet and two for air exhaust. Reactors were continuously mixed with a magnetic stirrer and aerated with 0.5L/min compressed air through a diffusor stone. The light intensity was kept at 8000 lux (approx. 110 µmol $m^{-2}s^{-1}$) with dark and light cycles of 12h/12h. Cultures were kept at a temperature of 25 °C and pH level 7.5-8.0. Figure 3.1. shows the sketch of reactor design.

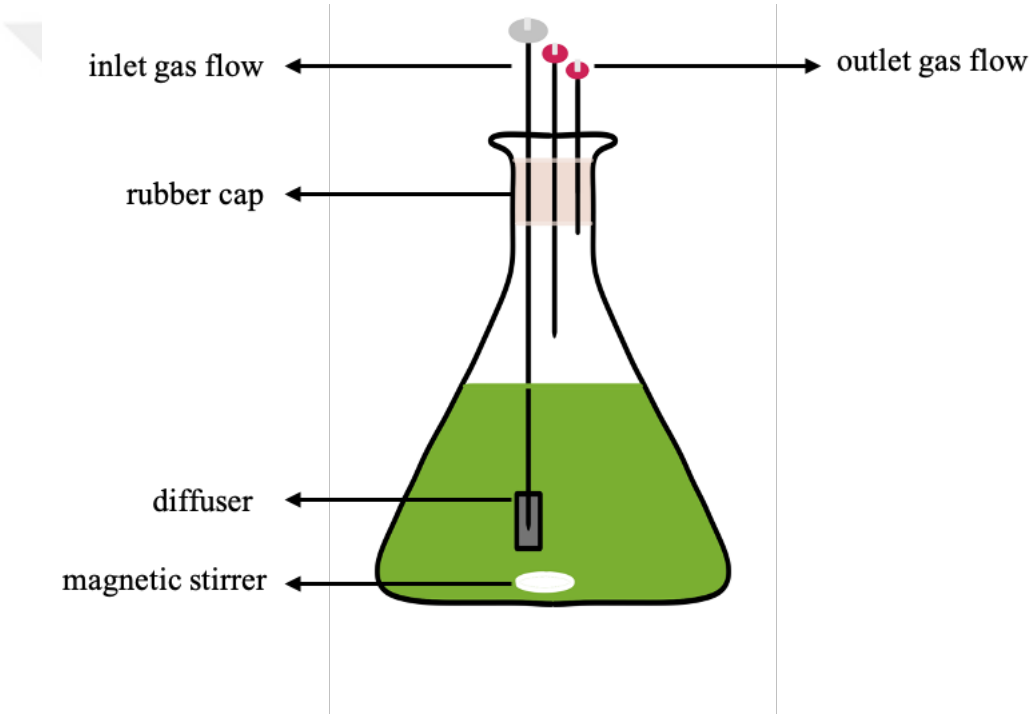

Figure 3.1. Reactor for seed growth.

In order to determine the growth curve of *Synechocystis* sp., optical density (OD) measurements were taken daily and number of cells were measured every other day. pH levels were also monitored daily with a pH probe (Handylab 680FX, SI Analytics, Weilheim, Germany). OD values were measured at 730 nm wavelength using spectrophotometer (DR 3900, Hach Lange, Manchester, United Kingdom) and number of cells were counted by the help of hemocytometer under a light microscope (Boeco, Hamburg, Germany).

3.3. Experimental Reactor Setup

Once the cultures reached late-exponential phase, they were harvested using a centrifuge (Model U-320R, Boeco, Hamburg, Germany). The cultures were centrifuged at 4500 rounds per minute (rpm) at 25 °C for five minutes, and pellets were washed once with designated medium before resuspending in 50 mL medium. The cell concentration in the inoculation seed was then determined under light microscope with hemocytometer. Figure 3.2. shows *Synechocystis sp.* cells under light microscope under 40x objective (400x magnification in total). The seed cultures were then inoculated into 115 mL serum bottles with a working volume of 100 mL at a starting cell concentration of 1×10^8 cells/mL. All batches were continuously mixed with magnetic stirrer at 450 rpm and illuminated with white LED lamps at 8000 lux (approx. 110 µmol $m^{-2}s^{-1}$). Bottles were flushed with argon just after the preparation to washout oxygen and black rubber septa were used to close the bottles. The setup was kept 5 or 6 days depending on resilience in different media. All glassware and rubber septa were autoclaved for sterilization prior to utilization.

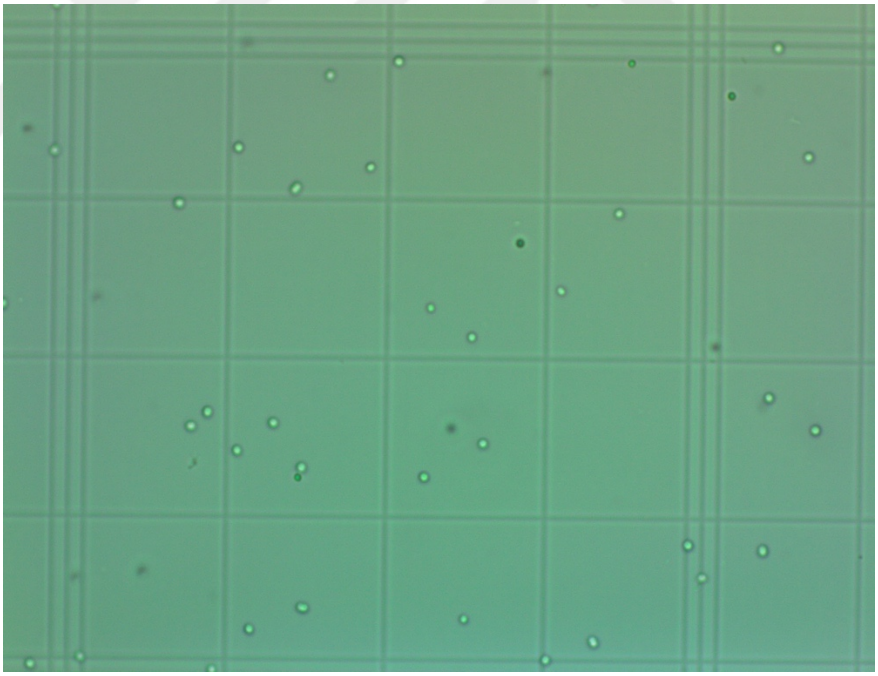

Figure 3.2. *Synechocystis sp.* cells under light microscope.

3.4. Experimental Conditions

Four different medium compositions were assayed to investigate their effects on hydrogen production in *Synechocystis sp.* First, BG-11 medium as specified in Table 3.1. and Table 3.2. prepared as baseline condition. Then, the medium was modified with nitrogen and sulfur depletion,

separately. For nitrogen depletion (BG-11(-N)), same components without $NaNO_3$ were used. Sulfur depletion (BG-11(-S)) was prepared by replacing $MgSO_4.7H_2O$ with proper amount of $MgCl_2.6H_2O$ without changing 0.3 mM Mg^{+2} composition in the medium. Similarly, $ZnSO_4.7H_2O$ was replaced with $ZnCl_2$ for sulfur depletion in BG-11 trace metal solution. For the last experimental setup, 5 g/L sodium thioglycolate was mixed with BG-11 medium and named as BG-11° for disambiguation. pH level of BG-11° was adjusted to 7.4 with 0.02M HEPES buffer for slow oxidation of thioglycolic acid. All media were autoclaved at 121 °C for 15 minutes before utilization. Temperature varied between 25-27 °C. Experiments were completed with three biological replicates. Conditions of the experimental setup is given in Table 3.3.

Table 3.3. Experimental conditions.

	i	ii	iii	iv
Initial Headspace Gas	Argon	Argon	Argon	Argon
Temperature (°C)	25-27	25-27	25-27	25-27
Light	8000 lux	8000 lux	8000 lux	8000 lux
Medium	BG-11	BG-11(-N)	BG-11(-S)	BG-11°

Figure 3.3. shows the experimental setup of the bioreactors. During dark phase all illumination was cut off, including dim daylight. Temperature was continuously checked with thermometer and positions of reactors were arranged that each has got same irradiance during light phase.

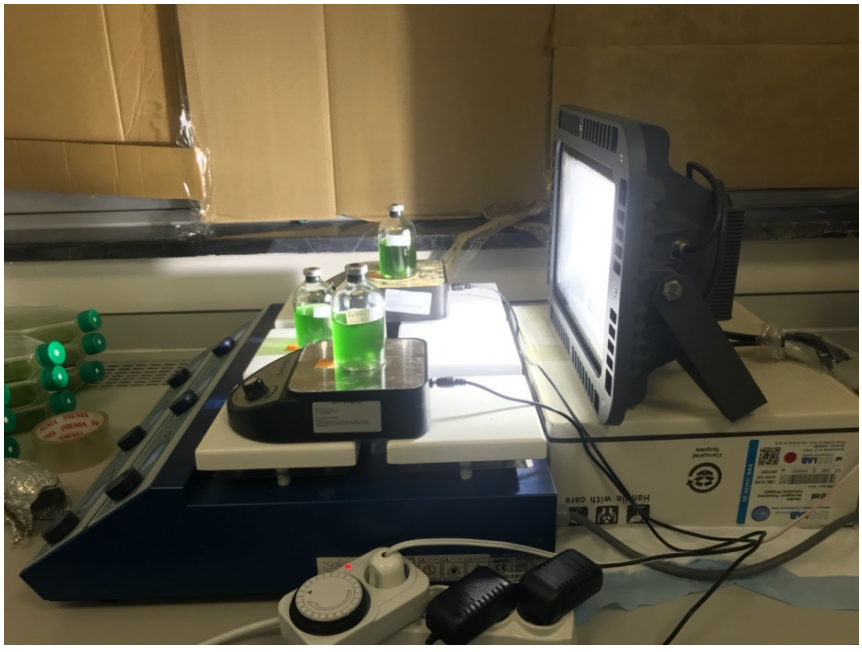

Figure 3.3. Experimental setup.

3.5. Measurements

For hydrogen gas analysis three different sampling methods were performed. Hydrogen accumulation was measured by sampling the headspace and analyzing gas composition of the serum bottle reactor. Activation of dark hydrogen production was analyzed via small vial sampling. Hydrogenase activities were measured using MV. Each method is further explained below. For hydrogen analyses, 6 mL samples were taken daily.

3.5.1. Headspace Sampling

Once the reactors were prepared, two different time dependent headspace gas analyses were done; during light and dark phase. First, headspace gas pressure was measured with a pressure transducer (Traceable, VWR, U.S.) for accurate calculation of hydrogen gas amount. Then 100 mL gas sample was taken using a 1mL syringe. Sample composition was analyzed with gas chromatography.

3.5.2. Small Vial Sampling

Each day, 1 mL of culture sample was taken with sterile syringe. It is inoculated into a sterile amber GC vial with total volume of 2 mL. It is then flushed with Argon and put on orbital shaker upside down for a day. First gas analysis was done after 1 h of sampling, and the second was after 24 h. Headspace gas pressure in vial was measured. Total gas composition was then determined.

3.5.3. Sampling for Hydrogenase Activity

In vivo hydrogenase activity was determined using the method derived from Antal and Lindblad (Antal and Lindblad, 2005). Briefly, cell pellet was resuspended in the reaction mixture containing MV and sodium dithionite in phosphate buffer. Evolved hydrogen gas was determined from GC analysis.

Reagents were prepared as follows: 40 mM sodium dithionite and 4 mM reduced MV solutions were separately prepared fresh in 50 mM potassium phosphate buffer at pH 7.0 each time prior to analysis. First, potassium phosphate buffer is prepared. Ultrapure water was boiled for 10 minutes for oxygen removal in water bath and then cooled. For 500 mL 50 mM pH 7.0 phosphate buffer,

2.336 g K_2HPO_4 and 1.577 g KH_2PO_4 were added. pH level was checked with pH meter. MV is found in chlorinated form as methyl viologen dichloride hydrate. The reduced form was prepared by modifying Tris with potassium phosphate buffer in the method from Trudiatger (Trudiatger, 1970). Accordingly, MV and sodium dithionite solutions were prepared in anoxic environment to prevent reoxidation of reduced molecules. Before starting, two 42-mL amber vials with septum cap were flushed with argon for 15 minutes to remove oxygen. 10 mL buffer was added via syringe to minimize oxygen contact. 40 mM sodium dithionite solution was prepared by adding 1.74 g %85 pure sodium dithionite into 50 mM pH 7.0 potassium phosphate buffer. The vial was then flushed with argon one more time for 15 minutes to remove any oxygen interferences. For 4 mM MV solution, 0.124 g 98% pure methyl viologen dichloride hydrate was added in 10 mL potassium phosphate buffer. 20-30 µL of 40 mM sodium dithionite solution was added for further removal of any remaining oxygen. Similar to sodium dithionite solution, the vial was flushed with argon for 15 minutes one more time.

Blank amber vials were flushed with argon for 15 minutes to obtain anaerobic environment. First, 5 mL sample was taken from serum bottle reactor. It was centrifuged at 4500 rpm for 5 minutes at 25 °C, washed with buffer solution once, and pellet was resuspended in 3 mL 40 mM sodium dithionite solution in 50 mM K-phosphate buffer. The suspension was injected into amber vial via syringe. Then 3 mL 4 mM MV solution in 50 mM potassium phosphate buffer was added similarly. Final concentration of reaction mixture was 2 mM MV and 20 mM sodium dithionite in 50 mM pH 7.0 K-phosphate buffer and the volume was 6 mL. After 24 hours in 42 mL amber vials at room temperature on orbital shaker, headspace pressure was measured and gas samples taken from the headspace of the vial were analyzed in gas chromatography (Antal and Lindblad, 2005).

Sampling from serum bottle causes vacuum. To prevent any interference in following sampling processes, argon gas was injected to balance reactor pressure. Sampling was done during light phase.

After total chlorophyll a determination, total *in vivo* hydrogenase activity is given in terms of µmoles of hydrogen per hour per gram chlorophyll a.

3.5.4. Gas Analysis Method

Gas analyses were conducted by using gas chromatography (GC2014, Shimadzu, Japan) equipped with thermal conductivity detector (TCD). 100 µL gas samples were analyzed by manually injecting 100 µL gas sample via gas tight syringe into capillary column (Carboxen 1010, Supelco) in

splitless mode. Chromatography column was 30 m in length and 0.53 mm in inner diameter. For run method, the oven was kept at 35 °C, detector was at 230 °C and SPL unit at 200 °C. Argon was used as the carrier gas with a column flow of 3.0 mL/min. The method was run for 6 minutes, which is sufficient for hydrogen, oxygen and nitrogen peaks. Oxygen and nitrogen peaks were not clearly separated via this method.

Calibrations with respect to area under the chromatogram curve were done for each gas by injecting 99.99 % hydrogen, 99.99% oxygen and 99.99% nitrogen gases in volumes of 2, 5, 10, 20 and 40 μL. Mole equivalent to each volume was calculated by using ideal gas law and the calibration curves in amount of gas vs. area were obtained. Sample compositions were determined accordingly. It was assumed that pressure in syringe was 1 atm and temperature was 298 K. Mole of gas in injection volume was determined by equation 3.1;

$$n=\frac{PV}{RT} \tag{3.1}$$

where;
P: pressure (bar)
V: Volume of injection (L)
R: Gas constant (0.08314 Lbar/Kmol)
T: Temperature (K)
n: amount of gas (mol)

Therefore, calibration curve in area vs. amount of gas was obtained. For sample analysis, initially amount of gas in the syringe should be determined from equation 3.2. It was assumed that pressure in the syringe is 1 atm.

$$n_1=a\times A+b \tag{3.2}$$

where;
n_1: amount of gas in syringe (mole)
A: gas peak area
a: slope of calibration curve
b: calibration curve constant

Figure 3.4. shows moles vs area calibration curve for hydrogen. Data are shown in Appendix B1. The R^2 of the curve is 0.98, and the equation for calibration is;

$$n_{Hydrogen}=(3.45319\times10^{-5}\times Area)+3.08587\times10^{-2} \quad (3.3)$$

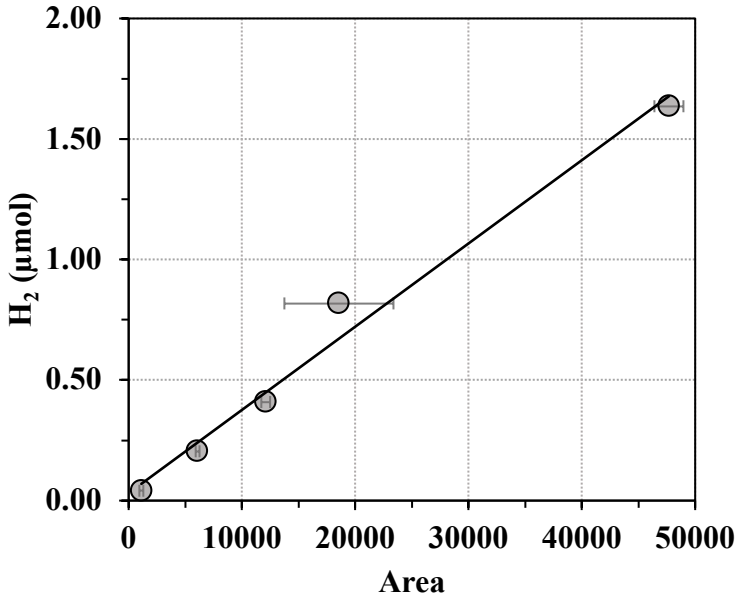

Figure 3.4. Hydrogen calibration curve.

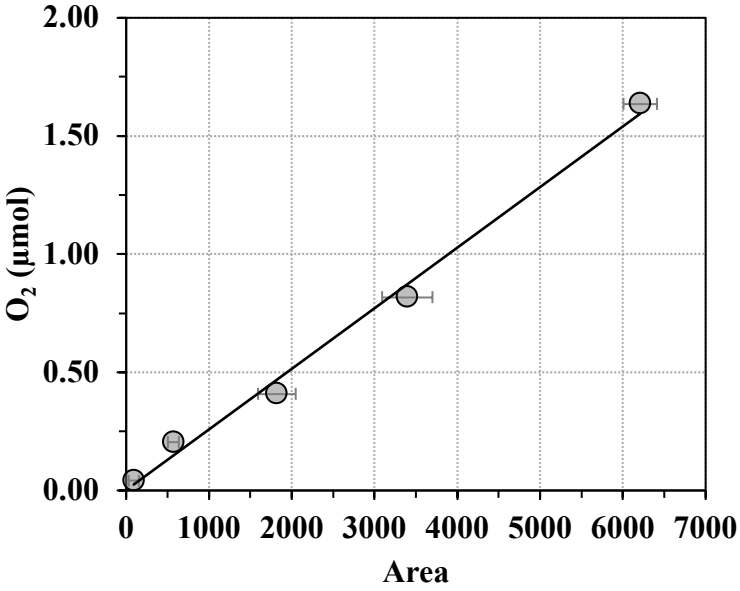

Figure 3.5. Oxygen calibration curve.

In same manner, calibration curve for oxygen was obtained by using data in Appendix B2 and shown in Figure 3.5. R^2 is 0.99 and the equation is;

$$n_{Oxygen}=(2.56413\times10^{-4}\times Area)+1.78084\times10^{-3} \quad (3.4)$$

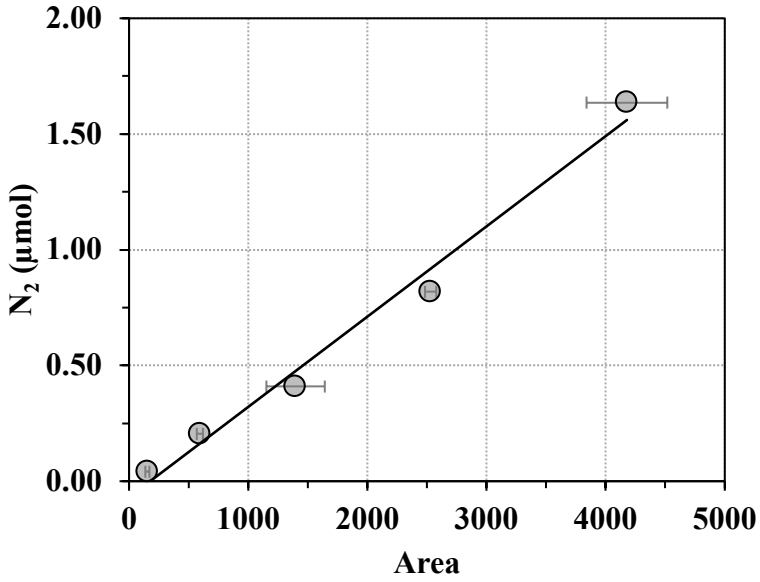

Figure 3.6. Nitrogen calibration curve.

Lastly, the calibration curve for nitrogen is shown in Figure 3.6. Data from Appendix B3 were used to plot the graph. R^2 is 0.98 and the equation is;

$$n_{Nitrogen}=(3.89998\times10^{-4}\times Area)-6.91064\times10^{-2} \quad (3.5)$$

As vial pressure is higher than atmospheric pressure, amount of gas is proportionally higher than that of the syringe. Total amount of gas in moles in vials was calculated from equation 3.6;

$$n_{vial}=\frac{n_1\times P_{vial}\times V_{vial}}{P_{syringe}\times V_{syringe}} \quad (3.6)$$

where,

P_{vial}: Pressure of amber vial (bar)

V_{vial}: Volume of gas in amber vial (L)

$P_{syringe}$: Pressure in syringe (bar)

$V_{syringe}$: Volume of injection (L)

n_{vial}: amount of gas in amber vial (mol)

Pressure in syringe was assumed to be 1.01325 bar. $V_{syringe}$ was always 100 µL and headspace volume of amber vial was always equivalent to 36 mL, which was V_{vial}.

3.5.5. Dissolved Oxygen Measurement

Dissolved oxygen (DO) in liquid medium of BG-11° is measured with DO probe (FDO 1100 IDS, SI Analytics, Weilheim, Germany). For this measurement, a separate serum bottle reactor was cultivated in same conditions. Each day, simultaneously with gas sampling, 10 mL sample was taken into a 50 mL falcon tube. Probe was put in the sample until DO value became stable. Probe was previously calibrated with humid sponge. The unit is mg/L.

3.6. Chlorophyll a Analysis

When the rate of hydrogen production is given with respect to pigment content, it is essential to determine total chlorophyll content. The cyanobacterium *Synechocystis sp.* possesses only chlorophyll a, therefore it is used as reference pigment content for hydrogen production. The process includes sample preparation, chlorophyll extraction, spectrophotometric absorbance measurement and empirical quantification. First, sample was prepared as follows. 5 mL sample was collected and centrifuged for 5 minutes at 4500 rpm. The wet pellet was washed one time with potassium phosphate buffer (pH 7.0) and then stored in refrigerator at -20 °C for a week. During preliminary experiments for extraction ability of solvents, it was found that technical methanol is slightly more effective than HPLC grade 90% acetone, and significantly better extractant than technical ethanol. Thus, methanol was chosen for chlorophyll extraction in *Synechocystis sp.*

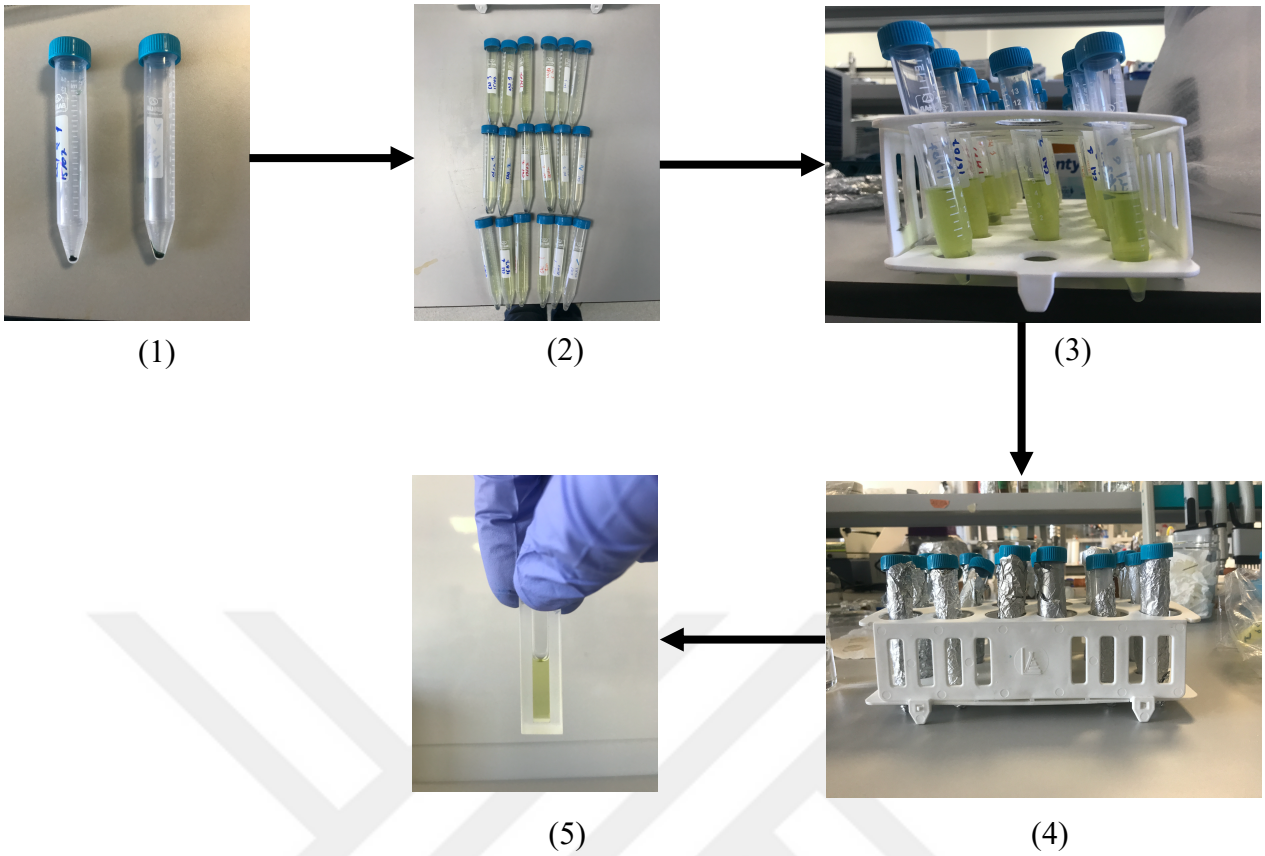

Figure 3.7. Chlorophyll a extraction steps. Samples were taken from the reactor and centrifuged. They were stored at -20°C until the day of extraction (1). Samples were resuspended in methanol and stored at 4 °C in dark for two hours (2)(3)(4). 1 mL were taken in quartz cuvette and absorbance were measured (5).

For extraction steps, pellets were suspended in pure methanol for two hours in dark at 4 °C. 5 mL solvent was added into 15 mL falcon tube containing the pellet and the tube was covered with aluminum foil. It was previously found that cell disruption methods homogenization and sonication were not significantly effective on extraction with alcoholic solvents (Sartory and Grobbelaar, 1984). Therefore, pellets were only suspended in the solvent without any disruption. After the extraction step, extracts were centrifuged at 4 °C 4500 rpm for 5 minutes to remove cell materials. 1 mL supernatant, free from turbidity, was taken for spectrophotometric analysis. All absorbance measurements were taken against blank methanol sample. Absorbance value at 750 nm was checked to ensure whether the sample is turbid or not. If the absorbance value is equal or greater than 0.005, it indicates that the sample is turbid, and should be clarified further by repeated centrifugation. Then, an empirical estimation is needed for chlorophyll determination. Extraction steps can be followed explicitly on Figure 3.7. Chlorophyll a concentration was found by equation 3.7 derived from Ritchie (Ritchie, 2006).

$$C_{\text{chlorophyll a}} = \frac{\left(12.9447(A_{665}\text{-}A_{750})\right)V_{\text{solvent}}}{lV} \tag{3.7}$$

where;

$C_{\text{chlorophyll a}}$ = concentration of chlorophyll in the sample ($\mu g_{\text{chlorophyll a}}$ per mL_{medium})
A_{665} = Absorbance Value at 665 nm against blank sample
A_{750} = Absorbance Value at 750 nm against blank sample
V_{solvent} = volume of solvent used (mL)
l = spectrophotometric cell length (cm)
V = sample volume (mL)

Then, total chlorophyll a content in 5 mL sample was determined by:

$$M_{\text{chlorophyll a}} = C_{\text{chlorophyll a}} \times 5 \text{ mL} \tag{3.8}$$

where;

$M_{\text{chlorophyll a}}$ = Total mass of chlorophyll a in 5 mL sample ($\mu g_{\text{chlorophyll a}}$)

Total hydrogen production rate was determined by;

$$v_{\text{hydrogen}} = \frac{n_{\text{hydrogen}}}{M_{\text{chlorophyll a}} \times h} \tag{3.9}$$

where;

v_{hydrogen} = hydrogen gas production rate (µmol per gram-chlorophyll a hour)
n_{hydrogen} = mol of hydrogen gas in vial (µmol)
h = reaction time (hour)

4. RESULTS AND DISCUSSION

This chapter focuses growth parameters of *Synechocystis sp.* and various gas production rates with respect to experimental media compositions. Hydrogenase activity and hydrogen gas production rates are investigated.

4.1. Growth of *Synechocystis sp.*

In the course of cyanobacterial growth, three replicates with 300 mL working volume were grown under 8000 lux and 0.3 L/min air flow at approximately 27 °C. Figure 4.1. shows growth curve with respect to OD_{730}. Exponential growth was observed between the 3rd and 7th day, followed by a slow transition into stationary phase. As OD values were not stabilized due to continuous evaporation from the cultures, stationary phases cannot be precisely observed. However, it was accepted that 7th or 8th day is the late-exponential phase/early-stationary phase in current bioreactor systems (Figure 4.1).

There is no conclusive agreement on which stage is to harvest for hydrogen production in the literature. Touloupakis et al., maintained the culture until stationary phase to reach maximum carbohydrate accumulation (Touloupakis et al., 2016). Burrows et al. incubated *Synechocystis sp.* very concentrated at 10^9 and 10^{10} cells/mL, but did not provide the growth phase (Burrows et al., 2008; Burrows et al., 2009). Late-exponential phase were preferred in other studies (Antal and Lindblad, 2005; Dutta and Vermaas, 2016).

OD, pH and cell concentration values data are shown on Appendix A, on Table A.1. and Table A.2.

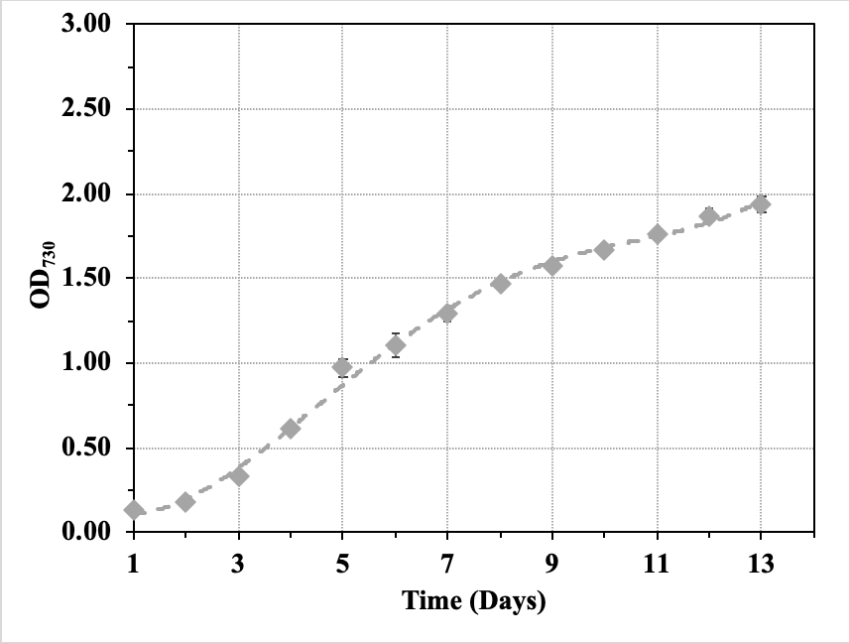

Figure 4.1. Growth curve for *Synechocystis sp.*

pH started just below 8.0 and fluctuated between 9.0 to 10.0 as can be seen in Figure 4.2. Cell number per mL was determined on every other day and shown in Figure 4.3.

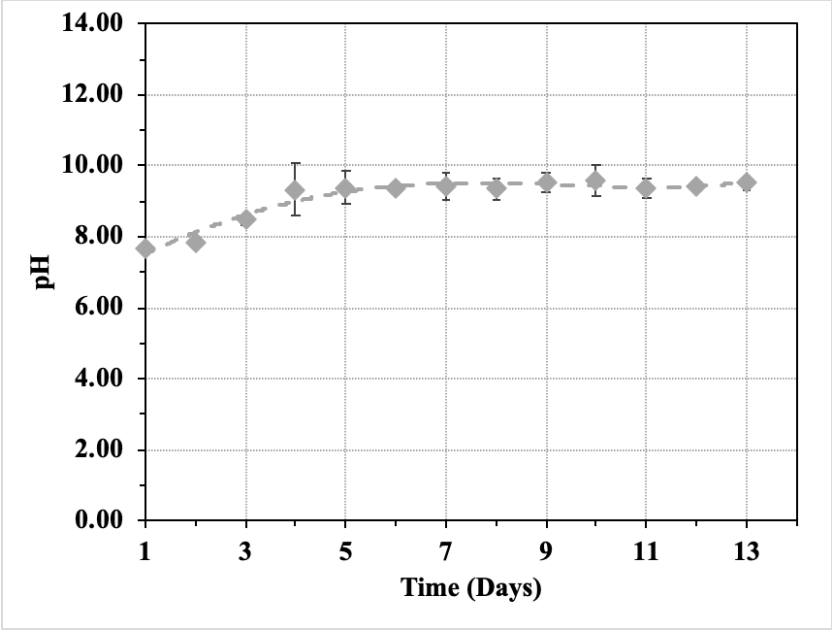

Figure 4.2. pH vs time.

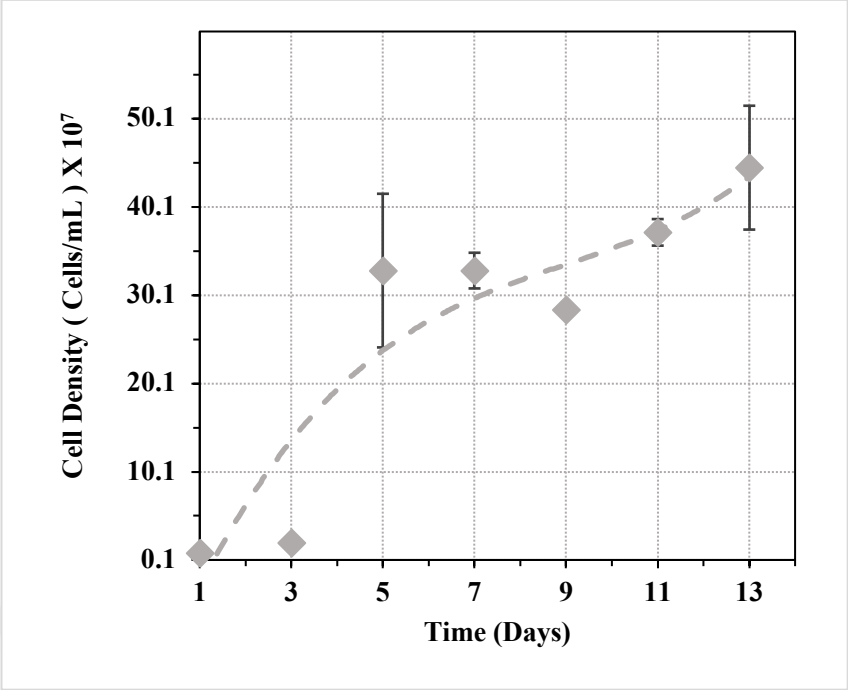

Figure 4.3. Cell density vs time.

Four different reactor setups are named with respect to their media composition in order to prevent confusion. BG-11, BG-11(-N), BG-11(-S) and BG-11° media are named as Reactor 1 (R1), Reactor 2 (R2), Reactor 3 (R3) and Reactor 4 (R4), respectively.

4.2. Initial Screening Experiments

Initial screening experiments were held in different manner. The aim was to detect hydrogen detection in fast screening tests. First, cyanobacterium was grown in BG-11 medium for biomass accumulation, and this stage were called pre-culture. Then, two days of adaptation in designated medium in serum bottle is followed by experimental analysis stage. BG-11(-N) and BG-11(-S) are known for their effect on hydrogen production in *Synechocystis sp*. For this reason, they have been chosen to compare with BG-11 medium. Light regime, volume and cell density have been varied. Setup 4 and 5 had distinctive reactor design; serum bottle outflow is connected to reverse graduated cylinder filled with water, to eliminate headspace overpressure in the reactor and it was estimated that generated gas would be accumulated in there. It was assumed that gas amount would be determined by water displacement, and composition would be analyzed in GC. However, no water displacement was observed due to low volume and productivity. Instead, all hydrogen measurements were done by direct headspace measurements or using GC vial sampling without adding MV and sodium dithionite as explained in Section 3.5.1. and 3.5.2.

Table 4.1. shows all experiments done in detail. As working volume, 1.5 mL, 80 mL, 100 mL and 110 mL were chosen. In Setup 1 and 2, two different volumes were used for experimental setup stage; 1mL working volume in 2 mL GC vial and 30 mL working volume in 40 mL amber vial. Vials were flushed with argon to get rid of oxygen, and they were incubated in dark. Gas sampling time varied between those setups. No hydrogen was observed in BG-11 medium, but it was detected qualitatively in BG-11(-N) and BG-11(-S) media in trace amount, hard to measure quantitatively.

Only significant hydrogen detection was observed when 30 mL cell suspension sample were taken and incubated in dark. Anaerobiosis, and nitrogen and sulphur deprivation separately triggered hydrogen generation. Since hydrogen was not observed in any of reactor headspace, it was assumed that volume is not primarily important. However, headspace pressure should be watched to make a conclusive statement, because hydrogen production may be suppressed under high pressure.

Table 4.1. Initial screening experiments for hydrogen detection.

#	Pre-culture	Adaptation					Experimental Setup	Hydrogen
		Medium	Volume	Light	Cell Density (cells/mL)	Duration		
1	4th day	BG-11	80 mL	12h L/D cycle with aeration	10^8	48 H	Samples transferred to 2mL and 40mL vials. Flushed with argon. Total 48H dark. First sampling after 10H	Not detected
		BG-11 (-N)	80 mL	12h L/D cycle with aeration	10^8	48 H	Samples transferred to 2mL and 40mL vials. Flushed with argon. Total 48H dark. First sampling after 10H	Detection in large vial
		BG-11 (-S)	80 mL	12H L/D cycle with aeration	10^8	48 H	Samples transferred to 2mL and 40mL vials. Flushed with argon. Total 48H dark. First sampling after 10H	Detection in large vial

2	4th day	BG-11	80 mL	12H L/D cycle with aeration	10^8	41 H	Samples transferred to 2mL and 40mL vials. Flushed with argon. Total 41H dark. First sample after 30mins.	Not detected
		BG-11 (-N)	80 mL	12H L/D cycle with aeration	10^8	41 H	Samples transferred to 2mL and 40mL vials. Flushed with argon, Total 41H dark. First sample after 30mins.	Possibly after 30min
		BG-11 (-S)	80 mL	12H L/D cycle with aeration	10^8	41 H	Samples transferred to 2mL and 40mL vials. Flushed with argon. Total 41H dark. First sample after 30mins.	Possibly after 30min
3	5th day	BG-11	80 mL	12H L/D cycle with aeration	10^8	48 H	Flushed with argon. Total 48H dark. Gas samples were taken from reactors, no vial sampling. First sample after 30mins.	Not detected
		BG-11 (-N)	80 mL	12H L/D cycle with aeration	10^8	48 H	Flushed with argon, Total 48H dark. Gas samples were taken from reactors, no vial sampling. First sample after 30mins.	Not detected
		BG-11 (-S)	80 mL	12H L/D cycle with aeration	10^8	48 H	Flushed with argon, Total 48H dark. Gas samples were taken from reactors, no vial sampling. First sample after 30mins.	Not detected

4	4th day	BG-11	100 mL	12H L/D cycle w/aeration	10^8	48 H	Analysis at dark. After fourth day of experimental phase, reactor put back to illumination.	Not detected
		BG-11 (-N)	100 mL	12H L/D cycle with aeration	10^8	48 H	Analysis at dark. After fourth day of experimental phase, reactor put back to illumination.	Not detected
		BG-11 (-S)	100 mL	12H L/D cycle with aeration	10^8	48 H	Analysis at dark. After fourth day of experimental phase, reactor put back to illumination.	Not detected
5	4th day	BG-11	110 mL	12H L/D cycle with aeration	10^8	48 H	Analysis at dark. After 30min, 24H and 48H samples were taken. No displacement.	Not detected
		BG-11 (-N)	110 mL	12H L/D cycle with aeration	10^8	48 H	Analysis at dark. After 30min, 24H and 48H samples were taken. No displacement.	Not detected
		BG-11 (-S)	110 mL	12H L/D cycle with aeration	10^8	48 H	Analysis at dark. After 30min, 24H and 48H samples were taken. No displacement.	Not detected
6	4th day	BG-11	110 mL	12H L/D cycle with aeration	10^8	48 H	Continuation of Setup 5. Reactors were put back at illumination.	Not detected
		BG-11 (-N)	110 mL	12H L/D cycle	10^8	48 H	Continuation of Setup 5. Reactors were put	Not detected

				with aeration			back at illumination.	
		BG-11 (-S)	110 mL	12H L/D cycle with aeration	10^8	48 H	Continuation of Setup 5. Reactors were put back at illumination. No H2	Not detected
7	4th day	BG-11	100 mL	12H L/D cycle with aeration	10^8	48 H	Analysis at dark. After 30min and 24H samples were taken.	Not detected
		BG-11 (-N)	100 mL	12H L/D cycle with aeration	10^8	48 H	Analysis at dark. After 30min and 24H samples were taken.	Not detected
		BG-11 (-S)	100 mL	12H L/D cycle with aeration	10^8	48 H	Analysis at dark. After 30min and 24H samples were taken.	Not detected
8	7th day	BG-11	100 mL	Continuous illumination with aeration	10^8	48 H	Light cycle. First analysis is during light, later are taken during dark cycle. After 1H, 24H and 48H samples were taken.	Not detected
		BG-11 (-N)	100 mL	Continuous illumination with aeration	10^8	48 H	Analysis at dark. After 1H, 24H and 48H samples were taken.	Hydrogen is detected on 48th hour.
		BG-11 (-S)	100 mL	Continuous illumination with aeration	10^8	48 H	Light cycle. First analysis is during light, later are taken during dark cycle. After 1H, 24H and 48H samples were taken.	Not detected
9	6th day	BG-11	100 mL and 1.5mL	12H L/D cycle	$2x10^8$	48 H	Analysis at dark. After 30min and 24H samples were taken.	Not detected

		BG-11 (-S)	100 mL and 1.5mL	12H L/D cycle	$2x10^8$	48 H	Analysis during light. After 30min and 24H samples were taken.	Not detected
10	6th day	BG-11°(2g/L thioglycolate)	50 mL	Continuous illumination in closed bottle	$2x10^8$	48 H	Starting headspace gas is air. Gas sampling after 24H	Not detected
		BG-11 (+ 20mM dithionite)	50 mL	Continuous illumination in closed bottle	$2x10^8$	48 H	Completely bleached after 18H of incubation	Not detected
		BG-11 (-S) (+ 2g/L thioglycolate)	50 mL	Continuous illumination in closed bottle	$2x10^8$	48 H	Starting headspace gas is air. Gas sampling after 24H	Not detected
		BG-11 (-S) (+ 20mM dithionite)	50 mL	Continuous illumination in closed bottle	$2x10^8$	48 H	Completely bleached after 18H of incubation	Not detected

Even though hydrogen was detected in large vial, smaller 2 mL GC vials were used in following experiments due to need for excess biomass. The experiment was held for 5 days, which makes the use of 30 mL suspension on each measurement unfeasible. On the other hand, reactor headspace gas analysis in the dark were made after 10 hours, which is compatible with screening assay. However, in any case no significant direct hydrogen production was observed. Therefore, it was focused more on hydrogenase enzyme activity measurement via reduced MV and sodium dithionite.

4.3. Chlorophyll a Content

Chlorophyll measurement along the experiment is a way to observe reactor growth, like OD or dry-weight measurement. In this study, chl a was measured for 6 days, whole time course of the experiment. Appendix D shows absorbance values for chl a determination.

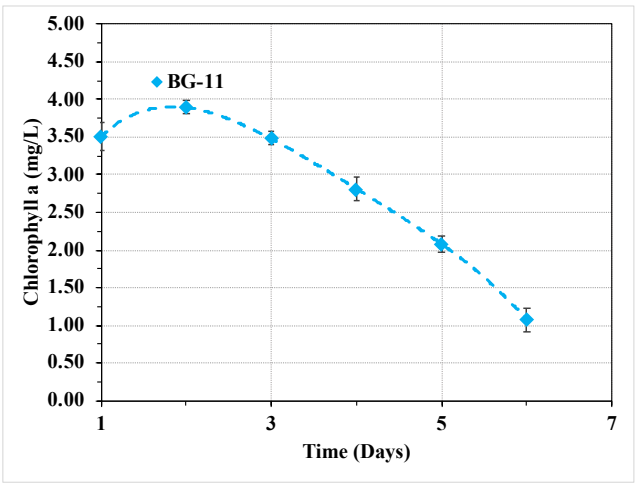

Figure 4.4. Chl a concentration of R1.

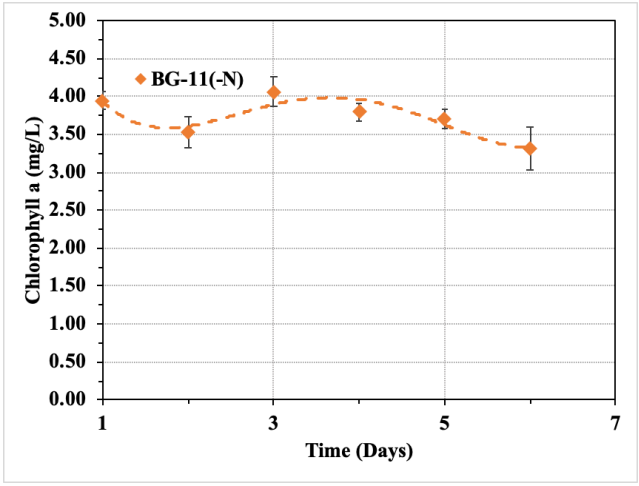

Figure 4.5. Chl a concentration of R2.

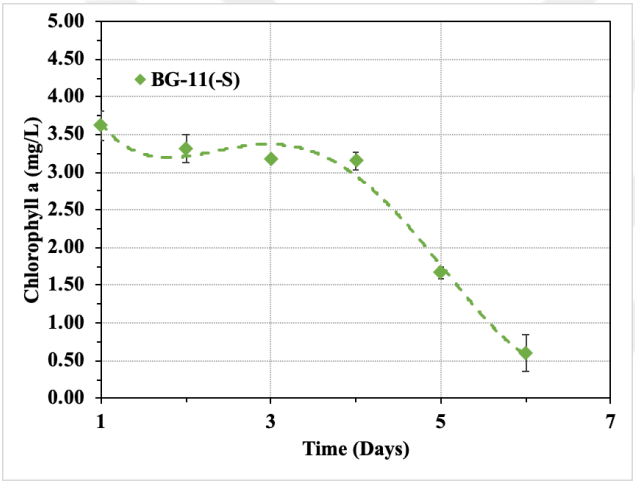

Figure 4.6. Chl a concentration of R3.

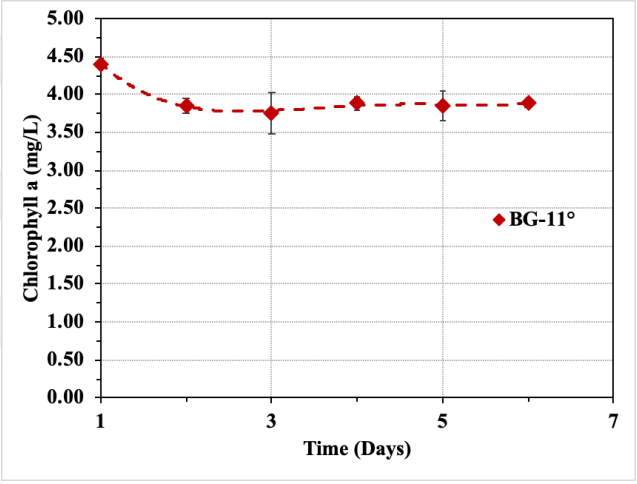

Figure 4.7. Chl a concentration of R4.

Chl a concentration of all reactor setups can be seen in Figure 4.4., Figure 4.5., Figure 4.6. and Figure 4.7. Approximately similar starting chl a concentrations were aimed. Reactors were incubated with a cell concentration of 10^8 cells/mL. Despite a small increase in chl a after 24 hours, the control group R1 significantly bleached during the course of the experiment. Once possibility is that even in BG-11 medium, cells were not able to accumulate carbohydrates, causing degradation of chl a instead. However, to give a conclusive remark, carbohydrate accumulation should be investigated. Similar effect, without any increase in first days, was observed in R3. In Figure 4.8., state of each culture on 6th day can be seen. The bleaching can be clearly observed in R1 and R3. Different than Richaud et al. proposed, bleaching occurred in sulphur starved cells (Richaud et al., 2001). Due to nitrogen starvation, metabolism of R2 was affected as well. The loss of pigment elements, or chlorosis, is likely to happen when nitrogen is limited or deprived completely due to catabolism of phicobiliproteins, LHC, antennas, and chl a (Antal et al., 2006). Similar to previous study,

Touloupakis et al. also detected sharp decrease in pigment concentration when the culture was transferred into nitrogen depleted medium (Touloupakis et al., 2016). Krasikov et al detected the deceleration of cell growth, loss phycocyanin content and constant chl a over phycocyanin concentration in *Synechocystis sp.*, indicating loss of pigment material (Krasikov et al., 2012). However, in this study pigment loss was not observed even on 6th day, as can be seen in Figure 4.8.(C).

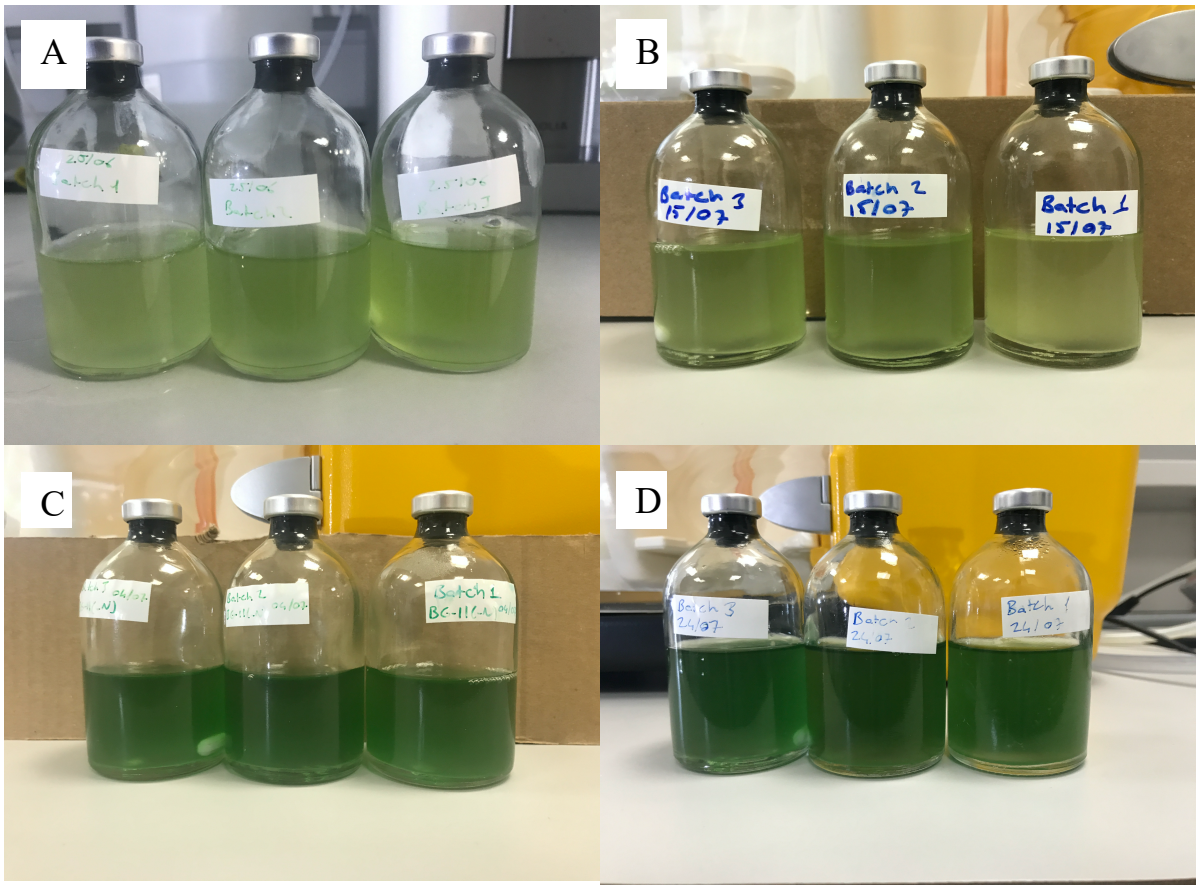

Figure 4.8. Reactors on 6th day. (A) BG-11; (B) BG-11 (-S); (C) BG-11 (-N); (D) BG-11°.

On the other hand, almost constant pigment concentration was observed in medium with thioglycolate compound. One reason is that thiol and disulfide groups may provide electrons in electron transport chain. Also, one possibility is that those reactive groups may be sulfur source for thiol and disulfide containing proteins such as thioredoxin.

4.4. Overall Biological Hydrogen Production

In the course of this study, three different hydrogen measurements were performed. Headspace gas composition were observed, hydrogenase activity was measured by artificial electron donor MV,

and small culture sampling in GC vials was done for gas production analysis. Some common comments for all reactor setups can be made. Appendix C shows gas chromatography results obtained after headspace gas measurements. In terms of headspace gas composition, there were no hydrogen observation at all throughout the study in any of medium composition. This may be due to several possibilities. Plausibly in dark phase, respiration was not enough to consume all remaining oxygen, which had concentrations of above 1mM. Therefore, the existence of oxygen is the core drawback inhibiting hydrogen generation.

Another reason might be the overall bioreactor design. It was stated that hydrogenase is not able to produce much hydrogen against existing backpressure (Das et al., 2014). Serum bottles were tightly capped without allowing any gas inflow or outflow. Firstly, before starting reactor it was flushed with argon, and this created an inner pressure in headspace of reactor. Also, argon gas was injected after each culture sampling to overcome vacuum pressure. Headspace volume might not efficiently high for accumulation. That was the reason of testing another reactor design in initial screening experiments, however none of gas species accumulation, including oxygen, was achieved in that design having reverse graduated cylinder connected to the outstream gas. Much more higher headspace volume, reaching up to 90 to 100 mL could have been investigated for triggering the production of hydrogen.

One possibility is the growth phase of cells. In this study, cells were harvested at late-exponential phase of growth and then incubated in complete fresh medium. Melnicki et al. proposes that hydrogen production decreases in purple sulphur bacteria, which possess nitrogenase enzyme, at stationary phase (Melnicki et al., 2008). However, one significant difference is that in this study complete fresh medium for cell incubation was used, whereas in that study, cells were regrown in succinate added old medium, and hydrogen production was ceased when the substrate was completely consumed. But overall, it was reported that growth does not seem to a requirement for hydrogen production (Melnicki et al., 2008). This is supported by other research, which conducted hydrogen analysis using late-exponential or stationary phase cultures for inoculation, mentioned in Section 4.1.

First, it was observed that during first day of the light phase oxygen production was never ceased. Theoretically, in sulfur deprivation medium it was expected that inhibition of PSI causes disruption in photolysis, and oxygen generation is cut off. However, either the oxygen consumption was never stopped during light phase or the consumption never exceed the production rate. Even in sulphur starvation, oxygen concentration remained above 2mM.

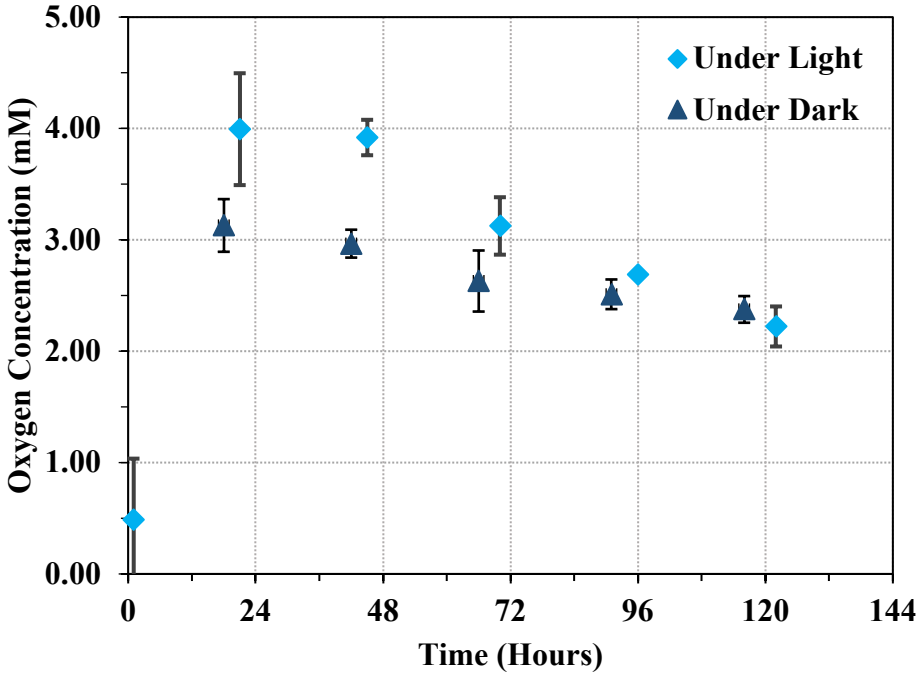

Figure 4.9. Oxygen concentration in the headspace of R1.

For R1, it can be said that photosynthetic ability and respiration were working well as complete growth medium was provided. Headspace oxygen concentration can be followed in Figure 4.9. At the end of each dark cycle, oxygen was slightly consumed, leaving the level between 3 to 2.3 mM. However, as soon as the lights were turned on, oxygen concentration jumped to a level of 4 mM in the first two days. Along the course of experiment, oxygen composition follows a similar trend that of chl a in Figure 4.4., which indicates a decrease in photosynthetic rate as the cells lost their pigment. Also, the concentrations of dark and light phase converge to similar values towards the 5th and 6th days. This may be explained by dying off of the culture, and eventually bleached. Cournac et al reported that even oxygen in micromolar level is able to suppress hydrogen generation and causes hydrogen uptake in wild-type *Synechocystis sp.* PCC 6803 (Cournac et al., 2002). Only exception is the transient state from dark to light phase, which triggers hydrogen production for less than a minute. Therefore, current assay falls into macro level comparing to this study and make it difficult for observation any possible hydrogen accumulation in the headspace.

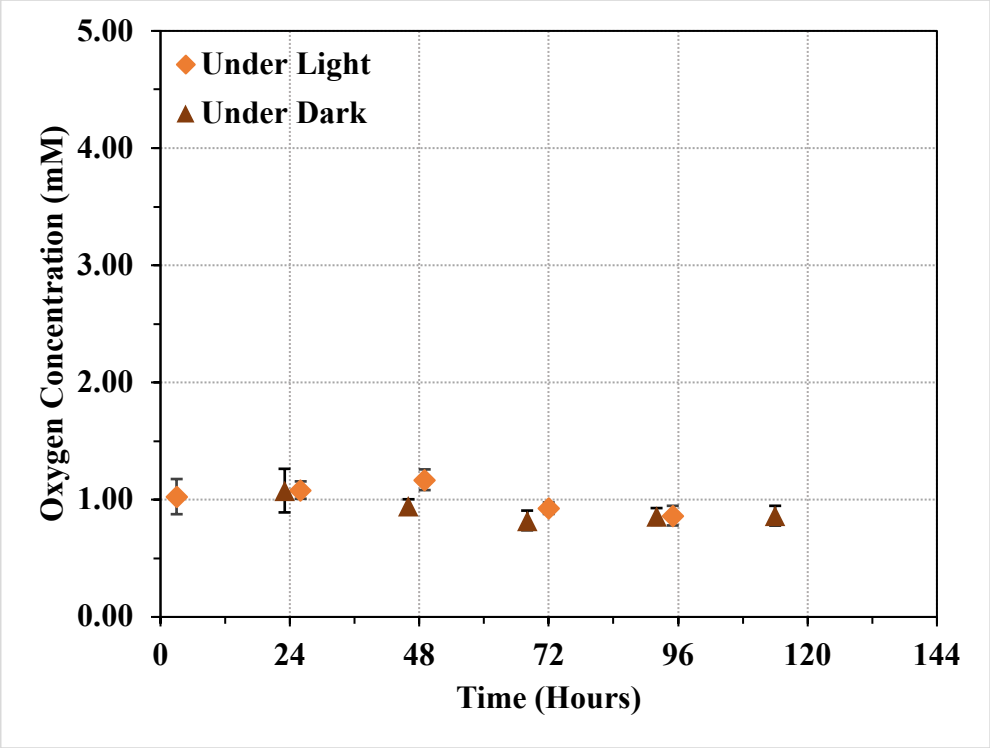

Figure 4.10. Oxygen concentration in the headspace of R2.

In Figure 4.10., effect of nitrogen starvation on oxygen production in *Synechocystis sp*. can be observed. Interestingly, there is no fluctuations of concentration between light and dark phases, and headspace concentration remains constant at around 1 mM. Krasikov et al. determined that nitrogen starvation cease the oxygen generation in *Synechocystis sp*., which is in line with presented results (Krasikov et al., 2012).

Sulphur starvation did not significantly affect headspace oxygen concentration. The trend, shown in Figure 4.11., is much similar to that of R1. Melis et al. found that rate of respiration passes the rate of photosynthesis after 24 to 30 hours of sulphur deprivation in *Chlamydomonas reinhardtii* cells during light phase (Melis et al., 2000). However, it was never observed total consumption of oxygen in sulphur deprived medium in this study.

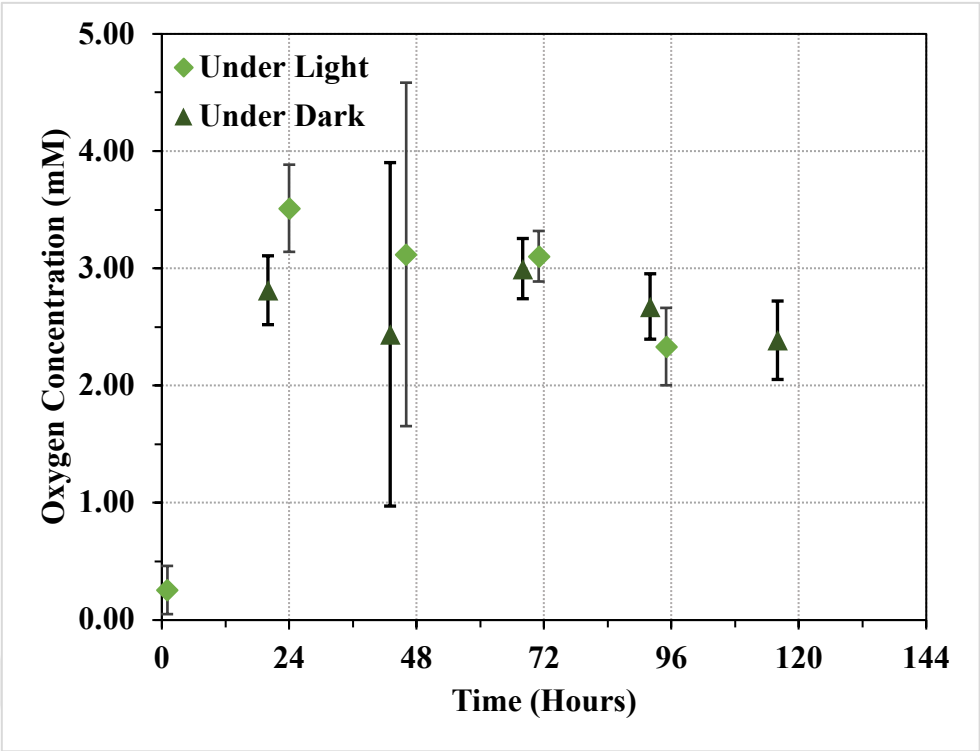

Figure 4.11. Oxygen concentration in the headspace of R3.

Much different from other medium compositions, BG-11° medium was successful in oxygen removal in gas phase. Oxygen gas was not observed in headspace after the inoculation either during light or dark phase, indicated in Figure 4.12. However, gaseous oxygen removal apparently was not enough for hydrogen production. Figure 4.13. shows dissolved oxygen both in blank BG-11° and R4. Although significantly reduced, sodium thioglycolate salt was not totally effective on oxygen removal. Dissolved oxygen was never below 0.45 mg/L. This might hinder gaseous hydrogen generation. Appendix F shows dissolved oxygen data.

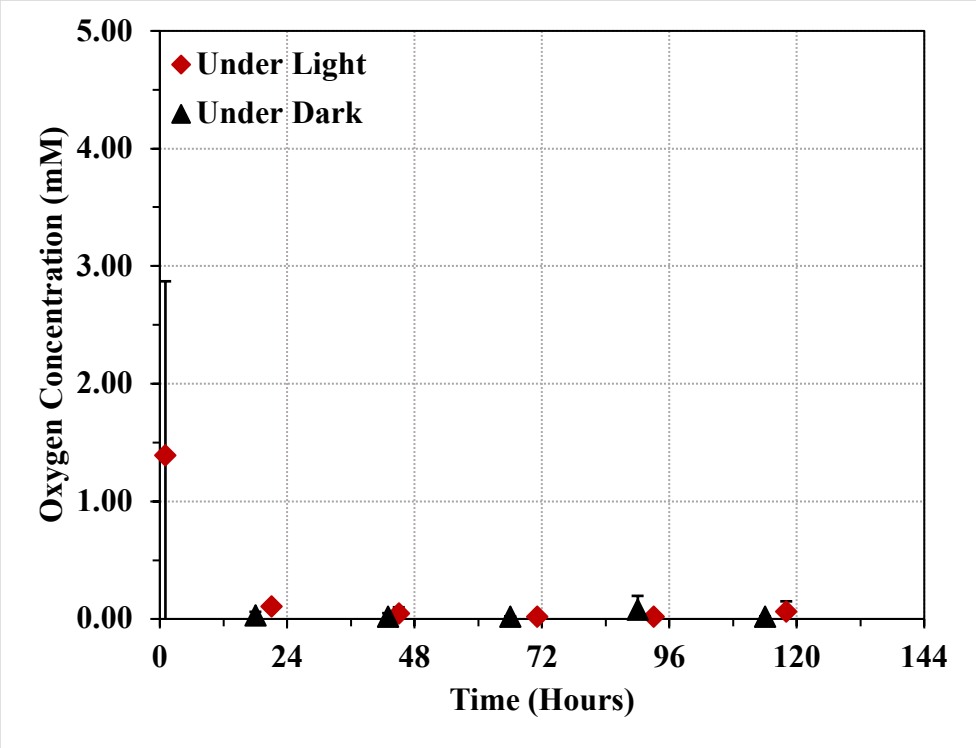

Figure 4.12. Oxygen concentration in the headspace of R4.

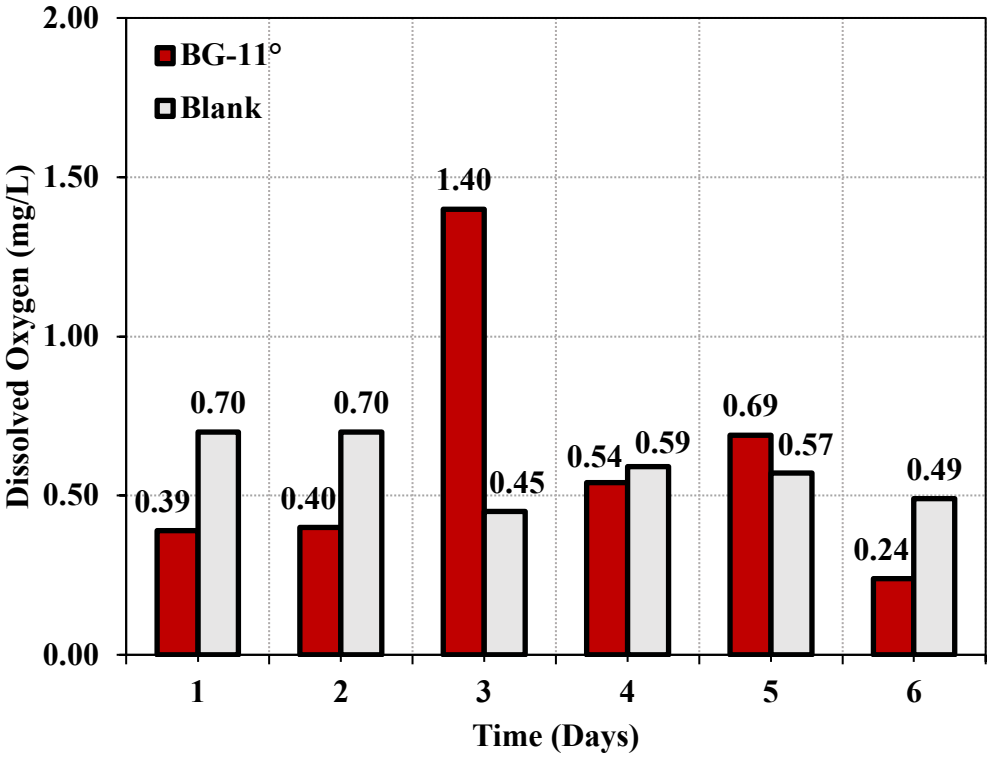

Figure 4.13. Dissolved oxygen in BG-11° setup.

On the other hand, GC vial sampling was troublesome for analysis. No hydrogen generation was observed in any of media composition. Convenient results were not observed (data not shown); first

sampling after one hour were not sufficient for any gas accumulation and second sampling were not possible due to vacuum effect when the first sample was taken from the vial.

4.5. Hydrogenase Activity

Hydrogenase activity, detected by reduced MV and sodium dithionite, indicates potential of the enzyme productivity. Reduced MV is a strong electron donor to hydrogenase. In this experiment, hydrogen evolution by hydrogenase enzyme was conducted via MV reduced by sodium dithionite in dark argon atmosphere. All calculations were made using data from Appendix E. Overall, it can be said that the minimum enzyme activity falls around 30 µmol H_2 mg chl a^{-1} h^{-1}, which was detected in R2. The highest level is 87.99±1.11 µmol H_2 mg chl a^{-1} h^{-1}, seen on the 5th day of sulphur deprived medium. Hydrogenase activity rate closer to R3 setup was expected in BG-11° medium, however it remained as one of the lowest, with a rate value between 30 to 35 µmol H_2 mg chl a^{-1} h^{-1} in the course of the study.

Activity in BG-11 medium started at 41.76 ±0.97 µmol H_2 mg chl a^{-1} h^{-1}, decreased on 3rd day, and finally increased up to 66.15 ± 2.43 µmol H_2 mg chl a^{-1} h^{-1} (Figure 4.14.). This jump probably is not decoupled from decreasing chl a content seen in Figure 4.4.

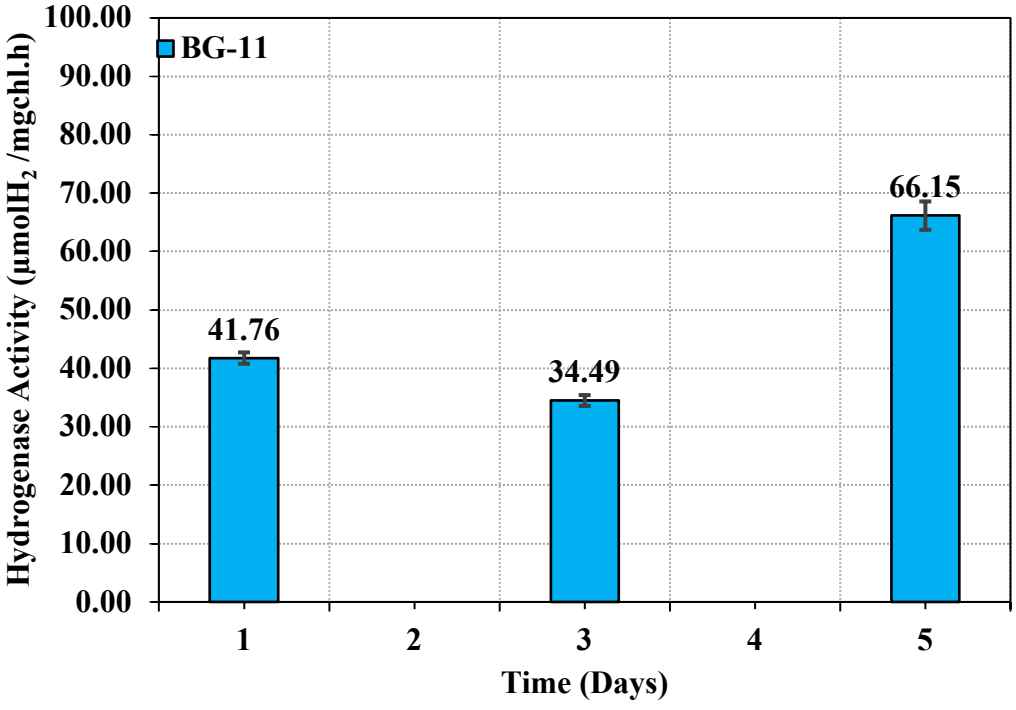

Figure 4.14. Hydrogenase activity of R1.

Table 4.2. Hydrogenase activity in the presence of reduced MV.

Species	Highest hydrogenase activity with reduced MV in the course of experiment	Conditions	Reference
Synechocystis sp. PCC 6803	235.5 µmol H_2 mg chl a^{-1} h^{-1}	BG11 (1 mM NaNO3), constant light, bubbling with air and 1% CO2	(Schütz et al., 2004)
Synechocystis sp. PCC 6803	2.02 ±0.14 µmol H_2 mg Pr^{-1} h^{-1}	300 min preincubated under H2 atmosphere	(Antal et al., 2006)
Synechocystis sp. PCC 6803	1.8 µmol H_2 mg Pr^{-1} h^{-1}	7th day of BG11 without sulphate, 15 mM NH4Cl, 8 mM NaHCO3 and 10 mM HEPES	(Antal and Lindblad, 2005)
Gloeocapsa alpicola	2.3 µmol H_2 mg $Pr^{-1}h^{-1}$	3th day of BG11 without sulphate, 15 mM NH4Cl, 8 mM NaHCO3 and 10 mM HEPES	(Antal and Lindblad, 2005)
Chlamydomonas reinhardtii	28 µmol H_2 mg chl a^{-1} h^{-1}	30 minutes after anaerobiosis, pulse illumination	(Kosourov et al., 2018)
Synechocystis sp. PCC 6803 triple oxidase mutant	Approx.135 µmol H_2 mg chl a^{-1} h^{-1}	Sulphur deprived BG-11 with 5 mM NH_4Cl in the presence of tungstate	(Gutthann et al., 2007)
Synechocystis sp. PCC 6803 hik30 mutant	Approx. 78 µmol H_2 mg chl a^{-1} h^{-1}	BG-11	(Gutekunst et al., 2014)
Synechocystis sp. PCC 6803	859.2±36.6 µmol H_2 mg chl a^{-1} h^{-1}	Nitrogen and sulphur deprived BG-11 with 750 µM β-mercaptoethanol	(Baebprasert et al., 2010)
Synechocystis sp. PCC 6803	30-84 µmol H_2 mg chl a^{-1} h^{-1}	Nitrogen or sulphur starvation, or BG-11 with 5 g/L sodium thioglycolate	This study

Some hydrogenase activity with presence of reduced MV and sodium dithionite is given in Table 4.2. Nitrogen-limiting medium is far better than any other setup or genetic modification, with an activity rate of 235.5 µmol H_2 mg chl a^{-1} h^{-1}. Note that some of the rates are given in terms of total protein content; *Gloeocapsa alpicola* by (Antal and Lindblad, 2005), and *Synechocystis sp*.by both (Antal et al. 2006) and (Antal and Lindblad, 2005). In this study, it was not possible to approach a value this high. Probably, complete starvation has less effect than high deprivation. Burrows et al. showed that optimized nitrogen and sulphur concentration has higher influence than complete starvation (Burrows et al., 2008) Nitrogen starvation and sodium thioglycolate addition from this study also give competitive results with *Chlamydomonas reinhardtii* under pulse illumination, but far under hik30 mutant and triple oxidase mutant in the presence of tungstate. Baebprasert et at. found

the highest hydrogenase activity at 70°C for a short period, which is not sustainable (Baebprasert et al., 2010).

Nitrogen starvation did not induce in higher hydrogen generation for all three measurements Figure 4.15.). Similar to change in chl a concentration, the production remained on the minimum activity.

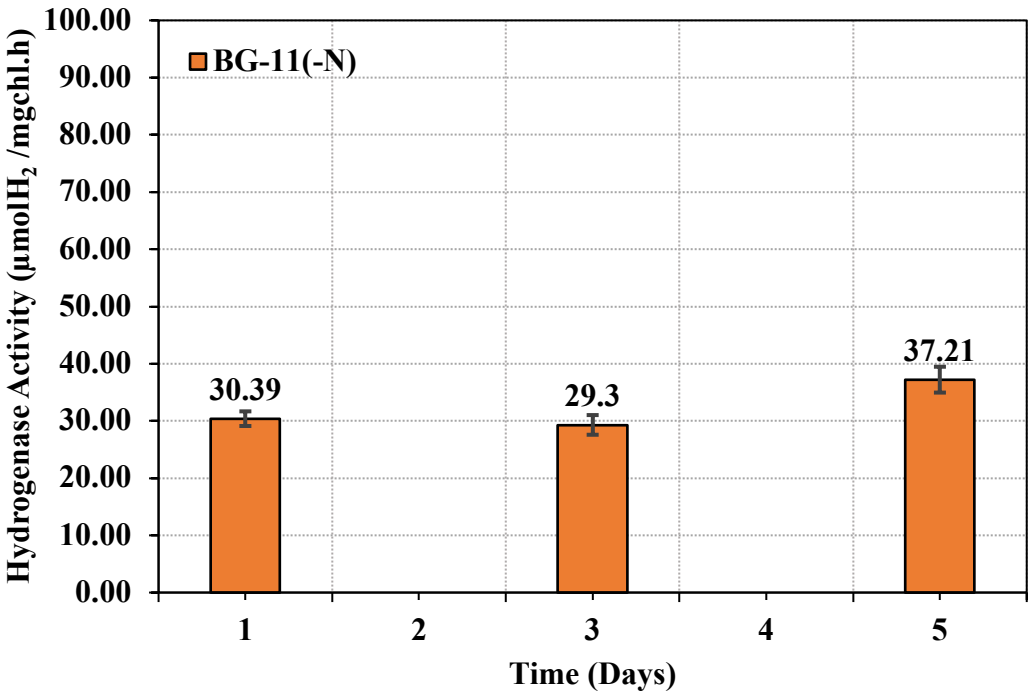

Figure 4.15. Hydrogenase activity of R2.

Higher hydrogenase activity in R3 can be explained in several ways (Figure 4.16.). One is the inhibition of PSII activity, which leads to cease of water splitting and oxygen evolution. This phenomenon was not quantitively observed in this research but discussed in others (Antal and Lindblad, 2005; Laurinavichene et al., 2006; Melis et al., 2000). Another possibility is that the cell might use accumulated carbohydrate or lipid compound. Under sulphur deprivation of *Synechocystis sp*., it was found that genes which are responsible of fatty acid and lipid biosynthesis was highly upregulated (Zhang et al., 2008). Sulphur deprivation leads to a division of hydrogen production between both into photolysis and photofermentative pathways. This separation might trigger an increase in production.

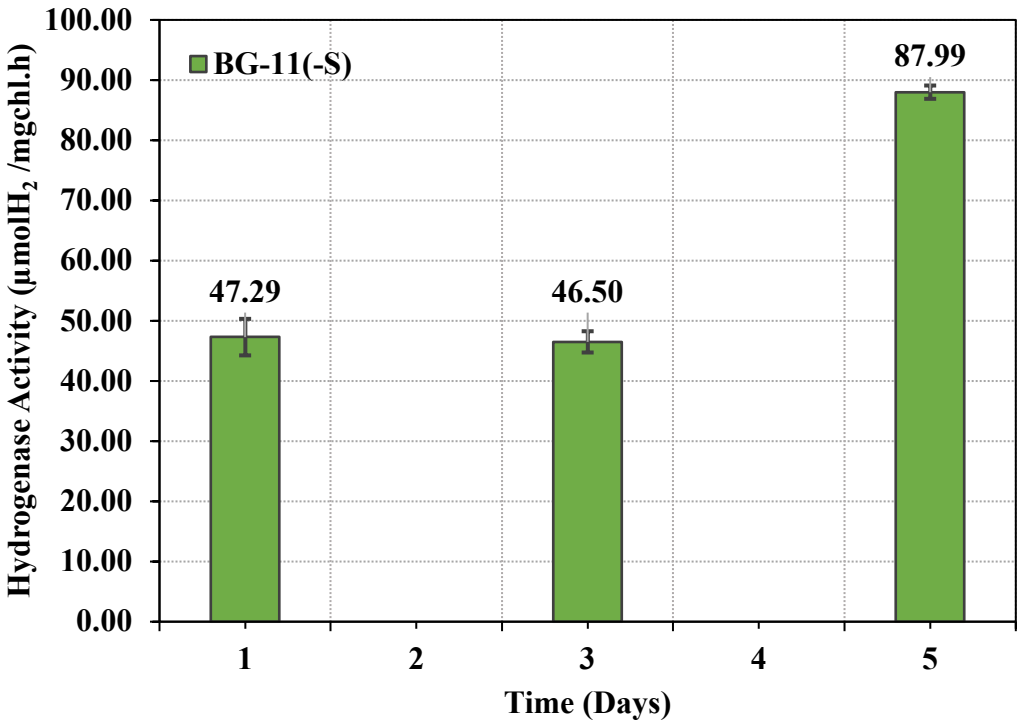

Figure 4.16. Hydrogenase activity of R3.

Sodium thioglycolate addition did not improve hydrogenase activity, plus the rate was even lower than that of BG-11 medium grown cells (Figure 4.17.). Even though oxygen was effectively removed, and cells were not damaged like to those of dithionite addition, the culture was even more vigorous to any other medium compositions. When thioglycolic acid is oxidized with air, apart from disulfides, it is possible to observe sulfuric acid and hydrogen peroxide as products (Cook and Steel, 1959). In BG-11° medium, formation of side products is not estimated, however disulfide compounds are likely to occur. In *Synechocystis sp.* thioredoxin protein, having cysteine-disulfide active site taking part in electron transport as an electron carrier and light dependent enzyme regulations (Navarro et al., 2000). Thiol/disulfide exchange is a reversible process, which can be affected by redox potential regulated by enzymatic activity in the suspension. Relation of redox kinetics should be further investigated for more clear explanation.

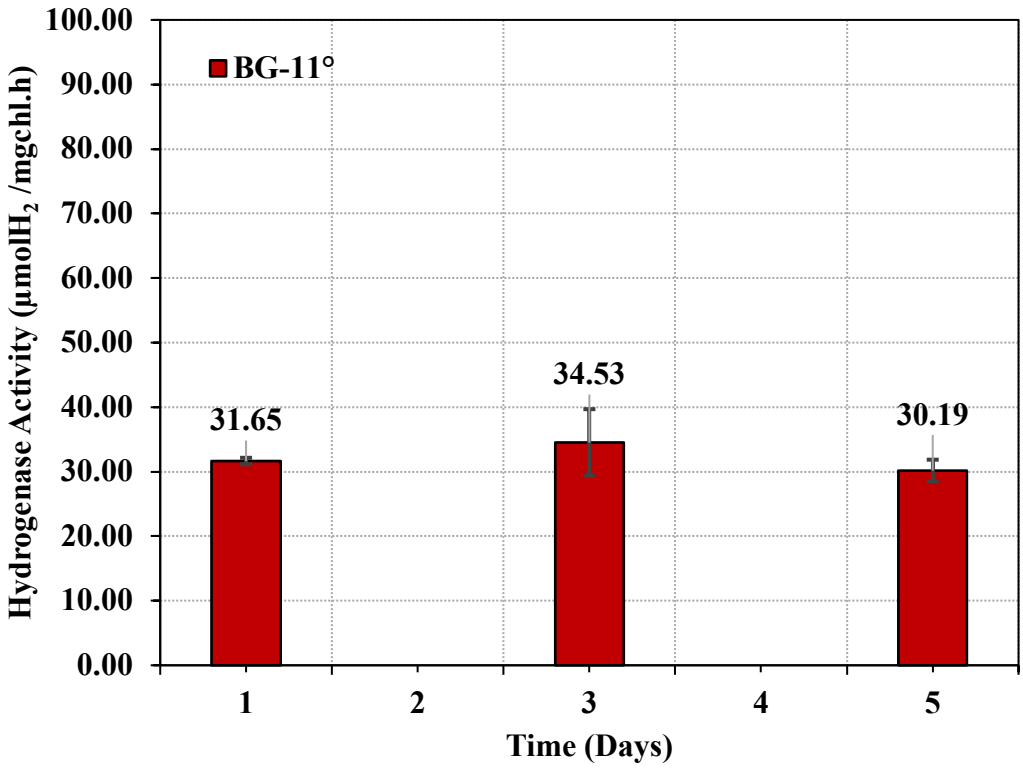

Figure 4.17. Hydrogenase activity of R4.

5. CONCLUSION

Energy requirements and instabilities in climate due to anthropogenic activities leads research towards sustainable alternatives for decades. Among them, due to its high energy density hydrogen is a promising medium for a radical energy transition system from fossil fuels. However as of today, there are so few carbon-neutral commercialized hydrogen production methods. Electrolysis, depending on electricity source, is considered as a sustainable process. On the other hand, biological approaches are on the rise. Microorganisms which are able to perform photolysis, photofermentation or dark fermentation are effectively under investigation for hydrogen production. Among them, photobiological hydrogen production had been on focus for several year due to its low requirement for input, namely only water and sun light.

Photolysis is the biological pathway, splitting water molecule into oxygen gas and hydrogen ions by means of photosynthetic reactions plus hydrogenase enzymes However, oxygen is a strong inhibitor for hydrogenase, ceasing hydrogen generation even in small quantities. There are various pathways for increasing the product yield: genetic modification, medium modification, immobilization or reducing agent utilization.

Synechocystis sp. is a non nitrogen-fixing cyanobacterium, possessing hydrogenase enzyme which can generate hydrogen gas by direct or indirect photolysis. In the course of this study, four different culture media composition were tested and compared for their performance. It was aimed to increase hydrogen production rate by removing oxygen. Culture media used were BG-11, BG-11(-N), BG-11(-S) and BG-11°. BG-11 medium were modified by subtracting nitrogen and sulphur components, separately. Main focal point was to measure effectiveness of reducing agent sodium thioglycolate, which was present in BG-11° medium. Three different measurement methods were undertaken, and samples were analyzed in gas chromatography; (1) direct headspace has measurement from reactor; (2) small GC vial sampling and measurement its headspace; and (3) hydrogenase enzyme activity detection by reduced MV and sodium dithionite. During headspace measurement, no hydrogen was detected in any of media composition. It was found that oxygen remained in the headspace and never consumed totally, except BG-11° medium. In contrast with literature, neither sulphur nor nitrogen starvation triggered rapid consumption of oxygen in the environment, even though bleaching occurred in sulphur starved medium. Thioglycolate was

effective in removal of oxygen gas, however low amount of dissolved oxygen might have prevented hydrogen generation.

Sampling in GC vials were not effective and there were no gas detection neither after 1 hour nor after 24 hours due to inner vacuum pressure caused by previous sampling.

Hydrogenase activity was measured with reduced MV and sodium dithionite under dark, and highest hydrogenase activity was found by cells cultured in BG-11(-S) medium on 5th day. The rate of activity in BG-11° medium was even lower than BG-11. One chance is that thiol or disulfide compound may serve as sulphur source or thioglycolate may interrupt redox potential within the culture, providing electrons to the electron transport chain.

Despite the biological limitations of oxygen toxicity on hydrogenase enzyme and analytical measurement difficulties, this study sheds light on the possibility of biological hydrogen production in *Synechocystis sp.* with further optimizations on bioreactor design and fine headspace sampling, higher hydrogen production values can be obtained. Nevertheless, enzyme activities within the range of literature values, offer possibility of using *Synechocystis sp.* ATCC27184 species for sustainable biohydrogen production under photoautotrophic conditions.

REFERENCES

Allakhverdiev, S. I., Thavasi, V., Kreslavski, V. D., Zharmukhamedov, S. K., Klimov, V. V., Ramakrishna, S., Los, D. A., Mimuro, M., Nishihara, H., Carpentier, R. 2010. Photosynthetic hydrogen production. Journal of Photochemistry and Photobiology C. Photochemistry Reviews, 11, 101-113.

Allen, M. R., Dube, O. P., Solecki, W., Aragón-Durand, F., Cramer, W., Humphreys, S., Kainuma M., Kala J., Mahowald N., Mulugetta Y., Perez, R., Wairiu, M., Zickfeld, K. 2018. Framing and Context. In V. Masson-Delmotte, P. Zhai, H.-O. Pörtner, D. Roberts, J. Skea, P. R. Shukla, A. Pirani, W. Moufouma-Okia, C. Péan, R. Pidcock, S. Connors, J. B. R. Matthews, Y. Chen, X. Zhou, M. I. Gomis, E. Lonnoy, T. Maycock, M. Tignor, T. Waterfield (Eds.), Global Warming of 1.5°C. An IPCC Special Report on the impacts of global warming of 1.5°C above pre-industrial levels and related global greenhouse gas emission pathways, in the context of strengthening the global response to the threat of climate change, sustainable development, and efforts to eradicate poverty, 49-91. In Press.

Amin, A. M., Croiset, E., Epling, W. 2011. Review of methane catalytic cracking for hydrogen production. International Journal of Hydrogen Energy, 36, 2904-2935.

Ananyev, G. M., Skizim, N. J., Dismukes, G. C. 2012. Enhancing biological hydrogen production from cyanobacteria by removal of excreted products. Journal of Biotechnology, 162, 97-104.

Antal, T., Krendeleva, T., Pashchenko, V., Rubin, A., Stensjo, K., Tyystjärvi, E., Los D.A., Carpentier R., Nishihara, H., Allakhverdiev, S. 2012. Photosynthetic hydrogen production: mechanisms and approaches. In N. Azbar and D. B. Levin (Eds.), State of the Art and Progress of Biohydrogen, 25-53, Bentham Science Publishers, Canada.

Antal, T. K., Lindblad, P. 2005. Production of H-2 by sulphur-deprived cells of the unicellular cyanobacteria Gloeocapsa alpicola and Synechocystis sp PCC 6803 during dark incubation with methane or at various extracellular pH. Journal of Applied Microbiology, 98, 114-120.

Antal, T. K., Oliveira, P., Lindblad, P. 2006. The bidirectional hydrogenase in the cyanobacterium Synechocystis sp. strain PCC 6803. International Journal of Hydrogen Energy, 31, 1439-1444.

Anwar, M., Lou, S., Chen, L., Li, H., Hu, Z. 2019. Recent advancement and strategy on bio-hydrogen production from photosynthetic microalgae. Bioresource Technology, 292, 121972.

Appel, J., Phunpruch, S., Steinmüller, K., Schulz, R. 2000. The bidirectional hydrogenase of Synechocystis sp. PCC 6803 works as an electron valve during photosynthesis. Archives of Microbiology, 173, 333-338.

Arar, E. 1997. In vitro determination of chlorophylls-a, b, c+ c and pheopigments in marine and freshwater algae by visible Spectrophotometry. Method 446.0. US Environmental Protection Agency. US Environmental Protection Agency, Washington.

Azbar, N., Kapdan, I. K. 2012. Use of immobilized cell systems in biohydrogen production. In N. Azbar, D. B. Levin (Eds.), State of Art and Progress in Production of Biohydrogen, 227-249., Bentham Science Publishers, Canada.

Baebprasert, W., Jantaro, S., Khetkorn, W., Lindblad, P., Incharoensakdi, A. 2011. Increased H2 production in the cyanobacterium Synechocystis sp. strain PCC 6803 by redirecting the electron supply via genetic engineering of the nitrate assimilation pathway. Metabolic Engineering, 13, 610-616.

Baebprasert, W., Lindblad, P., Incharoensakdi, A. 2010. Response of H-2 production and Hox-hydrogenase activity to external factors in the unicellular cyanobacterium Synechocystis sp strain PCC 6803. International Journal of Hydrogen Energy, 35, 6611-6616.

Bernát, G., Waschewski, N., Rögner, M. 2009. Towards efficient hydrogen production: the impact of antenna size and external factors on electron transport dynamics in Synechocystis PCC 6803. Photosynthesis Research, 99, 205-216.

Bozoglan, E., Midilli, A., Hepbasli, A. 2012. Sustainable assessment of solar hydrogen production techniques. Energy, 46, 85-93.

Brewer, J. H. 1940. Clear liquid mediums for the aerobic cultivation of anaerobes. Journal of the American Medical Association, 115, 598-600.

Burris, R. H. 1991. Nitrogenases. Journal of Biological Chemistry, 266, 9339-9342.

Burrows, E. H., Chaplen, F. W. R., Ely, R. L. 2008. Optimization of media nutrient composition for increased photofermentative hydrogen production by Synechocystis sp PCC 6803. International Journal of Hydrogen Energy, 33, 6092-6099.

Burrows, E. H., Wong, W. K., Fern, X., Chaplen, F. W. R., Ely, R. L. 2009. Optimization of pH and Nitrogen for Enhanced Hydrogen Production by Synechocystis sp PCC 6803 via Statistical and Machine Learning Methods. Biotechnology Progress, 25, 1009-1017.

Call, D., Logan, B. E. 2008. Hydrogen production in a single chamber microbial electrolysis cell lacking a membrane. Environmental Science and Technology, 42, 3401-3406.

Carere, C., Levinli, D. B. (2012). Role of Metabolic Engineering in Enhancing Hydrogen Yields. In N. Azbar, D. B. Levin (Eds.), State of the Art and Progress in Production of Biohydrogen, 188-203, Bentham Science Publishers, Canada.

Chader, S., Hacene, H., Agathos, S. N. 2009. Study of hydrogen production by three strains of Chlorella isolated from the soil in the Algerian Sahara. International Journal of Hydrogen Energy, 34, 4941-4946.

Cook, A., Steel, K. 1959. The Stability of Thioglycollate Solutions: Part I. Effects of Method of Preparation of Solutions, pH and Temperature upon the Oxidation of Thioglycollate. Journal of Pharmacy and Pharmacology, 11, 216-223.

Cournac, L., Guedeney, G., Peltier, G., Vignais, P. M. (2004). Sustained photoevolution of molecular hydrogen in a mutant of Synechocystis sp strain PCC 6803 deficient in the type I NADPH-dehydrogenase complex. Journal of Bacteriology, 186, 1737-1746.

Cournac, L., Mus, F., Bernard, L., Guedeney, G., Vignais, P., Peltier, G. 2002. Limiting steps of hydrogen production in Chlamydomonas reinhardtii and Synechocystis PCC 6803 as analysed by light-induced gas exchange transients. International Journal of Hydrogen Energy, 27, 1229-1237.

Das, D., Khanna, N., Dasgupta, C. N. 2014. Biohydrogen Production Fundamentals and Technology Advances, Taylor and Francis Group LLC, U.S.A.

Das, D., Veziroğlu, T. N. 2001. Hydrogen production by biological processes: a survey of literature. International Journal of Hydrogen Energy, 26, 13-28.

Demirbaş, A. 2008. The Importance of Bioethanol and Biodiesel from Biomass. Energy Sources, Part B: Economics, Planning, and Policy, 3, 177-185.

Dere, Ş., Güneş, T., Sıvacı, R. 1998. Spectrophotometric determination of chlorophyll-A, B and total carotenoid contents of some algae species using different solvents. Turkish Journal of Botany, 22, 13-18.

Dickson, D. J., Page, C. J., Ely, R. L. 2009. Photobiological hydrogen production from Synechocystis sp. PCC 6803 encapsulated in silica sol–gel. International Journal of Hydrogen Energy, 34, 204-215.

Dincer, I., Acar, C. 2015. Review and evaluation of hydrogen production methods for better sustainability. International Journal of Hydrogen Energy, 40, 11094-11111.

Dutta, I., Vermaas, W. F. 2016. The electron transfer pathway upon H_2 oxidation by the NiFe bidirectional hydrogenase of Synechocystis sp. PCC 6803 in the light shares components with the photosynthetic electron transfer chain in thylakoid membranes. International Journal of Hydrogen Energy, 41, 11949-11959.

Eckert, C., Dubini, A., Yu, J., King, P., Ghirardi, M., Seibert, M., Maness, P.C. 2012. Hydrogenase genes and enzymes involved in solar hydrogen production. In N. Azbar, D. B. Levin (Eds.), State of the Art and Progress in Production of Biohydrogen, 8-24, Bentham Science Publishers, Canada.

EIA. 2016. Annual Energy Outlook, U.S. Energy Information Administration. https://www.eia.gov/outlooks/aeo/ Date accessed July 2020.

Eroğlu, E., Melis, A. 2011. Photobiological hydrogen production: recent advances and state of the art. Bioresource Technology, 102, 8403-8413.

Farrington, J., Ebert, M., Land, E. J., Fletcher, K. 1973. Bipyridylium quaternary salts and related compounds. V. Pulse radiolysis studies of the reaction of paraquat radical with oxygen. Implications for the mode of action of bipyridyl herbicides. Biochimica et Biophysica Acta (BBA)-Bioenergetics, 314, 372-381.

FCHJU. 2014. Development of Water Electrolysis in the European Union, Fuel Cells and Hydrogen Joint Undertaking. https://www.fch.europa.eu/node/783 Date Accessed July 2020

Frey, M. 2002. Hydrogenases: hydrogen-activating enzymes. ChemBioChem, 3(2-3), 153-160.

Germer, F., Zebger, I., Saggu, M., Lendzian, F., Schulz, R., Appel, J. 2009. Overexpression, isolation, and spectroscopic characterization of the bidirectional [NiFe] hydrogenase from Synechocystis sp. PCC 6803. Journal of Biological Chemistry, 284, 36462-36472.

Ghirardi, M. L., Togasaki, R. K., Seibert, M. 1997. Oxygen sensitivity of algal H 2-production. Applied Biochemistry and Biotechnology, 63, 141.

Gutekunst, K., Chen, X., Schreiber, K., Kaspar, U., Makam, S., Appel, J. 2014. The bidirectional NiFe-hydrogenase in Synechocystis sp. PCC 6803 is reduced by flavodoxin and ferredoxin and is essential under mixotrophic, nitrate-limiting conditions. Journal of Biological Chemistry, 289, 1930-1937.

Gutthann, F., Egert, M., Marques, A., Appel, J. 2007. Inhibition of respiration and nitrate assimilation enhances photohydrogen evolution under low oxygen concentrations in Synechocystis sp. PCC 6803. Biochimica et Biophysica Acta (BBA)-Bioenergetics, 1767, 161-169.

Hahn, J. J., Ghirardi, M. L., Jacoby, W. A. 2007. Immobilized algal cells used for hydrogen production. Biochemical Engineering Journal, 37, 75-79.

Hallenbeck, P. C. 2013. Photofermentative Biohydrogen Production. In A. Pandey, J.-S. Chang, P. C. Hallenbeck, C. Larroche (Eds.), Biohydrogen,, 144-155, Elsevier, Poland

Hallenbeck, P. C., Abo-Hashesh, M., Ghosh, D. 2012. Strategies for improving biological hydrogen production. Bioresource Technology, 110, 1-9.

Happe, T., Schütz, K., Böhme, H. 2000. Transcriptional and Mutational Analysis of the Uptake Hydrogenase of the Filamentous CyanobacteriumAnabaena variabilis ATCC 29413. Journal of Bacteriology, 182, 1624-1631.

Henriques, M., Silva, A., Rocha, J. 2007. Extraction and quantification of pigments from a marine microalga: a simple and reproducible method. Communicating Current Research and Educational Topics and Trends in Applied Microbiology, 2, 586-593.

Hwang, J.-H., Kim, H.-C., Choi, J.-A., Abou-Shanab, R., Dempsey, B. A., Regan, J. M., Jung Rae, K., Hocheol, S., Nam, I.-H. Kim, S.-N. 2014. Photoautotrophic hydrogen production by eukaryotic microalgae under aerobic conditions. Nature Communications, 5, 1-6.

IEA. 2018 World Energy Outlook 2018. International Energy Agency. https://www.iea.org/reports/world-energy-outlook-2018 Date Accessed July 2020.

IEA. 2019. The Future of Hydrogen. International Energy Agency. https://www.iea.org/reports/the-future-of-hydrogen Date Accessed 2020.

IHA. 2020. Hydropower Status Report. International Hydropower Assosciation, England

Ivanova, G., Rákhely, G., Kovács, K. L. 2008. Hydrogen production from biopolymers by Caldicellulosiruptor saccharolyticus and stabilization of the system by immobilization. International Journal of Hydrogen Energy, 33, 6953-6961.

Jokel, M., Nagy, V., Tóth, S. Z., Kosourov, S., Allahverdiyeva, Y. 2019. Elimination of the flavodiiron electron sink facilitates long-term H_2 photoproduction in green algae. Biotechnology for Biofuels, 12, 1-16.

Kaneko, T., Sato, S., Kotani, H., Tanaka, A., Asamizu, E., Nakamura, Y., Miyajima, N., Hirosawa, M., Sugiura, M., Sasamoto, S. 1996. Sequence analysis of the genome of the unicellular cyanobacterium Synechocystis sp. strain PCC6803. II. Sequence determination of the entire genome and assignment of potential protein-coding regions. DNA Research, 3, 109-136.

Khetkorn, W., Lindblad, P., Incharoensakdi, A. 2012. Inactivation of uptake hydrogenase leads to enhanced and sustained hydrogen production with high nitrogenase activity under high light exposure in the cyanobacterium Anabaena siamensis TISTR 8012. Journal of Biological Engineering, 6, 19.

Khetkorn, W., Rastogi, R. P., Incharoensakdi, A., Lindblad, P., Madamwar, D., Pandey, A., Larroche, C. 2017. Microalgal hydrogen production–A review. Bioresource Technology, 243, 1194-1206.

Knoop, H., Zilliges, Y., Lockau, W., Steuer, R. 2010. The metabolic network of Synechocystis sp. PCC 6803: systemic properties of autotrophic growth. Plant Physiology, 154, 410-422.

Kosourov, S., Jokel, M., Aro, E.-M., Allahverdiyeva, Y. 2018. A new approach for sustained and efficient H_2 photoproduction by Chlamydomonas reinhardtii. Energy & Environmental Science, 11, 1431-1436.

Kothari, R., Buddhi, D., Sawhney, R. L. 2008. Comparison of environmental and economic aspects of various hydrogen production methods. Renewable and Sustainable Energy Reviews, 12, 553-563.

Krasikov, V., Aguirre von Wobeser, E., Dekker, H. L., Huisman, J., Matthijs, H. C. 2012. Time-series resolution of gradual nitrogen starvation and its impact on photosynthesis in the cyanobacterium Synechocystis PCC 6803. Physiologia Plantarum, 145, 426-439.

Laurinavichene, T. V., Fedorov, A. S., Ghirardi, M. L., Seibert, M., Tsygankov, A. A. 2006. Demonstration of sustained hydrogen photoproduction by immobilized, sulfur-deprived Chlamydomonas reinhardtii cells. International Journal of Hydrogen Energy, 31, 659-667.

Lichthentaler, H. 1987. Chlorophyll and carotenoids-pigments of photosynthetic biomembranes,-In: Colowick, SP., Kaplan, NO (ed): Methods in Enzymology, Vol, 148. In: Academic Press, Sandiego-New York-Berkcley-Boston–London–Sydney–Tokyo–Toronto.

Lindberg, P., Devine, E., Stensjö, K., Lindblad, P. 2012. HupW protease specifically required for processing of the catalytic subunit of the uptake hydrogenase in the cyanobacterium Nostoc sp. strain PCC 7120. Applied and Environmental Microbiology, 78, 273-276.

Lindberg, P., Schütz, K., Happe, T., Lindblad, P. 2002. A hydrogen-producing, hydrogenase-free mutant strain of Nostoc punctiforme ATCC 29133. International Journal of Hydrogen Energy, 27, 1291-1296.

Mackinney, G. 1941. Absorption of light by chlorophyll solutions. Journal of Biological Chemistry, 140, 315-322.

Madigan, M., Martinko, J., Bender, K., Buckley, D., Stahl, D. 2015. Brock Biology of Microorganisms. Pearson, U.S.A.

Masepohl, B., Hallenbeck, P. C. 2010. Nitrogen and Molybdenum Control of Nitrogen Fixation in the Phototrophic Bacterium Rhodobacter capsulatus. Recent Advances in Phototrophic Prokaryotes, 675, 49-70.

Masukawa, H., Mochimaru, M., Sakurai, H. 2002. Disruption of the uptake hydrogenase gene, but not of the bidirectional hydrogenase gene, leads to enhanced photobiological hydrogen production by the nitrogen-fixing cyanobacterium Anabaena sp. PCC 7120. Applied Microbiology and Biotechnology, 58, 618-624.

Melis, A., Happe, T. 2001. Hydrogen production. Green algae as a source of energy. Plant Physiology, 127, 740-748.

Melis, A., Zhang, L., Forestier, M., Ghirardi, M. L., Seibert, M. 2000. Sustained photobiological hydrogen gas production upon reversible inactivation of oxygen evolution in the green Alga Chlamydomonas reinhardtii. Plant Physiology, 122, 127-136.

Melnicki, M. R., Bianchi, L., De Philippis, R., Melis, A. 2008. Hydrogen production during stationary phase in purple photosynthetic bacteria. International Journal of Hydrogen Energy, 33, 6525-6534.

Meyer, J. 2007. [FeFe] hydrogenases and their evolution: a genomic perspective. Cellular and Molecular Life Sciences, 64, 1063.

Michaelis, L., Hill, E. S. 1933. Potentiometric studies on semiquinones. Journal of the American Chemical Society, 55, 1481-1494.

Montagud, A., Gamermann, D., Fernandez de Cordoba, P., Urchueguia, J. F. 2015. Synechocystis sp. PCC6803 metabolic models for the enhanced production of hydrogen. Critical Reviews in Biotechnology, 35, 184-198.

Muradov, N. 2017. Low to near-zero CO_2 production of hydrogen from fossil fuels: Status and perspectives. International Journal of Hydrogen Energy, 42, 14058-14088.

Murray, A., Gibbs, C., Longmore, A., Flett, D. 1986. Determination of chlorophyll in marine waters: intercomparison of a rapid HPLC method with full HPLC, spectrophotometric and fluorometric methods. Marine Chemistry, 19, 211-227.

Navarro, F., Martín-Figueroa, E., Florencio, F. J. 2000. Electron transport controls transcription of the thioredoxin gene (trxA) in the cyanobacterium Synechocystis sp. PCC 6803. Plant Molecular Biology, 43, 23-32.

Nikolaidis, P., Poullikkas, A. 2017. A comparative overview of hydrogen production processes. Renewable and Sustainable Energy Reviews, 67, 597-611.

Oh, Y.-K., Raj, S. M., Jung, G. Y., Park, S. 2013. Metabolic engineering of microorganisms for biohydrogen production. In Pandey, A., Chang, J.-S., Hallenbeck, P. C., Larroche, C. (Eds), Biohydrogen, 45-65, Elsevier,U.S.A.

Oreskes, N. 2005. The scientific consensus on climate change. Science, 307(5708), 355-355.
Pandey, A., Mohan, S. V. 2014. Biohydrogen Production: An Introduction. In Pandey, A., Chang, J.-S., Hallenbeck, P. C., Larroche, C. (Eds), Biohydrogen, 1-24, Elsevier, U.S.A.

Peterson, G. L. 1977 A simplification of the protein assay method of Lowry et al. which is more generally applicable. Analytical Biochemistry, 83, 346-356.

Porra, R. J. 2002. The chequered history of the development and use of simultaneous equations for the accurate determination of chlorophylls a and b. Photosynthesis Research, 73, 149-156.

Quarton, C. J., Tlili, O., Welder, L., Mansilla, C., Blanco, H., Heinrichs, H., Heinrichs, H., Leaver, J., Samsatli, N. J., Lucchese, P., Robinius, M., Samsatli, S. 2020. The curious case of the conflicting roles of hydrogen in global energy scenarios. Sustainable Energy & Fuels, 4, 80-95.

Rao, K. K., Cammack, R. 2001. Producing Hydrogen as a Fuel. In R. Cammack, M. Frey, R. Robson (Eds.), Hydrogen as a Fuel, 219-248, Taylor & Francis, London.

Ratnasamy, C., Wagner, J. P. 2009. Water gas shift catalysis. Catalysis Reviews, 51, 325-440.

Richaud, C., Zabulon, G., Joder, A., Thomas, J.-C. 2001. Nitrogen or sulfur starvation differentially affects phycobilisome degradation and expression of the nblA gene in Synechocystis strain PCC 6803. Journal of Bacteriology, 183, 2989-2994.

Rippka, R., Deruelles, J., Waterbury, J. B., Herdman, M., Stanier, R. Y. 1979. Generic Assignments, Strain Histories and Properties of Pure Cultures of Cyanobacteria. Microbiology, 111, 1-61.

Ritchie, R. J. 2006. Consistent sets of spectrophotometric chlorophyll equations for acetone, methanol and ethanol solvents. Photosynthesis Research, 89, 27-41.

Sartory, D., Grobbelaar, J. 1984. Extraction of chlorophyll a from freshwater phytoplankton for spectrophotometric analysis. Hydrobiologia, 114, 177-187.

Schmetterer, G. 1994. Cyanobacterial respiration. In The molecular biology of cyanobacteria 409-435, Springer, U.S.A.

Schmitz, O., Boison, G., Hilscher, R., Hundeshagen, B., Zimmer, W., Lottspeich, F., Bothe, H. 1995. Molecular biological analysis of a bidirectional hydrogenase from cyanobacteria. European Journal of Biochemistry, 233, 266-276.

Schmitz, O., Boison, G., Salzmann, H., Bothe, H., Schütz, K., Wang, S.-h., Happe, T. 2002. HoxE—a subunit specific for the pentameric bidirectional hydrogenase complex (HoxEFUYH) of cyanobacteria. Biochimica et Biophysica Acta (BBA)-Bioenergetics, 1554, 66-74.

Schütz, K., Happe, T., Troshina, O., Lindblad, P., Leitao, E., Oliveira, P., Tamagnini, P. 2004. Cyanobacterial H_2 production—a comparative analysis. Planta, 218, 350-359.

Steinman, A. D., Lamberti, G. A., Leavitt, P. R., Uzarski, D. G. 2017. Biomass and pigments of benthic algae. In Methods in Stream Ecology, Volume 1, 223-241, Elsevier.

Surzycki, R., Cournac, L., Peltier, G., Rochaix, J.-D. 2007. Potential for hydrogen production with inducible chloroplast gene expression in Chlamydomonas. Proceedings of the National Academy of Sciences, 104, 17548-17553.

Tamagnini, P., Axelsson, R., Lindberg, P., Oxelfelt, F., Wünschiers, R., Lindblad, P. 2002. Hydrogenases and hydrogen metabolism of cyanobacteria. Microbiology and Molecular Biology Reviews, 66, 1-20.

Tamagnini, P., Leitão, E., Oliveira, P., Ferreira, D., Pinto, F., Harris, D. J., Heidorn, T., Lindblad, P. 2007. Cyanobacterial hydrogenases: diversity, regulation and applications. FEMS Microbiology Reviews, 31, 692-720.

Tamagnini, P., Troshina, O., Oxelfelt, F., Salema, R., Lindblad, P. 1997. Hydrogenases in Nostoc sp. Strain PCC 73102, a Strain Lacking a Bidirectional Enzyme. Applied and Environmental Microbiology, 63, 1801-1807.

Tanaka, A., Melis, A. 1997. Irradiance-dependent changes in the size and composition of the chlorophyll ab light-harvesting complex in the green alga Dunaliella salina. Plant and Cell Physiology, 38, 17-24.

Tanaka, A., Tanaka, R. 2006. Chlorophyll metabolism. Current Opinion in Plant Biology, 9, 248-255.

Thauer, R. K. 1998. Biochemistry of methanogenesis: a tribute to Marjory Stephenson: 1998 Marjory Stephenson prize lecture. Microbiology, 144, 2377-2406.

Touloupakis, E., Benavides, A. M. S., Cicchi, B., Torzillo, G. 2016. Growth and hydrogen production of outdoor cultures of Synechocystis PCC 6803. Algal Research, 18, 78-85.

Trebst, A. 1972. Measurement of hill reactions and photoreduction. In Methods in Enzymology 24, 146-165 Elsevier.

Trudiatger, P. 1970. On the absorbancy of reduced methyl viologen. Analytical Biochemistry, 36, 222-225.

Ursua, A., Gandia, L. M., Sanchis, P. 2011. Hydrogen production from water electrolysis: current status and future trends. Proceedings of the IEEE, 100, 410-426.

Vignais, P. M., Billoud, B. 2007. Occurrence, classification, and biological function of hydrogenases: an overview. Chemical Reviews, 107, 4206-4272.

Vincent, I., Bessarabov, D. 2018. Low cost hydrogen production by anion exchange membrane electrolysis: A review. Renewable & Sustainable Energy Reviews, 81, 1690-1704.

Vogt, S., Lyon, E. J., Shima, S., Thauer, R. K. 2008. The exchange activities of [Fe] hydrogenase (iron–sulfur-cluster-free hydrogenase) from methanogenic archaea in comparison with the exchange activities of [FeFe] and [NiFe] hydrogenases. JBIC Journal of Biological Inorganic Chemistry, 13, 97-106.

Voloshin, R. A., Rodionova, M. V., Zharmukhamedov, S. K., Veziroglu, T. N., Allakhverdiev, S. I. 2016. Biofuel production from plant and algal biomass. International Journal of Hydrogen Energy, 41, 17257-17273.

Weber, J., Krujatz, F., Hilpmann, G., Grutzner, S., Herrmann, J., Thierfelder, S., Bienert, G., Illing, R., Helbig, K., Hurtado, A., Cuniberti, G., Mertig, M., Lange, R., Gunther, E., Opitz, J., Lippmann, W., Bley, T., Haufe, N. 2014. Biotechnological hydrogen production by photosynthesis. Engineering in Life Sciences, 14, 592-606.

Weiland, P. 2010. Biogas production: current state and perspectives. Applied Microbiology and Biotechnology, 85, 849-860.

Zhang, Z., Pendse, N. D., Phillips, K. N., Cotner, J. B., Khodursky, A. 2008. Gene expression patterns of sulfur starvation in Synechocystis sp. PCC 6803. BMC Genomics, 9, 344.

Zhu, H., Suzuki, T., Tsygankov, A. A., Asada, Y., Miyake, J. 1999. Hydrogen production from tofu wastewater by Rhodobacter sphaeroides immobilized in agar gels. International Journal of Hydrogen Energy, 24, 305-310.

APPENDIX A

Table A.1. OD and pH values for growth phase

	OD			pH		
Day	Batch 1	Batch 2	Batch 3	Batch 1	Batch 2	Batch 3
1	0.140	0.134	0.132	7.537	7.686	7.824
2	0.159	0.206	0.184	7.810	7.840	7.850
3	0.327	0.329	0.323	8.558	8.565	8.318
4	0.649	0.620	0.571	9.960	9.540	8.510
5	0.908	1.004	1.006	8.950	9.350	9.870
6	1.027	1.122	1.168	9.430	9.340	9.380
7	1.237	1.320	1.307	9.070	9.840	9.320
8	1.444	1.489	1.474	9.020	9.620	9.380
9	1.575	1.590	1.563	9.270	9.790	9.540
10	1.676	1.674	1.667	9.170	10.040	9.520
11	1.775	1.778	1.738	9.030	9.490	9.580
12	1.885	1.900	1.824	9.290	9.530	9.500
13	1.986	1.911	1.906	9.360	9.730	9.480

Table A.2. Cell number per mL for growth phase

	Cell count		
Day	Batch 1	Batch 2	Batch 3
1	7.69E+06	1.03E+07	9.19E+06
2			
3	2.18E+07	2.04E+07	1.85E+07
4			
5	2.44E+08	3.25E+08	4.18E+08
6			
7	3.06E+08	3.44E+08	3.37E+08
8			
9	2.89E+08	2.86E+08	2.78E+08
10			
11	3.88E+08	3.58E+08	3.71E+08
12			
13	5.23E+08	3.86E+08	4.28E+08

APPENDIX B

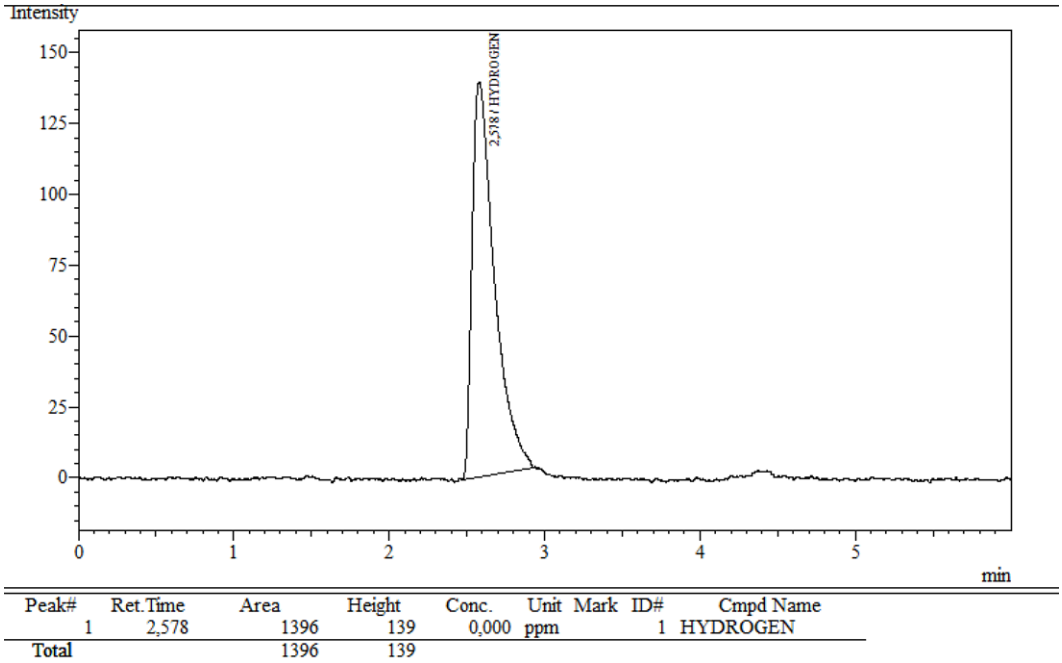

Figure B.1 Representative gas chromatogram for hydrogen calibration curve

Table B.1 Calibration curve data for hydrogen

Volume (µL)	Mean Area	SD	%RSD	Area1	Area2	Area3
1	1119.67	174.7265	15.60541	1047	1319	993
5	6084.00	169.3933	2.840227	6518	5842	5892
10	12096.67	387.9618	3.206491	12426	11669	12195
20	18557.67	4813.1011	25.93693	13254	19771	22648
40	47682.33	1280.2282	2.684926	46494	49038	47515

Table B.2 Calibration curve data for nitrogen

Volume (µL)	Mean Area	SD	%RSD	Area1	Area2	Area3
1	91.67	60.99	66.45	79	158	38
5	569.67	66.01	11.58	515	643	551
10	1820.33	227.31	12.49	2064	1614	1783
20	3395.67	304.08	8.96	3117	3350	3720
40	6209.67	202.32	3.26	6424	6183	6022

Table B.3 Calibration curve data for oxygen

Volume (μL)	Mean Area	SD	%RSD	Area1	Area2	Area3
1	153.67	17.2143351	11.29084	148	140	173
5	594.33	25.8907963	4.401019	565	604	614
10	1397.67	245.141456	17.52233	1115	1552	1526
20	2531.33	47.1628385	1.873728	2517	2493	2584
40	4178.67	339.031464	8.122036	3792	4425	4319

APPENDIX C

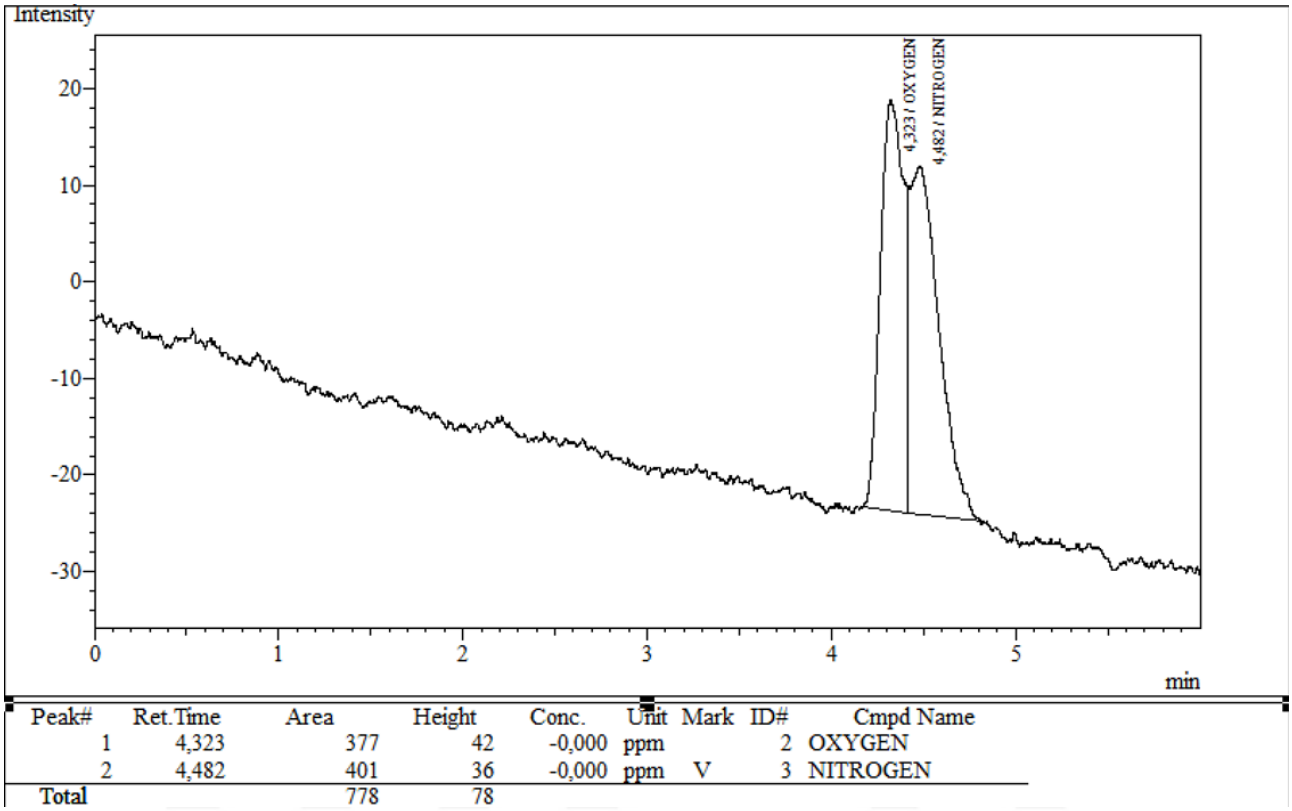

Figure C.1. Representative gas chromatogram for headspace gas analysis

Table C.1. Headspace gas analysis chromatogram areas and gauge pressures for R1

Day	Sample	Gas	Headspace Dark	Headspace Light	Headspace Dark		Headspace Light	
			Area	Area	Gauge P (bar)	Volume (L)	Gauge P (bar)	Volume (L)
1	1	O_2		117.8		0.021	0.078	0.021
		N_2		142.2		0.021	0.078	0.021
	2	O_2		0		0.021	0.022	0.021
		N_2		0		0.021	0.022	0.021
	3	O_2		398.9		0.021	0.05	0.021
		N_2		245.9		0.021	0.05	0.021
2	1	O_2	1200.3	1100	0.09	0.027	0.208	0.027
		N_2	315.2	236.5		0.027	0.208	0.027
	2	O_2	1040.5	1413	0.08	0.027	0.156	0.027
		N_2	300	205		0.027	0.156	0.027
	3	O_2	1150.2	1458.7	0.052	0.027	0.162	0.027

		N_2	219.9	211.5		0.027	0.162	0.027
3	1	O_2	1020.9	1260.7	0.104	0.038	0.164	0.038
		N_2	224.2	139.3		0.038	0.164	0.038
	2	O_2	1131.7	1455.6	0.066	0.038	0.092	0.038
		N_2	213.3	158.1		0.038	0.092	0.038
	3	O_2	1050.1	1378.6	0.064	0.038	0.096	0.038
		N_2	205.6	313.4		0.038	0.096	0.038
4	1	O_2	837	1011.8	0.076	0.044	0.084	0.044
		N_2	225	196.6		0.044	0.084	0.044
	2	O_2	983.6	1161.7	0.066	0.044	0.084	0.044
		N_2	228.1	186.1		0.044	0.084	0.044
	3	O_2	1049.7	1201.6	0.056	0.044	0.066	0.044
		N_2	202.7	304		0.044	0.066	0.044
5	1	O_2	876.7	913.4	0.13	0.055	0.132	0.055
		N_2	205.6	201.2		0.055	0.132	0.055
	2	O_2	813.5	924	0.124	0.055	0.124	0.055
		N_2	185.6	158.2		0.055	0.124	0.055
	3	O_2	914.9	948.2	0.108	0.055	0.108	0.055
		N_2	196.4	227.3		0.055	0.108	0.055
6	1	O_2	875.1	788	0.022	0.055	0.012	0.055
		N_2	224.5	242.3		0.055	0.012	0.055
	2	O_2	880.2	839.4	0.012	0.055	0.008	0.055
		N_2	121.6	161.2		0.055	0.008	0.055
	3	O_2	899.9	873.1	0.082	0.055	0.072	0.055
		N_2	215.2	209.9		0.055	0.072	0.055

Table C.2. Headspace gas analysis chromatogram areas and gauge pressures for R2

Day	Sample	Gas	Headspace Dark	Headspace Light	Headspace Dark		Headspace Light	
			Area	Area	Gauge P (bar)	Volume (L)	Gauge P (bar)	Volume (L)
1	1	O_2		365.4		0.021	0.26	0.021
		N_2		266.3		0.021	0.26	0.021
	2	O_2		270.8		0.021	0.318	0.021
		N_2		248.2		0.021	0.318	0.021
	3	O_2		305.7		0.021	0.18	0.021

		N_2		276.5		0.021	0.18	0.021
2	1	O_2	398.5	414.4	0.23	0.027	0.026	0.027
		N_2	262.9	434		0.027	0.026	0.027
	2	O_2	310.8	420.9	0.294	0.027	0.04	0.027
		N_2	281.3	320.5		0.027	0.04	0.027
	3	O_2	274.4	366.4	0.26	0.027	0.044	0.027
		N_2	282	286.1		0.027	0.044	0.027
3	1	O_2	376.8	453.8	0.028	0.038	0.038	0.038
		N_2	401.4	416.8		0.038	0.038	0.038
	2	O_2	329.7	442.9	0.042	0.038	0.056	0.038
		N_2	364	308.7		0.038	0.056	0.038
	3	O_2	337.8	386.5	0.048	0.038	0.06	0.038
		N_2	301.1	315.8		0.038	0.06	0.038
4	1	O_2	307.8	331.4	0.128	0.044	0.128	0.044
		N_2	439.2	446.6		0.044	0.128	0.044
	2	O_2	306.1	346	0.022	0.044	0.024	0.044
		N_2	388.4	420.8		0.044	0.024	0.044
	3	O_2	279	333.3	0.012	0.044	0.008	0.044
		N_2	307.9	370.3		0.044	0.008	0.044
5	1	O_2	257.9	315.2	0.152	0.055	0.156	0.055
		N_2	475.7	524.7		0.055	0.156	0.055
	2	O_2	334.7	310.1	0.054	0.055	0.05	0.055
		N_2	563.6	553.7		0.055	0.05	0.055
	3	O_2	300.1	272.3	0.104	0.055	0.1	0.055
		N_2	461.9	408.9		0.055	0.1	0.055
6	1	O_2	271.2	244.2	0.052	0.055	0.068	0.055
		N_2	525.6	440.1		0.055	0.068	0.055
	2	O_2	198.1	282.6	0.126	0.055	0.118	0.055
		N_2	421.7	555.2		0.055	0.118	0.055
	3	O_2	215.5	259.7	0.134	0.055	0.122	0.055
		N_2	418.6	359		0.055	0.122	0.055

Table C.3. Headspace gas analysis chromatogram areas and gauge pressures for R3

Day	Sample	Gas	Headspace Dark	Headspace Light	Headspace Dark		Headspace Light	
			Area	Area	Gauge P (bar)	Volume (L)	Gauge P (bar)	Volume (L)
1	1	O_2		0		0.021	0.238	0.021
		N_2		0		0.021	0.238	0.021
	2	O_2		146.5		0.021	0.118	0.021
		N_2		238.6		0.021	0.118	0.021
	3	O_2		132.8		0.021	0.112	0.021
		N_2		240.7		0.021	0.112	0.021
2	1	O_2	1201	1483.9	0.066	0.027	0.092	0.027
		N_2	375.3	397.1		0.027	0.092	0.027
	2	O_2	1089.8	1351	0.2	0.027	0.198	0.027
		N_2	301.9	347.5		0.027	0.198	0.027
	3	O_2	928.4	1149.9	0.156	0.027	0.164	0.027
		N_2	252.6	235.9		0.027	0.164	0.027
3	1	O_2	1205.6	1490.3	0.092	0.038	0.11	0.038
		N_2	313.2	285		0.038	0.11	0.038
	2	O_2	1213.4	1490.3	0.198	0.038	0.2	0.038
		N_2	297.1	285		0.038	0.2	0.038
	3	O_2	340	525.8	0.172	0.038	0.178	0.038
		N_2	0	129.2		0.038	0.178	0.038
4	1	O_2	1129.4	1217.5	0.194	0.044	0.15	0.044
		N_2	533.3	466.7		0.044	0.15	0.044
	2	O_2	1288.5	1337.8	0.072	0.044	0.048	0.044
		N_2	342.3	420.3		0.044	0.048	0.044
	3	O_2	1123	1203.9	0.044	0.044	0.028	0.044
		N_2	329.3	276		0.044	0.028	0.044
5	1	O_2	1267.6	1073.6	0.024	0.055	0.092	0.055
		N_2	502.8	506.1		0.055	0.092	0.055
	2	O_2	975.7	859.2	0.098	0.055	0.12	0.055
		N_2	379.4	283.8		0.055	0.12	0.055
	3	O_2	1017.7	812.2	0.09	0.055	0.104	0.055
		N_2	218.6	230.6		0.055	0.104	0.055
6	1	O_2	1017.4		0.07	0.055		0.055

		N_2	511.6			0.055		0.055
	2	O_2	1031.4		0.11	0.055		0.055
		N_2	317.3			0.055		0.055
	3	O_2	795.4		0.092	0.055		0.055
		N_2	220.3			0.055		0.055

Table D.4. Headspace gas analysis chromatogram areas and gauge pressures for R4

Day	Sample	Gas	Headspace Dark	Headspace Light	Headspace Dark		Headspace Light	
			Area	Area	Gauge P (bar)	Volume (L)	Gauge P (bar)	Volume (L)
1	1	O_2		372.5			0.096	0.021
		N_2		1092.1				0.021
	2	O_2		867.3			0.346	0.021
		N_2		3193.5				0.021
	3	O_2		30.3			0.1	0.021
		N_2		127.2				0.021
2	1	O_2	16.6	32.4	0.066	0.027	0.076	0.027
		N_2	307.2	364.6		0.027		0.027
	2	O_2	0	38.9	0.224	0.027	0.21	0.027
		N_2	192.8	285.7		0.027		0.027
	3	O_2	0	23	0.072	0.027	0.078	0.027
		N_2	256.3	255.4		0.027		0.027
3	1	O_2	0	0	0.144	0.038	0.112	0.038
		N_2	487.3	517.3		0.038		0.038
	2	O_2	0	28.1	0.023	0.038	0.192	0.038
		N_2	363.5	398.8		0.038		0.038
	3	O_2	0	0	0.114	0.038	0.09	0.038
		N_2	281.1	279.5		0.038		0.038
4	1	O_2	0	0	0.122	0.044	0.104	0.044
		N_2	535.9	516.1		0.044		0.044
	2	O_2	0	0	0.172	0.044	0.15	0.044
		N_2	338.1	398.2		0.044		0.044
	3	O_2	0	0	0.106	0.044	0.092	0.044
		N_2	258.9	312.9		0.044		0.044
5	1	O_2	0	0	0.102	0.055	0.11	0.055

		N_2	367.3	502.3		0.055		0.055
	2	O_2	68.5	0	0.104	0.055	0.154	0.055
		N_2	657.2	349.4		0.055		0.055
	3	O_2	0	0	0.076	0.055	0.092	0.055
		N_2	272.4	268		0.055		0.055
6	1	O_2	0	52.7	0.07	0.055	0.064	0.055
		N_2	438.2	760.7		0.055		0.055
	2	O_2	0	0	0.034	0.055	0.034	0.055
		N_2	278.7	364.1		0.055		0.055
	3	O_2	0	0	0.102	0.055	0.1	0.055
		N_2	1293.3	13028.9		0.055		0.055

APPENDIX D

Table D.1. Absorbance values for chlorophyll calculation for R1

Day	Sample	Absorbance at 750 nm	Absrobance at 665 nm
1	1	0.001	0.279
	2	0.003	0.284
	3	0.003	0.258
2	1	0.001	0.304
	2	0.003	0.309
	3	0.001	0.294
3	1	0.001	0.275
	2	0.002	0.273
	3	0.002	0.263
4	1	0.000	0.226
	2	0.003	0.207
	3	0.003	0.225
5	1	0.004	0.168
	2	0.002	0.153
	3	0.001	0.168
6	1	0.003	0.075
	2	0.000	0.079
	3	0.003	0.099

Table D.2. Absorbance values for chlorophyll calculation for R2

Day	Sample	Absorbance at 750 nm	Absrobance at 665 nm
1	1	0.003	0.301
	2	0.004	0.306
	3	0.005	0.32
2	1	0.001	0.292
	2	0.000	0.262
	3	-0.001	0.265
3	1	0.000	0.320
	2	0.000	0.325
	3	0.002	0.299
4	1	-0.001	0.299
	2	0.005	0.303
	3	-0.001	0.282
5	1	0.001	0.295
	2	-0.001	0.289

	3	-0.001	0.274
6	1	0.002	0.236
	2	0.000	0.278
	3	0.005	0.262

Table D.3. Absorbance values for chlorophyll calculation for R3

Day	Sample	Absorbance at 750 nm	Absrobance at 665 nm
1	1	0.002	0.297
	2	0.005	0.269
	3	0.002	0.281
2	1	0.005	0.268
	2	0.002	0.241
	3	0.003	0.268
3	1	0.001	0.244
	2	0.004	0.250
	3	0.002	0.250
4	1	0.001	0.254
	2	0.004	0.246
	3	0.001	0.237
5	1	0.000	0.131
	2	0.000	0.134
	3	0.002	0.125
6	1	0.000	0.025
	2	0.002	0.056
	3	0.004	0.064

Table D.4. Absorbance values for chlorophyll calculation for R4

Day	Sample	750	665
1	1	0.004	0.349
	2	0.003	0.338
	3	0.003	0.344
2	1	0.001	0.290
	2	0.000	0.303
	3	0.004	0.306
3	1	0.003	0.276
	2	0.005	0.290
	3	0.000	0.314
4	1	0.000	0.298
	2	0.001	0.309
	3	0.000	0.294

5	1	0.000	0.290
	2	0.001	0.316
	3	0.001	0.290
6	1	0.005	0.303
	2	0.000	0.305
	3	0.002	0.299

APPENDIX E

Table E.1. Hydrogenase activity measurement data for R1

Day	Hours	Sample	Hydrogen Area	Gauge Pressure (bar)	Time (h)	Total Volume (L)
1	0	1	205.5	0.218	23	0.036
		2	187.2	0.232	23	0.036
		3	210	0.146	23	0.036
3	48	1	171.2	0.114	25.5	0.036
		2	245.4	0.044	25.5	0.036
		3	219.3	0.07	25.5	0.036
5	96	1	234.1	0.216	24.5	0.036
		2	158.9	0.192	24.5	0.036
		3	127.6	0.276	*24.5*	0.036

Table E.2. Hydrogenase activity measurement data for R2

Day	Hours	Sample	Hydrogen Area	Gauge Pressure (bar)	Time (h)	Total Volume (L)
1	0	1	49.1	0.130	23	0.036
		2	76	0.120	23	0.036
		3	87.4	0.070	23	0.036
3	48	1	118.4	0.042	24	0.036
		2	101.4	0.208	24	0.036
		3	106	0.066	24	0.036
5	96	1	106	0.072	21	0.036
		2	121.8	0.152	21	0.036
		3	137.3	0.09	21	0.036

Table E.3. Hydrogenase activity measurements for R3

Day	Hours	Sample	Hydrogen Area	Gauge Pressure (bar)	Reaction Time (h)	Total Volume (L)
1	0	1	66.3	0.528	22	0.036
		2	52.4	0.564	22	0.036
		3	58.5	0.494	22	0.036
3	48	1	176.4	0.328	24	0.036
		2	194.2	0.266	24	0.036
		3	269.4	0.158	24	0.036
5	96	1	178.5	0.188	22	0.036
		2	150	0.236	22	0.036
		3	79.6	0.244	22	0.036

Table E.4. Hydrogenase activity measurements for R4

Day	Hours	Sample	Hydrogen Area	Gauge Pressure (bar)	Reaction Time (h)	Total Volume (L)
1	0	1	138.9	0.042	20	0.036
		2	141.3	0.038	20	0.036
		3	145.5	0.052	20	0.036
3	48	1	190.8	0.168	23	0.036
		2	144.8	0.066	23	0.036
		3	127.5	0.06	23	0.036
5	96	1	65.5	0.092	24	0.036
		2	82.1	0.11	24	0.036
		3	87	0.132	24	0.036

APPENDIX F

Table F.1. Dissolved oxygen data for R4

Day	Blank (mg/L)	Reactor (mg/L)
1	0.70	0.39
2	0.70	0.40
3	0.45	1.40
4	0.59	0.54
5	0.57	0.69
6	0.49	0.24